

AD/A-000 997

HEAT CIRCUITS OF THERMOELECTRIC  
DEVICES

G. K. Kotyrlo, et al

Army Foreign Science and Technology Center  
Charlottesville, Virginia

19 July 1974

DISTRIBUTED BY:

**NTIS**

National Technical Information Service  
U. S. DEPARTMENT OF COMMERCE



DEPARTMENT OF THE ARMY  
U.S. ARMY FOREIGN SCIENCE AND TECHNOLOGY CENTER  
230 SEVENTH STREET NE.  
CHARLOTTESVILLE, VIRGINIA 22901

TRANSLATION

In Reply Refer to:  
FSTC-HT-23- 853-74  
DIA Task No. T741801

Date: 19 July 1974

ENGLISH TITLE: Heat Circuits of Thermoelectric Devices

SOURCE: "Naukova Dumka", Kiev, 1973. Ukrainian SSR Academy of Sciences  
108 pp.

AUTHOR: Kotyrlo, G. K. Shchegolev, G. M.

LANGUAGE: Russian

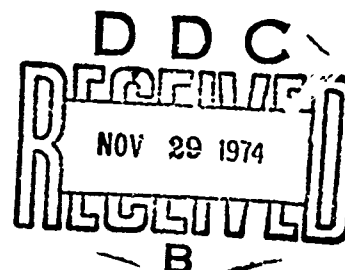
COUNTRY: USSR

REQUESTOR: GE - Turner

TRANSLATOR: Leo Kanner Associates [MAC]

ABSTRACT: A general discussion of thermoelectric devices is followed by a detailed mathematical analysis of the efficiency, temperature fields at the thermocouple junctions, the power level, etc. of various electrical power generator and refrigerator configurations. Single and two-stage designs of these devices are analyzed both qualitatively and quantitatively. A basic contrast between permeable and monolithic thermocouples is extensively developed in the book.

Reproduced by  
NATIONAL TECHNICAL  
INFORMATION SERVICE  
U S Department of Commerce  
Springfield VA 22151



NOTICE

The contents of this publication have been translated as presented in the original text. No attempt has been made to verify the accuracy of any statement contained herein. This translation is published with a minimum of copy editing and graphics preparation in order to expedite the dissemination of information.

Approved for public release. Distribution unlimited

AD A 000992

## TABLE OF CONTENTS

Foreword . . . . .	2
Chapter I	
The Fundamental Heat Circuit Elements of Thermoelectric Devices . . . . .	4
1. Heat Sources . . . . .	5
2. Heat Delivery and Dissipation Systems . . .	16
3. Power Sources . . . . .	28
Chapter II	
The Classification of Heat Circuits of Thermoelectric Devices . . . . .	31
1. Generator Circuits . . . . .	31
2. Circuits of Refrigerators, Conditioners and Heat Pumps . . . . .	55
Chapter III	
Features of Temperature Fields in Permeable Thermocouples . . . . .	60
1. Method of Calculating the Temperature Fields	63
2. Analysis of the Temperature Fields . . . . .	70
Chapter IV	
The Design of Thermoelectric Generators with Permeable Thermocouples . . . . .	74
1. The Design of a Generator Flushed by a Coolant Flowing from the Cold to the Hot Junctions . . . . .	75
2. Design of a Generator Where the Heat Carrier Blows Through from the Hot to the Cold Junctions . . . . .	95
3. Two-stage Generator Design . . . . .	109
Chapter V	
Thermoelectric Cooling Devices with Permeable Thermocouples . . . . .	117
1. Refrigerator Design Method . . . . .	118

2. An Operational Analysis of a Cooling Device	125
Conclusion . . . . .	130
Bibliography . . . . .	133



## FOREWORD

Thermoelectric devices have such valuable qualities as silent operation, reliability, the capability of operating for an extended period without servicing, compactness, and they are self-contained. It is just these qualities which explain the rather wide application of thermoelectric devices as well as which delineate the areas of their maximum distribution at the present time: powering the devices in space equipment, radio and meteorological stations, sea navigation buoys and various devices for ground and water transport, cathodic protection of piping and metallic installations.

The wider introduction of thermoelectric devices, in particular in stationary power engineering, is held back by their comparatively low power efficiency and the high cost per kilowatt. Because of this, a large number of laboratories and scientific organizations of the Soviet Union and many foreign countries are intensively carrying out investigations into the processes which take place during the operation of thermoelectric devices, and are

developing new semiconductor thermoelectric materials. Even more efficient and economical devices are being created as a result.

Efforts to increase the efficiency of thermoelectric devices are basically directed towards finding new materials with a high thermoelectric figure of merit  $z = \frac{e^2 \delta}{\lambda} / ^\circ K$ , the refinement as well as the development of the process engineering for interconnecting thermoelectric modules and for more effective heat transfer to the hot and cold surfaces of thermoelectric batteries, which assure minimal temperature losses, i.e. the finding of methods of effectively interlinking batteries with hot and cold heat sources.

Insufficient attention has been given to the development of new, more refined heat circuits and the analysis of their influence on the power efficiency of thermoelectric devices.

An attempt is made in the present work to consider the heat circuits of thermoelectric devices from the point of view of their thermodynamic efficiency, and evaluate the possible influence of the choice of heat circuit on the power efficiency of the batteries. It is interesting from this viewpoint to also consider thermoelectric batteries in which the primary quantity of heat is supplied or removed not through the surfaces of the hot and cold junctions, but within the thermocouples. Thermocouples are considered whose branches are made permeable to a substance being cooled when the battery is operated in a refrigerator mode, or a heat carrier (coolant) when operated as a generator of electrical power.

In permeable thermocouples, the internal heat exchange surface can be quite developed, a consequence of which is the fact that the heat exchange between the gas (liquid) passing through it and the solid material occurs at small temperature differences, i.e. almost reversibly. Such a heat exchange

system is responsible for the fundamental and essential features of thermocouple operation. In particular, new possibilities of influencing the cooling coefficient of a thermoelectric battery or its efficiency when operating in a generator mode are opening up.

## Chapter I

### The Fundamental Heat Circuit Elements of Thermoelectric Devices

The heat circuit of any thermoelectric device contains the usual common basic components irrespective of its function. A thermoelectric battery operating in any mode should have a hot and cold heat source, systems for delivering heat from the hot source to the hot junction and removing it from the cold junction to the cold sink, as well as an internal load which the battery powers in a generator mode, or an external power source when operating in refrigerator or heat pump modes.

Considering the existing battery design, it should be noted that they are basically made up of thermocouples of a rectangular shape and in a smaller number of designs, of ring-shaped thermocouples. More rarely employed are trapezoidal, cubic and other shapes which are chosen in the design of thermoelectric devices solely from considerations of connection convenience and operational peculiarities, since neither the shape nor the geometric dimensions of thermocouples exhibit an influence on the battery efficiency.

The main difficulties in making batteries are caused by the necessity of electrically connecting a significant number of p- and n- type elements.

However, there is no necessity to make up high power batteries by connecting the semiconductor materials in a series parallel configuration. Simpler and more reliable is the fabrication of batteries of any power from individual modules, which take the form of a few interconnected thermoelectric couples. Such low-power thermoelectric modules make it possible to fabricate a battery of any construction and power with the high reliability of series parallel connection.

Multistage thermocouples can also be analogously interconnected in low power modules. Many works [5, 16, 24] have been devoted to the technological questions of fabricating p- and n- type branches, their interconnection in thermoelectric modules and structural layout, so there is no point in going into these questions in detail.

We will consider in greater detail the other common circuit elements of thermoelectric devices which play an active part in the operation of the heat circuit and give it its characteristic features.

### 1. Heat Sources

One of the primary heat circuit components of thermoelectric generators is the source of heat energy, whose choice is of considerable significance in the design of the generator depending on the required length of its continuous operation, its function, useful electric power, etc.

The basic heat sources in generators already constructed at the present time and those being designed are combustion products of chemical fuels, radiant energy from the sun, radioisotopes, and nuclear reactors.

Chemical fuel is used primarily as a heat source in generators for ground service, which are employed for powering radio equipment, lighting, and the cathodic protection of metallic installations and piping which are located in difficult access regions.

In transport installations, where the dimensions and weight of the power supply system play a determining part, the use of a chemical fuel is inexpedient in the majority of cases since a large quantity of fuel is required to assure an extended period of generator operation.

In developing a heat source using chemical fuel, primary attention is given to the construction of the burner device and the selection of an optimum combustion chamber shape from the point of view of the organization of the burning process. The burner device and the combustion chamber should assure the requisite heat flow densities at the given hot junction temperature and a maximum completeness of fuel combustion. When high temperature thermoelectric materials are employed in the manufacture of the thermocouple branches, the solution of this problem can occasion substantial difficulties.

In principle, any types of chemical fuels can be used in thermoelectric devices - liquid, solid and gaseous. The working substances of various thermal cycles (steam, hot water, exhausted combustion products) can likewise be used as a heat source. In this case, the generator can be located at the most diverse points in the heat circuit of any heat-consuming installation. Where the waste heat from the working substances of thermal cycles or the exhaust gases from plants operating on the combustion products of organic fuels is utilized to obtain electrical energy, such generators will promote an increase in the power efficiency of the basic cycle.

Radiant energy from the sun is a promising and, in particular cases, inexpensive heat source for generators for space vehicles and ground service, which are located in meteorologically favorable regions of the earth.

The conditions favorable for generator operation are determined by the number of hours of sunshine and the total radiation reaching the surface of the earth in the given region [3].

The utilization of radiant energy from the sun as the sole heat source for a generator under space flight conditions is still rather complex and expensive. This is explained by the complexity and high cost of devices for focusing solar radiation, which create the heat flow densities necessary for normal generator operation, or of collectors, which absorb radiant energy, by the complexity of the devices for tracking focusing systems with a luminary when the space vehicle is rotating, and by the necessity for utilizing storage batteries during the time when the space vehicle is in the shade of the earth or another planet. However, solar converters for operation on board a space ship, operating at specified distances from the sun, at the present time already have an advantage in cost, weight per unit power, and reliability over systems with photoelectric elements, systems with a turbogenerator having a nuclear reactor heat source, etc. Such results were obtained in the comparison of various means of generating electrical power for converters having a useable power of up to 100 kw [29].

An interesting direction in the efforts to create solar generators for space service, the successful development of which will increase even more the role played by converters of this type, is the development and creation of heat batteries, which provide for the normal operation of the generator while the space vehicle is located in a shadow. The use of primarily lithium

fluoride and hydride is proposed for the heat-storing materials [32].

In the creation of solar generators for ground service, primary attention is devoted to the development of devices for focusing solar radiation with systems for daily tracking and yearly declination. A significant number of concentrator designs have been built and tested at the present time. Installations using a system of independent heating of each thermocouple from a separate reflector and with large diameter parabolic reflectors working on a group of thermocouples have been tested. Various systems of solar receivers which convert the radiant energy coming from the reflectors into heat energy have been developed [1].

Radioisotope heat sources have recently found wide application in the creation of generators for various purposes. The utilization of the heat which is emitted during radioisotope decay to heat the hot junctions of a generator makes it possible to create a reliable, self-contained, and comparatively long service life system of energy supply for application in space vehicles and operation on sea and land. In spite of the fact that radioisotope sources cannot provide for large heat flow densities, they are ideal heat sources for low power generators (tens and hundreds of watts), since they are small and simple to fabricate.

Radioisotope sources, in contrast to other heat sources, are suitable for application in thermoelectric installations and are characterized by a magnitude of emitted heat power which decreases with time. For this reason, in the choice of an isotope for a generator for one purpose or another, besides taking into account other factors it is necessary to choose a heat power or the isotope fuel taking into account the magnitude of the useable heat power required at the conclusion of the term of service of the given

device. Sometimes the isotope source is designed around the average value of its thermal power for the required operational lifetime of the generator.

The basic characteristics of radioisotopes suitable for application as generator heat sources are given in table 1. The data on the specific heat capacity of radioisotope fuel is taken from the literature [5, 16, 17, 29, 31, 34]. Some divergence in this data is explained by the difference in the specific weights of the radioisotope fuels which were used.

Table 1

Таблица 1

Изотоп 1.	Топливо 2.	Вид рас- пада 3.	Период полу- распада, лет 4.	Тепловая мощ- ность топли- ва, Вт/г 5.	Тепловая мощность чистого изотопы, Вт/г 6.
Po <sup>210</sup>	Po	$\alpha$	0.38	141.00	141.00
Cm <sup>242</sup>	Cm <sub>2</sub> O <sub>3</sub>	$\alpha$	0.15	99,5 — 120	120,00
Cl <sup>141</sup>	ClO <sub>2</sub>	$\beta - \gamma$	0,78	1,96 — 2,30	25,60
Pu <sup>239</sup>	PuC	$\alpha$	86.40	0,55 — 0,56	0,56
Pm <sup>147</sup>	Pm <sub>2</sub> O <sub>3</sub>	$\beta - \gamma$	2.60	0.16 — 0.31	0.31
Cs <sup>137</sup>	CsCl	$\beta - \gamma$	33.00	0,249 — 0,33	0,42
Sr <sup>90</sup>	SrTiO <sub>3</sub> SrO	$\beta - \gamma$	27,7 — 28,0	0,113 — 0,92	0,95
Co <sup>60</sup>	CO	$\beta - \gamma$	5.30	0,30	17,40
Ru <sup>106</sup>	Ru	$\beta - \gamma$	1.00	29,60	33,10
Cm <sup>241</sup>	Cm <sub>2</sub> O <sub>3</sub>	$\alpha$	17.60	2.30	2,80
Au <sup>198</sup>	Au	—	1.00	29,50	—
Cr <sup>132</sup>	—	$\beta - \gamma$	26.60	0,072	—
Tm <sup>170</sup>	Tm <sub>2</sub> O <sub>3</sub>	$\beta$	0.35	1.03	15,60
Tl <sup>204</sup>	Tl <sub>2</sub> O <sub>3</sub>	$\beta$	4.00	0.12	0,67
Ti <sup>225</sup>	ThO <sub>2</sub>	$\alpha$	1.90	111,00	170,60
U <sup>232</sup>	UO <sub>2</sub>	$\alpha - \gamma$	74.00	3.30	4,10
Am <sup>241</sup>	Am	$\alpha$	458.00	0,10	0,11

1. Isotope
2. Fuel
3. Type of decay
4. Half-life, years
5. Heat power of the fuel, watts/grams
6. Heat power of the pure isotope, watts/grams



The physical and chemical properties of the compounds which contain a radioactive isotope and are used in the form of a radioisotope fuel should meet a series of specific requirements. The fuel should be easy to prepare, should not react with the material of the fuel capsule, should be heat-resistant and have a high fusion temperature. The isotope concentration in the fuel should assure the required heat flow densities [20]. Once a fuel is obtained which meets these basic requirements, then various inert compounds or metallic additives are added to it, which has an influence on the specific weight of the fuel. This explains the divergence in data on the specific fuel power or radioisotope fuels published in Soviet and foreign literature.

At the present time, a rather large number of generators having a radioisotope heat source have been created, which has a number of advantages in comparison with other heat sources both under space conditions and in ground and sea installations having powers on the order of tens and hundreds of watts. However, their application is limited by biological harmfulness. The necessity of biological shielding leads to a substantial increase in the cost and difficulty of generator construction.

Nuclear sources of heat energy are utilized in the development of high-power generators. They assure extended self-contained operation of the thermoelectric device, and greater heat flow densities at high temperatures.

Two basic variants in the construction of nuclear reactors exist, which are distinguished according to the method of heat delivery to the hot junction of the generator: those having an intermediate heat carrier and those with indirect heat supply from heat-emitting elements of the reactor or its internal jacket. The basic characteristics of some nuclear reactors, designed

Table 2

Reactor type	Country	Heat power, kw	Temperature in the active region, °K	Fuel	Heat carrier	Weight, kg	Notes
SNAP-2(SDR)	USA	50	980	ZrH + 235	NaK	113.5	worked for 1000 hours
"Romashka"	USSR	40	2173	Uranium dicarbide plus 90% U-235	without heat carrier	--	--
SNAP-10	USA	15	--	ZrH + 235	without heat carrier	79 - 91	--
SNAP-10A	USA	40	838	--	NaK	123	43 days in an orbit of 1300 km in 1965
SNAP-8	USA	500	1088	ZrH + 235	NaK	228	enlarged variant of SNAP-2
Martin-Marietta Corp.	USA	--	--	ZrH + U	phosphorous trisulfide	--	projected design
Martin-Marietta Corp.	JSA	2500	--	UO <sub>2</sub> + H <sub>2</sub> O	boiling water	--	--

for the heating of the hot junctions of generators are given in Table 2.

By means of nuclear reactors in which the heat is transferred from the active region to the hot junctions of the generator by a heat carrier, it is possible to provide for isothermal heat delivery over the entire surface of the hot junctions, in particular where the substance used as a heat carrier changes its aggregate state in the given power cycle. Additionally, the intermediate heat carrier provides for partial radiation protection of the semiconductor substance. A nuclear heat source with an intermediate heat carrier makes possible independent construction and de-bugging of the generator and nuclear reactor. However, heat carriers in use at the present time do not permit complete utilization of the temperature possibilities of nuclear reactors and thermoelectric semiconductor materials.

In nuclear heat sources without an intermediate heat carrier, the thermocouples can be placed directly on the surface of the reflector, as was done in the Soviet nuclear thermoelectric plant "Romashka" [17] (Fig. 1). Heat emitting elements in the form of plates of uranium dicarbide enriched to 90% with U-235 are located in the cylindrical graphite body of the reactor. The active region is surrounded by a beryllium reflector, which makes it possible to obtain a temperature of  $1270^{\circ}$  K at the surface of the beryllium reflector. In this case, the temperature of the hot junctions of the thermocouples clamped against the surface of the beryllium reflector was  $1223^{\circ}$  K. It is obvious from the example of the "Romashka" plant just what importance is attached to the refinement of the system of contact heat exchange. With a further refined method of heat transfer between the contacting solid surfaces, it would be possible to achieve much smaller temperature differences between

the heating surface and the hot junctions, which would permit a more efficient utilization of the thermoelectric materials, whose maximum efficiency is achieved at maximum operating temperatures.

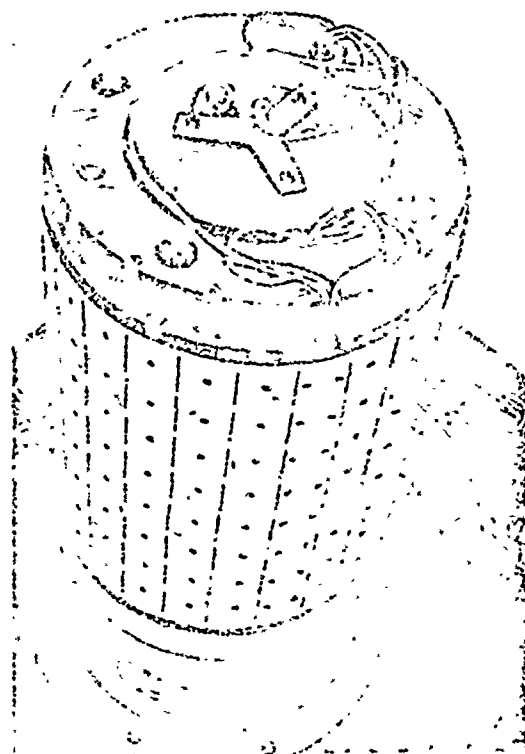


Figure 1. The nuclear reactor of the "Romashka" thermoelectric plant.

The SNAP-10 [29] thermoelectric plant is of a similar construction and is distinguished from the "Romashka" plant by the lower temperature of the hot junctions which is  $811^{\circ}\text{K}$ .

In plants of similar design, the plane surfaces of the nuclear reactor are not covered with thermocouples, and require reliable insulation to avoid heat losses, which are rather large.

Compactness and relative simplicity characterize those nuclear thermoelectric plants in which the thermocouples are superimposed on the heat-emitting

elements of the reactor. Any type of thermoelectric heat-emitting elements can be employed in the reactor with the condition that the heat carrier does not possess the property of electrical conductivity.

A series of structural variants of heat-emitting elements has been worked out, where these are co-located with thermocouples, however they all are modifications of a basic variant (Fig. 2). It can be seen from the

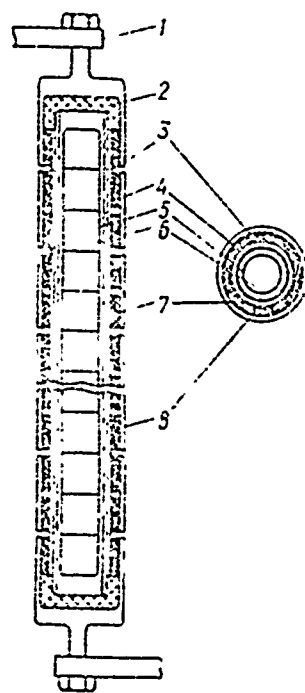


Figure 2. Thermocouples superimposed on heat-emitting elements:

- |                                |                    |
|--------------------------------|--------------------|
| 1. Current output conductors;  | 5 Fuel jacket;     |
| 2. Electrical insulators;      | 6. Fuel;           |
| 3. Hot thermocouple junctions; | 7. Thermocouples;  |
| 4. Electrical insulation;      | 8. Cold junctions. |

drawing that the thermocouples are arranged on the surface of the capsule with a separating medium. The heat-emitting elements in such a design can

be of any shape (the most widespread elements are in the shape of rods or plates).

When radioisotope and nuclear heat sources are used, the semiconductor thermoelectric materials are subject to the effect of various forms of radiation when operating, which can cause changes in their thermoelectric properties. The gamma radiation from radioactive isotopes and nuclear reactors, as well as neutron radiation from reactors, exerts the primary influence on the properties of the materials. Other types of radiation accompanying a fission reaction have little penetrating ability and are usually absorbed by the structural elements and exert no influence on the characteristics of the material. The questions which are connected with the influence of radiation on the properties of materials are at the present time still insufficiently studied. However, according to data in the literature, there exists a large number of semiconductor thermoelectric materials which are capable of operating satisfactorily under conditions of radioisotope and nuclear reactor heating of the hot junctions of a generator.

The surrounding medium is usually employed as a cold source in the heat circuits of thermoelectric devices. Depending on the purpose of the thermoelectric device, water, air or outer space can be considered a surrounding medium. The heat from the cold junctions of the generator or from the hot junctions of the refrigerator can be removed to the cold source either directly or by means of an intermediate heat carrier. The cold source has a substantial influence on the structural and power characteristics of a thermoelectric device, since the temperature level and the working medium determine the rate at which heat is removed from the junctions, which in turn

determines the structure and dimensions of the heat dissipation system.

## 2. Heat Delivery and Dissipation Systems

These systems play a significant part in the construction and operation of thermoelectric devices and plants. The choice in the method of delivering heat to the hot junctions of generators and the cold junctions of refrigerators is determined in many cases by the weight and dimension parameters of the devices, and their power efficiency. In the development of one type or another of thermoelectric devices, all the basic forms of heat transfer are usually employed -- heat conductivity, natural or forced convection and radiation -- depending on the purpose of the devices and the specifics of the operational conditions. Sometimes combined systems of heat transfer are employed, for example, the transfer of heat simultaneously by convection and radiation.

The process of transferring the heat by heat conduction occurs when the hot junctions of the generator which are directly clamped against the surface conducting the heat away are heated and when heat is conducted from its cold junctions to the surfaces in contact with them which absorb the heat. The converse is true in refrigerating devices. The heat conductivity of the materials of the thermocouple branches in these cases is of great significance in the structural design work on thermoelectric devices.

The direct transfer of heat from the source to the junctions of the thermoelectric device makes it necessary to create a heat junction consisting of several layers of materials of various thermal conductivity which are air-tight, electrically insulating, electrically connecting, etc. For

this reason, the calculation of heat transfer is made based on the relationships obtained for multilayered walls [28].

Nuclear thermoelectric systems of the "Romashka" and SNAP-10 type can serve as examples where the process of heat conductivity is utilized for conducting heat from the source to the hot junctions. In these systems, the thermocouples are arranged directly on the external jacket of the nuclear reactor. Heat is also supplied in a similar manner to the hot junctions in radioisotope generators (Fig. 3).

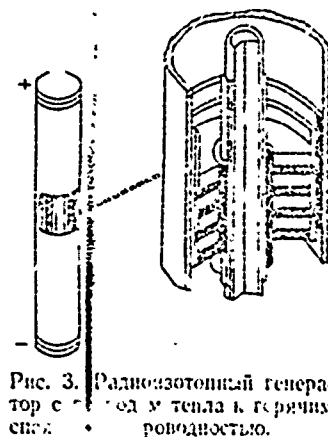


Figure 3. A radioisotope generator where heat is delivered to the hot junctions by thermal conductivity

In spite of the relative simplicity in laying out the heat transfer process using thermal conductivity, this method has a number of substantial drawbacks. For the contact between the heat-transmitting and the heat-absorbing surfaces, success is not always met in assuring the heat-flow densities necessary for normal operation of the device at a fixed temperature of the heat-absorbing surface. Additionally, it is not always possible to provide for a convenient structural connection of the generator with the heat



source. Such a connection can be the reason for additional heat losses.

Convective systems for heat supply and removal in thermoelectric devices employing gas, liquid or liquid metallic heat carriers are more efficient. Convective heat delivery systems permit doing away with the rigid structural connection between the generator and the heat source. For the case of nuclear reactor heating, the convective heat removal system maintains a lower temperature for the heat-emitting elements of the reactor at the same temperature of the hot junctions of the generator and realizing in this case the extraction of large heat flow densities from the active region of the reactor. The rate of heat removal for convective heating or cooling is determined by the speed at which the medium moves, its thermal physical properties and the shape and size of the heat emitting (or heat absorbing) surface.

Where heat is delivered or removed from the junctions of thermoelectric devices under conditions of natural (free) convection of the surrounding medium, the value of the coefficients are very low.

For the calculation of the heat output coefficients  $\alpha$  for plane walls and pipes, the following equations can be recommended [16]:

$$\left. \begin{aligned} Nu &= 1,15(GrPr)^{0,25} \text{ для } 1 \cdot 10^{-3} < (GrPr) < 5 \cdot 10^2, \\ Nu &= 0,51(GrPr)^{0,25} \text{ для } 5 \cdot 10^2 < (GrPr) < 2 \cdot 10^7, \\ Nu &= 0,135(GrPr)^{0,4} \text{ для } 2 \cdot 10^7 < (GrPr) < 2 \cdot 10^{13}, \end{aligned} \right\} (1)$$

where  $Nu = \frac{\alpha d}{\lambda}$ ,  $Gr = \frac{g \beta l^3 \Delta t}{\nu^2}$ ,  $Pr = \frac{\mu c_p}{\lambda}$ ,  $\beta$  is the volumetric expansion coefficient,  $\nu$  is kinematic viscosity,  $l$  is the typical dimension,  $\Delta t$  is the thermal head,  $\lambda$  is the coefficient of thermal conductivity,  $c_p$  is the heat capacity,  $\alpha$  is the heat transfer coefficient, and  $\mu$  is the dynamic

viscosity coefficient. In this case the value of  $\alpha = 3 - 6 \text{ watts/m}^2 \cdot \text{degrees}$ .

Where natural convection is used to increase the heat removal (heat delivery), the junctions are equipped with fins for the purpose of increasing the heat dissipating (heat absorbing) surface. In this case, the heat transfer coefficient from the finned surface to the surrounding medium depends on the shape, size and relative arrangement of the fins.

Natural cooling of the finned surfaces of junctions is primarily employed in those cases where questions of power efficiency make the considerations of the weight and size characteristics of thermoelectric devices of secondary importance.

A fin cooling system significantly increases the weight and size of a thermoelectric device and complicates its fabrication. However, under natural convection conditions it has little influence in increasing the power efficiency of the device. For this reason, when working with gaseous media blowers are often employed to increase the rate of heat transfer by creating a forced flow of gas along the vanes. In many cases, the expenditures of a part of the useful power developed by the generator to drive a blower is economically justified. For example, in generators for the cathodic protection of gas piping where an additional expenditure of gas which is burned does not play a substantial part, a blower installation which blows across the cold junctions, by increasing the rate of heat transfer makes it possible to obtain a significantly greater drop in temperatures at the junctions. This means it is also possible to obtain a greater useful power per unit volume of the thermoelectric material.

The conditions of heat transfer where the vanned surfaces of different configurations having ribs of various shapes are blower ventilated using

gas flows have been sufficiently well studied for their application in various thermal devices and installations for the operational conditions found there. However, all of this data is not generalized and there are no sufficiently clear-cut recommendations for computing the heat transfer coefficients from finned surfaces of cold and hot junctions of thermoelectric devices.

At SKB [unknown institute - translator's note] of semiconductor instruments, investigations into the heat transfer from the radiators of thermoelectric devices have been carried out. For radiators with a slotted gap, the data which was obtained on heat exchange is described by the equation [8]:

$$Nu = 1,55 \left( Pe \frac{d}{\lambda} \right)^{1/4} C, \quad (2)$$

where  $Pe = \frac{v d c_p \gamma}{\lambda}$ .

In this case gaps having a width of from 0.5 to 1.2 mm for hydraulic diameters of  $d = 1.6 - 2.2$  mm were investigated. From the point of view of optimal conditions for heat removal and aerodynamic resistance, the best gaps had a width of 1 - 1.2 mm. Such systems assured heat removal with a drop in temperatures of 2 - 4° K for heat flows at the junctions of the thermal batteries of 2 - 2.5 watts/cm<sup>2</sup>.

Sometimes it is more expedient to cool the fin junctions with water. A comparison of the effectiveness of air and water heat removal from the hot junctions of a thermoelectric conditioner [26] showed that the application of water cooling can substantially increase the cold productivity of the conditioner and its cooling coefficient with a significant reduction in the height and number of fins. Thermoelectric devices using water cooling

of the junctions are more expedient when employed on boats, sea navigation buoys, in deep sea apparatus, etc.

The application of water cooling in the majority of cases makes it possible in general to eliminate the vanes on the cold junctions of generators or the hot junctions of refrigerators, which significantly simplifies the technology of battery fabrication. However, difficulties arise in this case which are connected with salt encrustations, the presence of mechanical impurities in the water, etc. The coefficients of heat exchange in such cooling systems are computed in accordance with the well-known empirical equations [18]. Specifically for turbulent flow of liquids and gases in channels:

$$Nu = 0.023 Re^{0.8} Pr^{0.4}, \quad (3)$$

where  $Re = \frac{Ud}{\nu}$ ,  $d$  is the channel diameter, and  $U$  is the velocity of coolant flow.

To improve the conditions for heat removal from cold junctions of the generator, a method of absorbing the heat in an evaporating liquid has likewise been proposed where the liquid is subsequently delivered to the surrounding medium through a condenser with a developed heat dissipating surface [31]. Freon - 113 with an evaporation temperature of 320° K has been used as a liquid cooling agent. The design did not require pumps for pumping the coolant back, since the condensate was returned to the cold junction from the condenser by the force of gravity.

Heat delivery systems with liquid metal heat carriers are attracting attention in connection with the utilization of nuclear reactors as a heat source for generators. Such heat carriers, in comparison with gaseous ones,

offer the possibility of significantly reducing power losses during pump-through, improving the heat exchange process and reducing the pressure in the nuclear reactor circuit. However, at the present time the possible temperatures for semiconductor thermoelectric materials and nuclear reactors exceeds those possible for liquid metallic heat carriers whose maximum working temperature does not exceed 1100 - 1200° K.

The heat dissipation coefficients for the case of liquid metal flow can be computed from the following relationships [7]:

for turbulent flow in circular pipes

$$\begin{aligned} Nu &= 5 + 0.0021 Pe, \\ Nu &= 5 + 0.0025 Pe^{0.8}; \end{aligned} \quad (4)$$

for longitudinal flow around the rod bundles

$$Nu = 6 + 0.006 Pe; \quad (5)$$

for conditions of free convection

$$\begin{aligned} Nu &= 0.67 \left( \frac{Pr^2 Gr}{1 + Pr} \right)^{1/4} \text{ for } \frac{1}{11} \leq Gr < 10^5, \\ Nu &= 0.16 \left( \frac{Pr^2 Gr}{1 + Pr} \right)^{1/4} \text{ for } Gr < 10^3. \end{aligned} \quad (6)$$

It is recommended that the determining dimension in these relationships be taken as: the altitude for vertical walls, the diameter for pipes. The relationships given here have received experimental confirmation not only for the case of molten metals, but also for oil, water and air [7].

Quite effective in many cases are systems of heat supply and removal within the thermocouples. In this case, the thermocouple branches should be made permeable. The permeability can be created from one junction to another by the most diverse methods. This method can even use finely

porous thermocouples fabricated using the methods of powder metallurgy, and made up of individual pipes or rods of a sufficiently small diameter which are sintered together in order to improve electrical contact. The thermocouples can also be perforated by electric arc, electrochemical or laser drilling of small-diameter holes as well as by special stamping methods.

In designing such systems it is necessary to know the value of the heat dissipation coefficients both within the thermocouples between the semiconductor material and the heat carrier (coolant) blown through it, and at both surfaces, the hot and the cold.

Heat exchange inside porous capillary bodies is characterized by a high rate due to the very developed heat exchange surface. In view of the very small flow cross-section of the channels through which the heat-dissipating or the heat-absorbing substance blows, it does not obey the laws of heat exchange for flow in pipes and channels.

In finely porous thermocouples fabricated using the methods of powder metallurgy, the internal heat exchange surface is for all practical purposes undefined, since there are observed non-penetrating and uneven pores, pinching of the pores in the material, etc. Volumetric heat transfer coefficients  $\alpha^*$ , watts/cm<sup>3</sup>. deg., are usually employed in such systems. The usual geometric magnitudes cannot be used as a defining dimension in the heat-exchange equation because the geometric characteristics of the capillaries cannot be reproduced in the stamping process. A magnitude characterizing the hydraulic properties of the given sample is usually employed in these cases.

Many works have been devoted to the investigation of heat exchange

within finely porous bodies which are flushed with various substances. However, no general relationship for computing the heat transfer coefficient has been found up to now since its magnitude is determined by a large number of factors which are difficult to assess - the properties of the material, the stamping technology, the size of the initial powder, blow-through velocity of the substance, etc.

The heat exchange surface within a thermocouple can be determined precisely where permeable thermocouples are fabricated by stacking rods together or drilling small-diameter openings. The heat transfer coefficient  $\alpha$ , watts/cm<sup>2</sup> . deg., is used in the calculations for perforated thermocouples. The heat exchange per unit volume within a material having a large number of capillaries has been insufficiently investigated. At the present time there are no reliable formulas for the engineering calculations of perforated systems.

The temperature fields within permeable walls which are flushed by a substance, will be considered in more detail in the following.

Heat exchange at the external surfaces of permeable thermocouples is complicated by the fact that the substance is either drawn off or injected through the capillaries. For example, when a drop in temperatures is created at the junctions of the generator by means of flushing with a coolant directed from the cold junctions to the hot ones, the heat exchange conditions at the hot and cold side of the generator will be entirely different. The coolant which exits the capillaries on the hot side, creates a gaseous layer between the hot junctions and the heating flow which significantly increases the difficulty of heat transfer from the heating flow. The

greater the output of the substance which is blown through, the thicker this layer is, which has a temperature many times lower than the temperature of the heating flow, which means there is also a smaller heat transfer coefficient  $\alpha$ . The heat transfer coefficient  $\alpha_1$  from the permeable wall to the external flow from the outlet side of the purging substance can be computed from the formula

$$\frac{\alpha_1}{\alpha_H} = 1 - 0,19 \left( \frac{M_2}{M_1} \right)^b \frac{\rho v_w}{\alpha_H}, \quad (7)$$

which has been experimentally confirmed for a broad range of parameter changes [19]; where  $b = 0.35$  when  $0.2$  less than  $\frac{M_2}{M_1}$  less than  $1$ , and  $b = 0.7$  when  $1$  less than  $\frac{M_2}{M_1}$  less than  $8$ ;  $\alpha_H$  is the heat transfer coefficient at the nonpermeable wall;  $M_2$  and  $M_1$  are respectively the weights of the primary flow and the substance being blown through;  $\rho v_w$  is the specific consumption of the substance being blown through.

On the cold side of the generator where the coolant enters the capillaries, the rate of heat transfer increases due to a thinning of the viscosity of the layer against the wall.

Two variants of the thermal conditions can be considered for the side where the substance enters the permeable wall. For the case where the substance exits through the surface within the permeable wall, it can be assumed that heat losses into the surrounding medium from the cold side of the wall are absent. The heat leaving the surface of the wall, returns within the wall with the substance blown back in. In this case there is no point in talking about a coefficient of heat transfer  $\alpha$  as a magnitude



characterizing the quantity of heat removed from the surface.

However, if a portion of the medium flow blows through a permeable wall, while another portion flushes its surface externally, then there is an irreversible heat loss from the cold side of the wall. It is just this portion of the heat flow which is of the greatest interest and importance in considering the thermal equilibria of thermoelectric devices with permeable thermocouples. When carrying out heat calculations for such devices, it is always essential to know the quantity of heat which is irreversibly removed beyond their limits into the surrounding medium. The heat transfer coefficient  $\alpha$  from the permeable wall to the coolant flow washing it, which characterizes the irreversible heat loss from the given wall section, can be determined from the following relationships [14]:

$$\begin{aligned} \text{Nu} &= 1.68 \cdot 10^{-3} \text{Re}_{in}^{1.74} (\text{Re}_{\omega} \frac{l}{d_{eqv}})^{-1.24} (\frac{l}{d_{eqv}} \Pi)^{3.34} \\ &\text{for } \frac{l}{d_{eqv}} \Pi < 2 \\ \text{Nu} &= 0.017 \text{Re}_{in}^{1.74} (\text{Re}_{\omega} \frac{l}{d_{eqv}})^{-1.24} \\ &\text{for } \frac{l}{d_{eqv}} \Pi > 2 \end{aligned} \quad (8)$$

where  $l$  is the channel length. Taken as a defining dimension in these relationships is the equivalent channel diameter,  $d_{eqv}$ , formed by the permeable thermocouples and the impermeable walls of the structure;

$\text{Re}_{in} = \frac{\rho U_{in} d_{eqv}}{\mu}$  is Reynold's number based on the flow velocity across the permeable thermocouples;  $\text{Re}_{\omega} = \frac{\rho U_{\omega} d_{eqv}}{\mu}$  is Reynold's number

based on the blow through velocity of the cooling substance through the thermocouples;  $\Pi = \frac{P_{pr}}{P}$  is the ratio of the portion of the perimeter  $P_{pr}$  taken up by the permeable walls to the total perimeter of the channel. This correction takes into account the fact that in the structural formulation of the thermoelectric device, the coolant (cooling substance, heat carrier) will be moving in the channel, and one or a few walls of the channel will appear as permeable thermocouples. The relationships given above were obtained experimentally as a result of studying the heat transfer from finely porous walls when air was sucked out through them [14].

Systems using radiative heat dissipation are employed in the operation of thermoelectric devices in outer space. Such devices should have a cooler-radiator for removing heat from the junctions. In this case, heat is delivered to the radiating surfaces from the junctions either by means of thermal conductivity or an intermediate heat carrier. The quantity of heat dissipated by radiation into outer space can be determined from the Stefan - Boltzman equation:

$$Q = F \epsilon \sigma T^4 \quad (9)$$

where  $\epsilon$  is the level of characteristic black body heat radiation, and  $\sigma = 5.68 \cdot 10^{-8} \text{ watts/m}^2 \cdot \text{deg}^4$  is a constant.

The dependence of the area  $F$  of a heat exchange radiator on the temperature  $T$  of its surface for a fixed level of heat dissipation  $Q$  can be seen from this equation.

A ground service variant of the thermoelectric converter of the "Romashka" space power plant can serve as an example of such a system. In this case, heat dissipation was effected by radiation from a finned surface of the cold junctions into a medium which simulated outer space

conditions (Fig. 4).

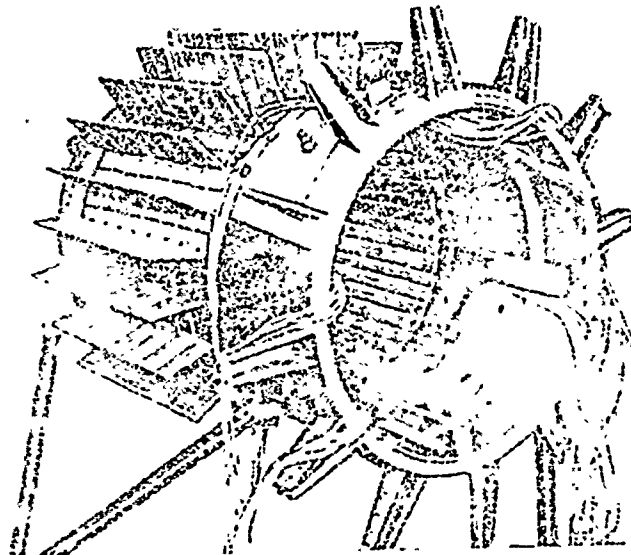


Рис. 4. Термоэлектрический преобразователь ядерной реакторной системы «Ромашка».

Figure 4. The thermoelectric converter of the "Romashka" nuclear reactor system.

### 3. Power Sources

If one of the basic elements for generators is the source of thermal energy, then the power source has considerable influence on the operation of thermoelectric cooling devices, conditioners, thermostats and heat pumps. The choice of this source plays a substantial part since a high level low-voltage direct current is required for the operation of thermoelectric devices. Storage batteries, rectifiers and current converters, and DC generators which match the parameters of the given device are usually considered as power sources.

The powering of thermoelectric devices for everyday service and fixed

industrial devices where electrical power is available is accomplished from the mains in the majority of cases using rectifiers. However rectifiers produce direct current with a certain percent of pulsating DC. The presence of an alternating component in the rectified current can be quite significant for certain rectifier device circuits. Current pulsation leads to significant degradation in the power characteristics of conditioners or heat pumps, and batteries operating in refrigerator modes. Therefore to preclude this pulsation, filters of various types are used, the most widespread being semiconductor diodes - germanium, silicon, selenium and copper oxide.

However, the use of filters for smoothing the pulsations is sometimes made difficult since the semiconductor thermobatteries require large currents reaching hundreds of amperes. At the present time, high current germanium diodes for currents of 1000 amps and greater which operate at a sufficiently high efficiency, are being industrially produced.

Investigations which were carried out in the semiconductor laboratory of the Odessa technological institute of the food stuff and refrigeration industry, have shown that the current pulsations flowing through the thermobatteries significantly influence their power characteristics. The reduction in cooling productivity and the cooling coefficient of plants in comparison with the computed values (for computations based on DC without pulsations) can amount to 20 - 50% and more depending on the operational temperature level of the thermobatteries, for the case of the presently most widespread practice of using single phase full-wave rectification [20].

The power parameters of devices operating with large temperature differences at the junctions of the thermocouples are degraded particularly

severely. These circumstances force us to strive to maximally smooth the pulsations in current feeding thermoelectric devices. If it is impossible for any reason to eliminate or reduce the current pulsations, then the actual design calculations should be made with formulas which take into account their influence on the operation of the device.

Storage batteries are used to power thermoelectric devices which operate where there is no electrical power available from the mains. The necessity for using storage batteries arises primarily in the operation of non-stationary devices. The operation of thermoelectric devices directly from a battery is limited in time by its capacity. Because of the fact that such devices use large currents at low voltages, the battery is discharged rather quickly. For this reason, to increase the operational life of the thermoelectric device which uses a battery, current converters are often employed which convert the relatively high-voltage low-current battery output into a high-current low-voltage supply. The presence of a converter naturally leads to additional losses, and the efficiency of the supply circuit is significantly reduced.

Thermoelectric generators can often be successfully employed as a power source for thermoelectric cooling devices, heaters and conditioners. The generator design can assure obtaining the DC parameters at the output necessary for powering the refrigerator or heater.

## Chapter II

### The Classification of Heat Circuits of Thermoelectric Devices

The common packaging of the basic components considered in Chapter I makes it possible to create various circuits for thermoelectric devices. The creation of an effective thermoelectric plant is impossible without a detailed analysis of the mutual interaction of elements of heat circuits which are rigidly interconnected during operation.

The heat circuits of thermoelectric devices are usually classified from the viewpoint of the difference in the methods of delivering and removing heat at the junction surfaces of the thermocouples. It is expedient to consider generator circuits and base their comparison on the heat source as one of the basic components of the device. As far as the circuits of thermoelectric cooling devices, conditioners and heat pumps are concerned, distinguishing between them on the basis of different systems of heat supply and removal is justified.

#### 1. Generator Circuits

The circuits of generators where the hot junctions are heated by combustion products are shown in Figure 5. Heat is delivered to the hot junctions by convection from a gaseous flow of combustion products or an organic fuel. These circuits are distinguished by the methods used to create temperature drops at the junctions and the dissipation of heat from the cold junctions of the generator.

Devices which are made as shown in the diagram of Figure 5 a, in

which the heat is dissipated by free convection from a finned surface on the cold junctions, are usually employed in difficult access localities where it is impossible to constantly monitor their operation. In particular, they can be utilized for cathodic protection of gas and oil pipe lines, located at points distant from population centers. Under these conditions, the power efficiency of the power source does not play a substantial part, since there is very cheap fuel available for combustion in the burner device of the generator, while the dominant factor becomes the reliability for extended operation of the device without maintenance.

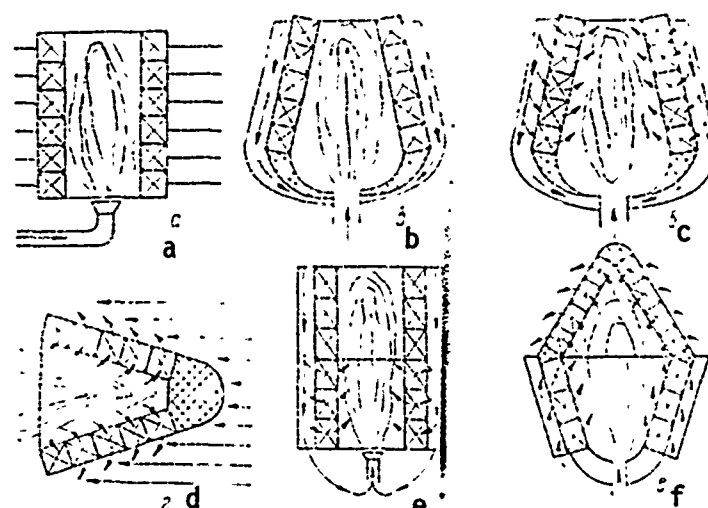


Рис. 5. Схемы генераторов с обогревом горячих спаев продуктами сгорания.

Figure 5. Diagrams of generators where the hot junctions are heated by combustion products.

A generator fabricated in such a fashion will have a very low efficiency. In the general case, the efficiency of any generator where the hot junctions are heated by combustion products, is determined from the following expression:

$$\eta = \frac{N}{8Q_p^H},$$

where  $N$  is the useable electrical power developed by the generator;  $B$  is the fuel consumption;  $Q_p^H$  is the heat generating capacity of the burned fuel.

It is well-known [6], that the useful electric power taken from the generator terminals, depends on the properties of the thermoelectric materials employed,  $z$  and  $\lambda$ , the battery dimensions,  $\delta$  and  $F$ , the temperature drop across the junctions  $\Delta T$  and the ratio of load resistance to internal resistance  $m$ , i.e.:

$$N = \frac{z\lambda m}{\delta(m+1)^2} \Delta T^2 F [8m].$$

It is apparent from this, that for a given material the determining factor is the temperature drop across the junctions, for which the developed electrical power varies as the square. The creation of the maximum possible temperature drops across the battery junctions is conditioned in the usual case by two such factors: the maximum achievable working temperature of the hot junctions which is limited by the properties of the semiconductor thermoelectric material which is used, and the rate of heat dissipation from the cold junctions. In this case, it is hypothesized that a heat flow density necessary to maintain to maximum temperature of the hot junctions for any cooling rate of the cold junctions can be assured from the hot side of the thermobattery. The required heat flow density in the burning region can be achieved by changing the fuel expenditure and the excess oxidate ratio, as well as by creating optimum aerodynamic conditions for a high heat-exchange rate. Naturally, when cooling the cold junctions by free convection into the surrounding medium, it is impossible to assure the removal of large quantities of heat because of the very low heat transfer coefficients under these conditions. This means that it is impossible to achieve any kind of



large temperature drops across the junctions. For this reason, in designs based on the drawing shown in Fig. 5 a, the useful power derived per unit surface of the thermobattery is usually very small. An external view of one of the first Soviet generators, the TGG-10, which was fabricated along the lines of the diagram shown in Fig. 5 a, is shown in Fig. 6. This generator developed a useful power of 10 - 12 watts at a current level of 1 amp [4].

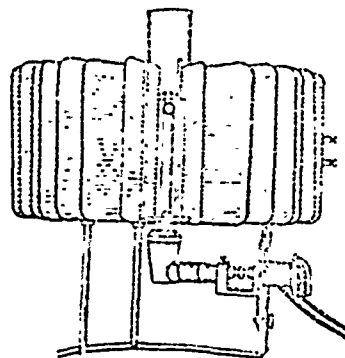


Figure 6. The TGG-10 generator.

The efficiency of devices operating on combustion products are still rather low at the present time, primarily for two reasons. In the first place, all of the heat derived from the cold junctions is dissipated into the surrounding medium and lost without serving any purpose, and, in the second place a substantial amount of heat is lost with the exhaust gases. While it still might be possible to deal with the first heat loss somehow by effecting heat regeneration (see Fig. 5 b), the matter is more complicated in the case of heat losses with the exhaust gases.

The combustion products leave the thermoelectric device with a temperature exceeding that of the hot junctions. Such a situation exists in all of the designs produced at the present time (see Fig. 5 a and b), as well as in the circuits shown in Fig. 5 c and d which have not yet been considered. The heat which is lost with the exhaust gases in generators running on organic fuels appears to be basic for determining their low efficiency.

For the case where the branches of the thermocouples are fabricated from high-temperature thermoelectric materials, the combustion products leaving

the device have a high temperature and can be used in any other heat utilizing device as a working medium. In this case, the generator plays the part of a high temperature addition to the basic cycle increasing its power efficiency. The overall efficiency of such a combined cycle is determined according to the following relationship [27]:

$$\eta_k = \eta_0 + \eta_\tau \psi (1 - \eta_0),$$

where  $\eta_0$  is the efficiency of the basic cycle;  $\eta_\tau$  is the efficiency of the high temperature addition (efficiency of the generator);  $\psi$  is the coefficient equal to the ratio of the heat delivered to the generator, to the heat transferred directly to the additive cycle.

When a generator is used as a high temperature addition to a cycle which has an efficiency commensurate with its efficiency, the efficiency of the combined cycle can be increased almost two times. This will be the case when a high temperature generator is utilized jointly with a low temperature one.

The structural diagram of a generator intended for operation using organic fuel and fabricated according to the diagram with recovery of the heat which is removed from the cold junctions (see Fig. 5 b) is shown in Fig. 7. This generator which was developed in the USA can be made with a variety of useable electric power levels [16]. The design of such a generator provides for the possibility of utilizing any liquid organic fuel. The liquid fuel is located in a fuel tank under excess pressure. When the generator is operating, it is fed through a line into the carburetion chamber. Upon the evaporation of the fuel in the carburetion chamber, air is sucked in there from the surrounding medium through an inlet opening, and a gas-air mixture is formed in the chamber which is then fed into the combustion chamber.

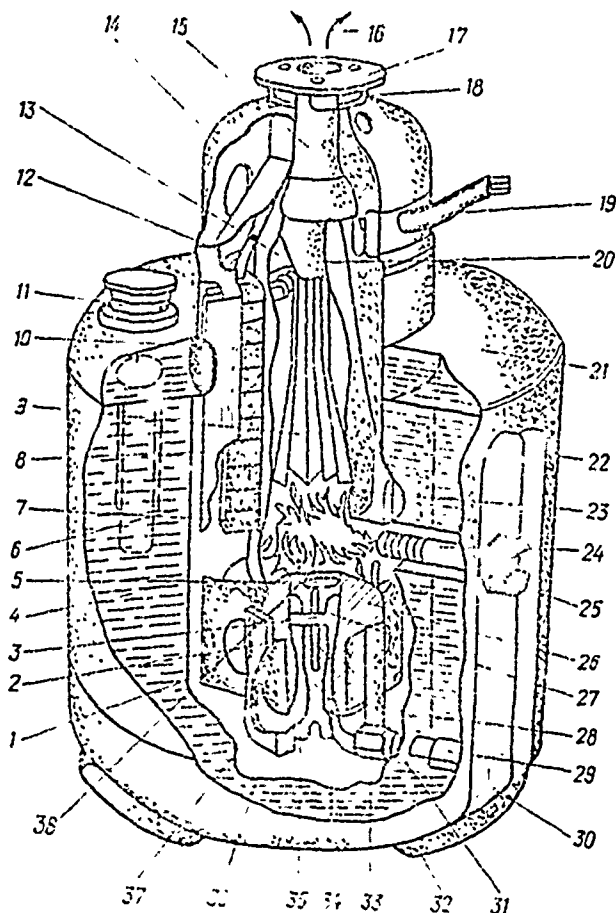


Figure 7. The construction of a typical generator which operates on liquid fuel:

- |                           |  |
|---------------------------|--|
| 1. Stiffening ribs;       | 20. Profiled cone;                     |
| 2. Ejector;               | 21. Fuel container;                    |
| 3. Radial fuel channels;  | 22. Frame cowl;                        |
| 4. Liquid fuel;           | 23. Combustion chamber cowl;           |
| 5. Axial fuel valve;      | 24. Igniter;                           |
| 6. Thermobatteries;       | 25. Ignition device;                   |
| 7. Carburetion chamber    | 26. Bottom of the carburetion chamber; |
| 8. Cooling surface;       | 27. Annular fuel line;                 |
| 9. Combustion chamber;    | 28. Air flow channel;                  |
| 10. Heating surface;      | 29. Nozzle;                            |
| 11. Fuel pump;            | 30. Frame;                             |
| 12. Air outlet opening;   | 31. Fuel line;                         |
| 13. Flow mixer;           | 32. Supports;                          |
| 14. Housing;              | 33. Regulating valve;                  |
| 15. Exhaust pipe;         | 34. Fuel flow channel;                 |
| 16. Exhaust opening;      | 35. Ejection channels;                 |
| 17. Cap;                  | 36. Air inlet opening;                 |
| 18. Flange;               | 37. Air cavity;                        |
| 19. Current output leads; | 38. Bottom of the combustion chamber.  |

Heat is delivered to the hot junctions of the thermocouples from the combustion products using fins which are mounted on the combustion chamber surface. The finned surface of the cold junctions is cooled by air which is circulated by the pressure difference between the inlet and outlet openings, which is created by the venturi action of the exhaust gas flow. A partial recovery of the heat removed from the cold junctions of the generator is realized by transmitting it through the cooling surface and the wall of the fuel container to the fuel.

Diagrams of generators which differ in principle from those made at the present time in the method of creating a temperature drop at the junctions are shown in Figures 5 c and d.

As has been noted in Chapter I, the thermocouples of such generators should be permeable to the blow-through of a substance in a direction from one of the junctions to another. When a device based on the diagram shown in Figure 5 c is operated, the cooling medium blowing through the permeable thermocouples and which in removing the heat within the thermocouples creates a temperature drop across their height, upon exiting the surface of the hot junctions mixes with the heating flow. On the other hand, in a device which operates according to the diagram shown in Figure 5 d, the hot gas blowing through the thermocouples transmits the heat within them and having created a temperature drop across the junctions exits the surface of the cold junctions and mixes with the cooling flow.

The primary distinction between these systems and those now being made consists in the fact that the basic quantity of heat is supplied (removed) not through the surfaces of the hot (cold) junctions, but within the thermo-

couples through their highly developed internal heat exchange surface.

As noted above, owing to the characteristics of heat exchange in finely porous or capillary systems, the heat from the ventilating current is transmitted to the material of the thermocouple branches (or vice versa) with an insignificant difference in the temperatures of the heat-exchanging medium, i.e. almost thermodynamically reversibly. This implies that within the thermocouples, the temperatures of the material and the ventilating substance will be the same or very close to one another over their entire height. The temperature profiles in the blow-through systems and their influence on the power characteristics of thermoelectric devices will be considered in subsequent chapters.

The fabrication of permeable thermocouples from many thermoelectric semiconductor materials will present no particular difficulties in comparison with the fabrication of monolithic thermocouples from the same materials.

The technology of stamping finely porous permeable samples is well worked out for a whole series of both metallic and metallic-ceramic materials and requires only finishing work for many semiconductor thermoelectric alloys. It is apparent from operational experience that the creation of permeable thermocouple branches is a completely resolvable problem. The greatest complexity in the creation of finely porous batteries is offered by the solution of the problem of series parallel connection of the branches of the thermocouples while preserving the permeability of the interconnected surfaces.

In considering the expediency of using permeable thermocouples from the point of view that there is an inadequately developed technology for their fabrication at the present time, it should be noted that permeability can be created using not only the methods of powder metallurgy but also other

methods. For example, permeable thermocouples can be obtained by means of electrochemical or electric arc drilling of sufficiently small diameter openings in monolithic thermocouples which are manufactured in accordance with a well-known and well-developed technology. The electrode with which the openings are made can be fabricated in the form of a comb which permits the simultaneous piercing of a set number of openings. Such a method of creating permeability is entirely justified when working with comparatively soft thermoelectric materials. Thermoelectric modules consisting of five p - n pairs, whose branches are made from thermoelectric semiconductor materials on a Bi, Te and Se base are shown in Fig. 8. In each square

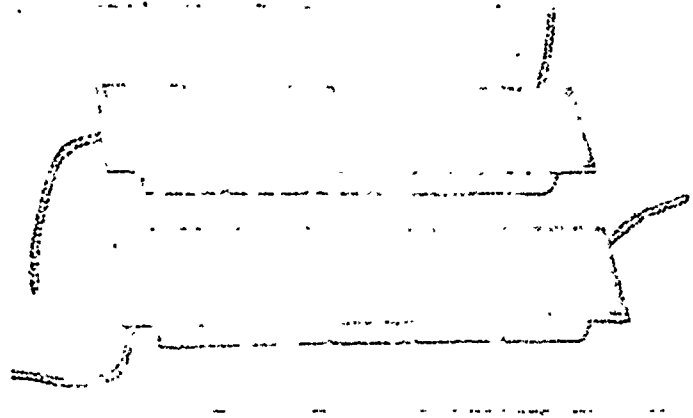


Figure 8. Thermoelectric modules with permeable thermocouples.

centimeter of the material of the branches in these modules, there are fifteen openings with a diameter of 0.45 - 0.55 mm. The divergence in hole diameters is explained by the fact that the tungsten electrodes of the comb were not ideally even and parallel with respect to each other.

For hard, difficultly fuseable materials (for example silicide), electric arc processing requires a lot of time, and for this reason this method is little used for the fabrication of a large number of holes. Therefore, thermocouples of refractory thermoelectric materials can be manufactured using the method of drop casting or press forming a powder. At the present time, test samples of perforated thermoelectric modules of high-temperature materials have been obtained using the manufacturing methods of press-forming powder metallurgy. Thermocouples can likewise be obtained by sintering previously pressed small-diameter rods or pipes or by other methods.

The diagram shown in Figure 5 c permits complete recovery of the heat removed from the cold junctions of the battery as does the diagram of Figure 5 b, however it has a large number of advantages in comparison with the latter.

In the operation of a generator in accordance with the second diagram, the temperatures of the heating and cooling currents, and thus the temperatures of the junctions, will change sharply along the length of the generator. Additionally, for the case of convective heat delivery to the hot junctions and convective cooling of the cold junctions, significant parasitic temperature drops exist both at the hot side of the thermobattery (between the heating flow and the hot junctions), and at its cold side (between the cold junctions and the cooling flow). Fin cooling of the junctions is employed to reduce these temperature differences, which makes the construction of the generator significantly more complex and difficult. This hinders the possibility of more or less completely utilizing the maximum temperature head, between the initial temperature of the heating gas and the temperature of the cooling substance at the inlet to the device.

The circuit shown in Figure 5 c makes it possible to eliminate a substantial number of the defects of the circuit shown in Figure 5 b.

In the first place, when using permeable thermocouples such operational modes are possible that sufficiently large velocities of the blow-through medium assure equal or almost entirely equal cold junction temperatures and coolant temperatures. Consequently, it is possible to almost completely exclude a parasitic drop in temperature at the cold side, which maintains the temperature of the cold junctions of the battery constant over its entire length and close to the temperature of the cold source. For example, this is possible by sectionalizing the delivery of the cooling medium, when the length of the sections is chosen in such a fashion that the coolant does not have time to warm up in the cooling canal by the time it reaches the inlet to the capillaries at the side of the cold junctions.

Secondly, either an oxidizer or a fuel can be employed in such a generator as a cooling medium which is blown through the permeable thermocouples. The oxidizer (fuel) which is fed in along the length of the generator also makes it possible to maintain the temperature of the hot junctions nearly constant over the length of the generator, i.e., as calculations show, at a quite significant distance from the combustion chamber (from the first thermocouples). This is achieved by gradually burning up the fuel in the oxidizer injected through the thermocouples, or vice versa, by burning the fuel which is blown through the thermocouples, in the current of the oxidizer which is fed in surplus over the first thermocouples.

Despite the difficult conditions of heat supply to the hot junctions (see Chapter I), the circuit considered here yields the maximum temperature



drop at the junctions, most completely utilizing the temperature head established between the hot and cold heat sources.

In such a fashion, under ideal conditions the circuit considered here can assure constant temperatures for the heating and cooling currents over the entire length of the battery while preserving the maximum temperature drops at the junctions. In this case, the cooling medium consumption necessary for creating the same temperature drops at the junctions of the circuit of Figure 5 c is incommensurably smaller than is the case for the operation of the circuit shown in Figure 5 b, even when finned cooling of the cold junctions of the batteries is present in the latter circuit.

A comparison of the power parameters of devices based on the circuits shown here when they are used as a high-temperature addition to some thermal cycle (the consumption and parameters of the hot gas input flow are given) shows that the circuit of Figure 5 c assures a significantly greater useful electric power, other conditions being equal. A more detailed analysis of the operation of a generator made according to the diagram shown in Figure 5 c will be set forth in the following chapter.

If in the circuit of Figure 5 c the temperature drop across the junction of the battery is created by blowing coolant from the cold junctions to the hot ones (against the heat flow), then in the circuit of Figure 5 d, the temperature drop at the junctions is created by blowing the heat carrier in the opposite direction. In devices which are built based on such a heat circuit, the high temperature combustion products blow through the permeable thermocouples from the hot junctions to the cold ones, and in giving up their heat within the material of the thermocouples create the conditions for

normal generator operation at a sufficiently high rate of heat removal from the surface of its cold junctions. Owing to the high rate of heat exchange on the hot side when heating gas enters the capillaries, these circuits make it possible to have the temperature of the hot junctions approach as closely as possible the temperature of the hot source. If the combustion products flowing across the first thermocouples of the generator have the same temperature, then the temperature of the hot junctions can be maintained constant along the length of the generator where hot gas is delivered to the thermocouples either sectionally (as in the cooling case) or from a closed volume perpendicular to the hot junctions. Such a circuit permits maximally utilizing the temperature possibilities of the heat carrier. A generator based on this circuit, is suitable for application as a device which utilizes the heat of the exhaust gases of any heat-using device. In particular, the utilization of such a device as a second-stage generator which is made based on the circuit of Figure 5 c yields a significant increase in the efficiency of the thermal cycle of this device (see Figure 5 f) [27].

In contrast to all of the circuits considered above, the circuit in Figure 5 d makes it possible to reduce to a minimum the loss of heat with exhaust gases. In fact, owing to the high rate of heat exchange within the thermocouples, real conditions can be created to assure that the heat carrier exits the cold side of the junctions at a temperature close to the temperature of the cold junctions. For this reason, the heat carrier will leave the device at a temperature close to the temperature of the surrounding medium given a sufficiently high internal cooling rate for the cold junctions.

Combined generator heat circuits are shown in Figures 5 e and f. The

circuit shown in Figure 5 e represents two generators based on the circuits of Figure 5 b and c and co-located in one independent unit. The first high-temperature stage of such a generator makes it possible to obtain the maximum possible temperature drop for the given conditions at the junctions by injecting fuel through the permeable thermocouples and gradually burning it in an oxidizer fed in excess to the input. The second stage of the device under consideration, the low temperature one, utilizes the exhaust heat from the first stage combustion products and increases the overall efficiency of the plant.

The circuit of Figure 5 f is most efficient in generators which run on organic fuel. It permits the operation of both generator stages while realizing the maximum possible temperature drop at the junction and in this case, reduces the heat losses from the side of the cold junctions and the losses with the exhaust gases to a minimum.

A more detailed analysis of the operation of circuits having permeable thermocouples (of this and the others described above), as well as the procedure for computing them will be set forth below.

Circuits of generators with nuclear reactor and radioisotope heating of the hot junctions are shown in Figure 9.

The circuits depicted in Figures 9 a and b are distinguished from the generator circuits using combustion products for heating which were considered above (see Figures 5 a and b) only by the method of heat delivery to the hot junctions. In this case, the hot junctions are heated by direct thermal contact with the heat-radiating surface. In these circuits, either an external nuclear reactor jacket or a capsule containing radioisotope fuel can be

considered as a heat-radiating surface. Circuits in which the utilization of heat which is liberated during the fission reaction of radioactive substances, is proposed for heating the hot junctions of thermocouples, have the same drawbacks as the analogous systems using combustion products for junction heating which were described above.

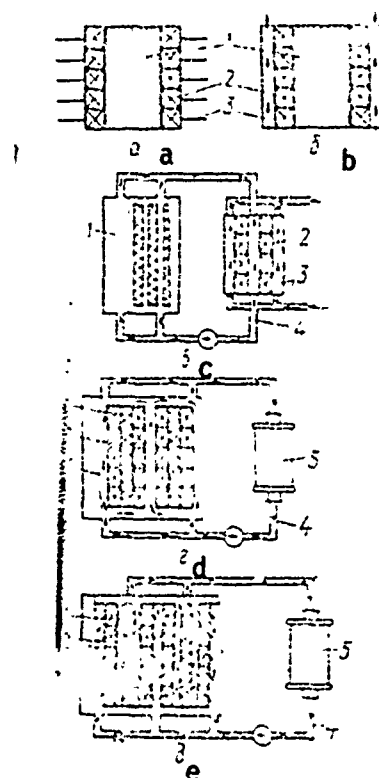


Рис. 9. Схемы генераторов с ядерно-реакторным и радиоизотопным нагревом.

Figure 9. Generator circuits with nuclear reactor and radioisotope heating:

1. The heating surface;
2. Thermocouples;
3. System for cooling the cold junctions;
4. Heat carrier loop;
5. Heat exchanger.

The circuit shown in Figure 5 b is most suitable when a device is employed where there is cold water for creating a large temperature drop at the junctions (for a high rate of heat removal from the cold junctions of the thermocouples). Such a circuit has been realized in a rather large number of generator designs for sea duty. The sea-going power system which was based on the SNAP-10 nuclear reactor intended for service in the space program can serve as an example. This system provides an electrical power of around 350 watts from 100 thermocouples.

In this device, the thermocouples are situated between the external surface of the reactor and the internal frame of the power plant. Heat dissipation from the cold junctions of the batteries is effected using thermal conductivity through the wall of the external frame into the ocean medium [33]. At the same time, a power system for space service based on the same reactor (Figure 9 a) where heat was dissipated by radiation from finned cold junctions, yielded a useful electrical power of only 250 watts.

The circuit of Figure 9 c is also rather widely used in the development and fabrication of thermoelectric devices for both space and sea-going service. The SNAP-10A thermoelectric system (Figure 9 c) functioned in a near-earth orbit at an altitude of 1300 km for 43 days in 1965, generating a useful power of more than 500 watts during initial operation (up until an accident). A schematic of the operational cycle of this plant is shown in Figure 10. Heat from the active region of the reactor is transmitted to the hot junctions of the thermocouples by a liquid metallic heat carrier, NaK-78. The given generator is made up of 2880 thermocouples, consisting of germanium - silicon alloys. Heat from the cold junctions in this circuit is likewise removed by

an intermediate heat carrier, which is cooled in the heat exchange radiator. The surface of the heat exchange radiator was  $5.8 \text{ m}^2$  at an average temperature of  $597^\circ \text{ K}$  [31, 34]. Thermoelectric converters for sea-going service having a useful electric power of 500 - 2000 watts were developed on the basis of this same nuclear system. Eutectic sodium - potassium was used both for delivering heat from the reactor to the hot junctions of the generator and for removing heat from the cold junctions to the heat exchanger which was cooled by sea water [33]. This system has successfully undergone a long period of testing.

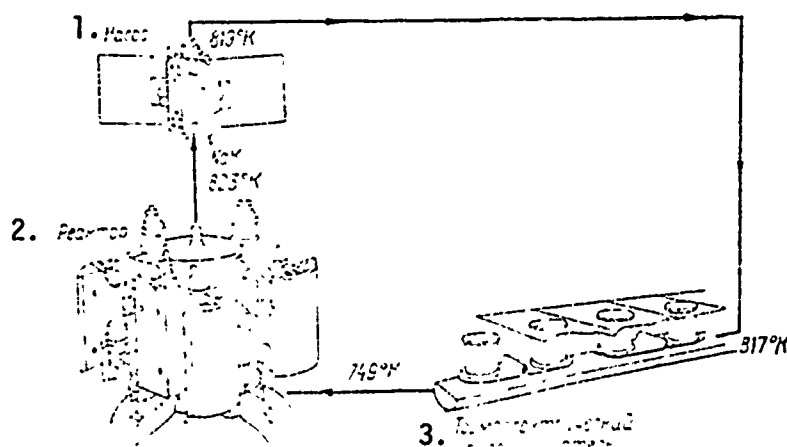


Figure 10. Diagram of the operational cycle of the SNAP-10A power plant.

1. Pump;                      2. Reactor;                      3. Thermoelectric converter.

A substantial advantage of the circuit depicted in Figure 9 c is the fact that the intermediate heat carrier serves as additional radiation shielding for the thermoelectric semiconductor materials. This makes it possible to somewhat increase the number of materials capable of operating

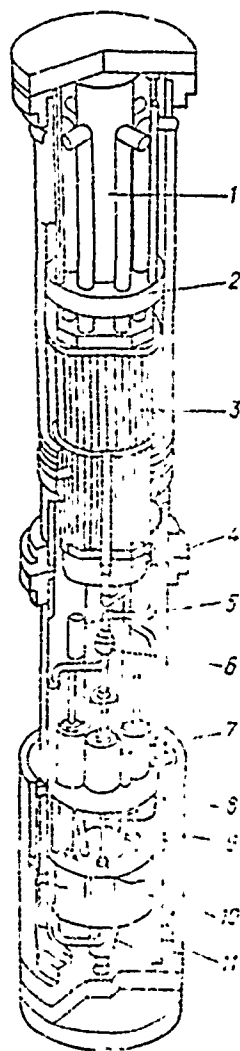
from a nuclear heat source. However such a system makes the utilization of high-temperature materials more difficult insofar as at the present time there is no adequate high-temperature heat carrier which meets the specific requirements for operation with nuclear power plants.

The deep sea device of "Neptune" system having an electrical power of 15 kw was designed on the basis of the circuit of Figure 9 c and is shown in Figure 11. The most technologically developed basic components of the SNAP-10A, SNAP-8, and SNAP-2 systems which were intended for space service are combined in the device [33]. The heat power of the nuclear system is 400 kw at a temperature in the active region of 938° K. The nuclear reactor is situated in the lower part of the device. The drive motors for the rods are located above the reactor and separated from its framework by shielding. The generator which consists of 12,000 elements of lead telluride is located in the central section of the power plant. Heat to the hot junctions of the thermocouples is supplied by liquid NaK-78 which is heated in the active region of the reactor from 700 to 938° K, while the heat from the cold junctions to the radiator is carried by boiling water which is circulated by its own natural forces. Heat is removed from the surface of the radiator by the surrounding sea water.

Generators can be made more compact where nuclear reactors are used for heating and the thermocouples are situated in the active zone directly on the heat emitting elements.

The circuits of such converters which are shown in Figure 9 d, in contrast to the circuits of Figure 9 c make it possible to avoid excess heat losses by the heat carrier in the piping, which connects the nuclear reactor with the

generator. Additionally, the indicated circuits offer the possibility of utilizing high-temperature thermoelectric materials. However, in the design of thermoelectric devices based on this circuit, particular attention should be given to the radiation resistance of the thermoelectric materials, insofar as under these conditions they will be operating without radiation shielding.



1. Instrument compartment;
2. Heat shielding;
3. Thermoelectric generator;
4. Water shielding;
5. Expansion compensator;
6. Pump;
7. Control rod drives;
8.  $\gamma$  radiation shielding;
9. Support shell;
10. Reactor;
11. Biological shielding.

Figure 11. Thermoelectric device of the "Neptune" system:



The circuit of Figure 9 e is distinguished from the heat circuit of Figure 9 d by the means which are used to create a temperature drop at the generator junctions and supply heat to the hot junctions. In the circuit of Figure 9 d, the heat carrier removes heat at the surface of the cold junctions and exits the boundaries of the active region of the reactor at a temperature somewhat lower than the temperature of the cold junctions. Heat is supplied to the hot junctions of the thermocouples from the jacket of the reactor heat-emitting elements.

In the circuit of Figure 9 e, provision is made for utilizing permeable thermocouples in the generator construction; at the junctions of these thermocouples a temperature drop is created by the blow-through of the heat carrier from the cold junctions to the hot ones. Taking the heat from within the thermocouples, the liquid or gaseous heat carrier exits into the space between the hot junctions and the jacket of the heat-emitting element, at a temperature somewhat lower than (or equal to) the temperature of the hot junctions. The heat carrier is heated up in the gap, contacting the jacketing of the heat-emitting elements, which are at a higher temperature; the heat carrier leaves the reactor boundary at a temperature equal to or greater than the temperature of the hot junctions. In this case, the heat to the hot junctions is supplied by convection from the jacket of the heat-emitting elements and by therm conductivity via the liquid metallic heat carrier or by convection and radiation when a gaseous heat carrier is employed.

It is apparent from a comparison of these two circuits, that in the circuit of Figure 9 e, all other conditions being equal, the utilization of heat from the hot source will be greater than in the circuit of Figure 9 d, since the heat carrier is heated to a higher temperature. However, this does not

mean that the efficiency of the device based on the circuit shown in Figure 9 e will be notably less than a device based on the circuit depicted in Figure 9 d. This should be considered in connection with the conditions of heat dissipation into the surrounding medium from the surface of the heat exchange cooler, which is delivered there with the heated heat carrier and should be dissipated prior to its being fed back into the nuclear reactor.

If heat from the surface from the heat exchanger is dissipated by either natural or forced convection, then the circuit of Figure 9 e has no advantages over the circuit of Figure 9 d, insofar as during an increase in the temperature head between the surface of the heat exchanger and the cooling medium, the quantity of heat which has to be dissipated increases. The linear relationship between the quantity of heat dissipated in the heat exchanger and the difference in temperature between the heat radiating surface and the cooling medium (in accordance with Newton's law)  $Q = \alpha F (T - t)$  does not permit a reduction in the surface of the heat exchanger or an increase in the degree of cooling of the heat carrier.

When heat is dissipated by radiation, the quantity of heat removed from the surface of the heat exchanger depends on the 4th power of its surface temperature (see (9)). Under these conditions, the circuit shown in Figure 9 e exhibits substantial advantages. The feed of the heat carrier into the heat exchange radiator at a temperature exceeding the temperature of the hot junctions of the generator, makes it possible to reduce its surface, or for the same surface, cool the heat carrier to a lower temperature, which in turn makes possible a greater temperature drop at the junctions of the generator.

An investigation of the parameters of refrigerator radiators which is

described in the literature [24], has shown that for liquid heat carriers, the dependence of the surface area of the refrigerator on the quantity of dissipated heat and the temperature of the heat carrier,  $T_{in}$ , at the input to the heat exchanger and at its output,  $T_{out}$ , has the form:

$$F = \frac{0}{\varepsilon \sigma} \cdot \frac{1}{3T_{out}^4} \cdot \frac{\left(\frac{T_{in}}{T_{out}}\right)^3 - 1}{1 - \frac{T_{out}}{T_{in}}}$$

Consequently, the circuit shown in Fig. 9 e permits an improvement in the size and weight characteristics of the power plant for the same electrical power by reducing the dimensions of the cooler radiator where the heat carrier is fed into it at a higher temperature than in the circuit of Fig. 9 d, and conversely, for the same surface areas of the heat exchange radiator in a device based on the circuit of Fig. 9 e, it is possible to obtain a greater useable electric power (a greater temperature drop at the junctions) than in the circuit of Fig. 9 d because of the more extensive cooling of the heat carrier. The comparison of the power efficiency of these thermal circuits requires more detailed and concrete calculations.

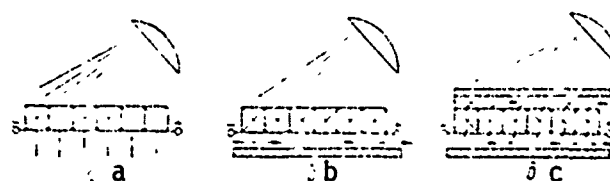


Рис. 12. Схемы генераторов с солнечным нагревом.

Figure 12. Diagrams of generators with solar heating.

The circuits of generators where the hot junctions are heated by radiant energy from the sun are shown in Fig. 12 and are differentiated

according to the methods used to create temperature drops across the thermocouple junctions. In all of these circuits, heat is delivered to the hot thermocouple junctions in the form of radiant solar energy. For this purpose, in units intended for ground service using such generators, devices for concentrating solar radiation are usually employed in view of the inadequate thermal density of solar radiation per unit of the earth's surface.

The heat which is removed from the surface of cold junctions of generators based on the circuits of Fig. 12 a and b is completely lost. It cannot be recovered due to the specificity of the heat energy source. The use of a heated cooling agent in any other heat utilizing devices is likewise inexpedient, insofar as it is at a low temperature, lower than the temperature of the cold junctions of the generator, which naturally has a negative effect on the efficiency of solar plants. However, for these devices which have a heat energy source "free of charge", the magnitude of the efficiency does not play such an important role as it does in generators having other heat sources for heating the hot junctions.

A more important factor determining the practicability of obtaining electrical energy using solar generators is their cost. The working out of technological processes for fabricating solar thermoelectric plants is in many respects connected with this cost reduction for devices to focus the radiant energy of the sun, and strictly speaking the further development of semiconductor batteries will permit their wider application in regions having a large number of days of sunshine.

A large number of generators with solar heating based on the circuits of Fig. 12 a and b have been fabricated and tested at the present time.

They are designed to obtain useful electrical powers of up to several tens and even hundreds of watts [3].

A solar generator which uses reflectors for concentrating solar energy, characteristically has a non-uniform distribution of thermal currents (including temperature) at the surface of the hot junctions of the semiconductor thermocouples. In this case, the thermal operational modes of the thermocouples in the battery vary, which has a negative effect on its overall efficiency. The non-uniformity in the heating of the hot junctions in many designs achieves rather large magnitudes, even hundreds of degrees. However, as noted in the literature [15], for some thermoelectric materials the heating non-uniformity can not only reduce the efficiency of generator operation, but can also somewhat increase it due to a further increase in operational efficiency of some thermocouples at temperatures varying from the design average. This circumstance is completely determined by the temperature dependence of the figure of merit,  $z$ , of the thermoelectric materials employed. If the quantity  $z$  increases with an increase in the temperature of the hot junctions, then the conversion efficiency grows in comparison with the operational efficiency of the device for the case of uniform heating, due to an increase in the temperature of the hot junctions for the average number of thermocouples determined by the generator design. When materials are used where the figure of merit varies inversely as the temperature, a non-uniformity in the thermal flow on the hot junction side causes a reduction in generator efficiency.

The effort to assure uniform temperature conditions in the battery thermocouples led to the creation of solar generators having thermocouples

of various heights and generators where each thermocouple was heated with its own concentrating reflector.

When the circuit of Fig. 12 c is employed, it is possible to obtain a coolant at a significantly higher temperature than in the circuit of Fig. 12 a and b, which provides for the possibility for its further effective utilization in other devices or in other stages of the generator. As has been noted above, in designs using permeable thermocouples, the coolant exits the surface of the hot junctions at a temperature close to the temperature of the junctions. In such a fashion, a generator based on such a circuit makes it possible to simultaneously obtain useful electrical power using solar energy and a hot heat carrier for further utilization.

## 2. Circuits of Refrigerators, Conditioners and Heat Pumps

In thermoelectric heating and cooling devices, the temperature difference at the hot and cold junctions of the thermocouples is created by the Peltier effects, which are manifested with the action of the flowing electrical current. In these devices, the DC power source is a component of the thermal circuit, analogous to the energy heat source in generators.

If the sources of heat energy define the various thermal circuits of generators, then the circuits of thermoelectric heating and cooling devices are expediently classified only from the point of view of the differences in the systems for supplying and removing heat.

Specific demands (see chapter I) are made on the DC power sources in order to assure normal operation of the device. In the analysis of the circuits of coolers, heaters and conditioners, the investigation of the influence of the type and characteristics of the power source on the other

circuit elements is of no interest so long as it meets all the necessary requirements. Consequently, the circuits of these devices are to be distinguished primarily according to the methods of supplying and removing heat from the junctions - radiation, convection (natural and forced) and heat exchange within the permeable thermocouples.

Possible circuits of coolers, heater and conditioners are shown in Fig. 13.

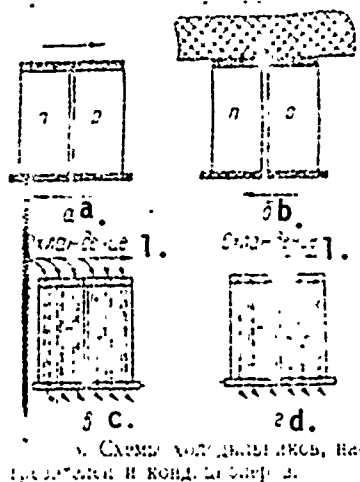


Figure 13. Circuits of refrigerators, heaters and conditioners.

#### 1. Cooling

Systems for supplying and removing heat by radiation are not used in practice in view of the low operational temperatures of the hot or cold junctions of these devices. Heat dissipation from cold junctions by radiation is achieved for practical purposes in thermoelectric refrigerators for space vehicles.

In the existing conditioner and cooler designs, the most widespread method of heat delivery and removal uses a convective gaseous or liquid flow across finned junctions. In this respect, batteries are classified

according to the nature of heat removal in the battery: of the type air - air, liquid - liquid, and a combined, liquid - gas. Batteries of all of these types operate according to the circuit shown in Fig. 13 a. Fins of various types are employed to increase the rate of the heat transfer process at the hot and cold junctions of such devices.

In some cases, the heat removal from the hot junctions or the heat supply to the cold junctions in refrigerating devices is accomplished not by means of convection at finned surfaces, but by means of contact heat exchange with a cooled or heat-absorbing surface. Such refrigerators are sub-classified into the mass - mass and mass - air types.

The circuit of a thermocouple in which heat exchange at one of the junctions is realized using convection with the surrounding medium, while at the other by contact heat exchange with the mass of the body, is shown in Fig. 13 b.

The basic circuit of a refrigerator shown in Fig. 14 corresponds to the circuit shown in Fig. 13 a [2]. In such a refrigerator which is intended for operation in a vehicle, heat is supplied to the cold junctions by the natural convection of the air contained in the cool volume. Heat is dissipated by the air flow washing over the hot junctions of the thermocouples. This design makes it possible to maintain temperature drops between the surroundings and the internal cooling volume of up to 298° K.

A diagram of a thermal battery module, the thermoelectric PTK-1 chamber, developed at the SKB semiconductor institute of the USSR Academy of Sciences, which is intended for the investigation of various devices is shown in Fig. 15 [25]. This module consists of two cascaded thermocouples and is capable of developing a cold productivity of 11 watts



where 453 watts of electrical power are consumed. Heat is delivered to the cold junctions of the thermocouples from the cooling volume via a finned surface, and heat is dissipated from the hot junctions to the body plate by contact heat exchange. To increase the rate of heat transfer in the plate, through perforations are made through which cooling water circulates. In this fashion, combined heat removal based on the circuits of Fig. 13 a and b is realized in this case.

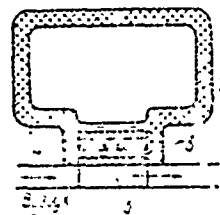


Рис. 14. Схем. авто-  
двигателя для автомо-  
биля.

Figure 14. Schematic of a vehicle air conditioner:

1. Heat insulation;
2. Refrigerating chamber;
3. Contact grease;
4. Heat conducting plate;
5. Cool air.

The circuits of permeable thermocouples in which the cooling medium blows through capillaries (pores) from the hot junctions to the cold ones, giving up heat to the material of the thermocouple branches over their entire height are shown in Fig. 13 c.

In permeable thermocouples, in contrast to monolithic types, heat is removed from the cooling medium not at the surface of the cold junctions,

but in the volume of the thermocouple. Heat can be dissipated from the surface of the hot junctions in two ways. When the cooling medium circulates in a closed loop, a device based on the circuit of Fig. 13 c is practicable. In this case, the cooling medium is fed into the thermocouples via channels made in the connecting plates of the hot junctions, while any other substance serves as a heat carrier for removing heat from the hot junctions.

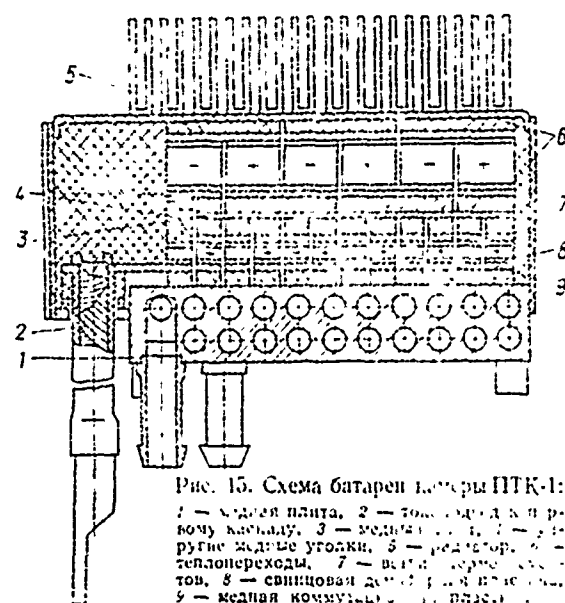


Figure 15. Schematic of the PTK-1 battery chamber:

1. Copper plate;
2. Current lead to the first cascade;
3. Copper leaf;
4. Flexible copper needles;
5. Radiator;
6. Thermal junctions;
7. Branches of the thermocouples;
8. Lead damping plate;
9. Copper connecting plate.

The operation of a permeable thermocouple using an open-ended circuit, shown in Fig. 13 d, is likewise possible when heat from the hot junctions is removed by the flow of a substance, some portion of which is sucked out through the permeable thermocouples being cooled.

The operation of permeable thermocouples cooled by medium flows will be considered in more detail in Chapter V.

### CHAPTER III

#### Features of Temperature Fields in Permeable Thermocouples

We will now consider in detail the principal distinctions in the delivery and dissipation of heat at the junctions of monolithic and permeable thermocouples.

Where permeable thermocouples are employed, the primary heat quantity is removed from or delivered to the material of the thermocouple branches not through the surface of the hot or cold junctions, but within the branches of the thermocouples. As has already been noted, the branches of thermocouples are made porous or perforated which causes them to have a highly developed internal surface. When a heat carrier or cooler is blown through such permeable thermocouples from one junction to another, the heat exchange process between the flushing substance and the material of the branches transpires at a very high rate. The enormously high rate of heat exchange under such conditions is achieved due to the extraordinarily developed heat exchange surface.

For finely porous pressed materials, the volumetric heat transfer

coefficients from the material of the wall to the gas blowing through the capillaries reach the order of  $10^5$  watts/m<sup>3</sup> x deg. In perforated walls with capillaries having a diameter of up to 1 mm, the heat exchange coefficients to the gas blowing through them can amount to 100 watts/m<sup>2</sup> · deg and more. In this case, the large heat exchange area makes it possible to transfer very large quantities of heat from the heat emitting surface to the heat absorbing medium, which determines the small temperature differences between the heat absorbing and heat emitting media, at which temperature the heat exchange takes place within the permeable thermocouples.

The temperature difference between the heat emitting surface and the heat absorbing medium during the heat exchange process determines the thermodynamic loss process. The smaller this difference, the greater are the losses as a result of the irreversibility of the heat exchange process. Consequently, in permeable thermocouples where the main quantity of heat is supplied (removed) within the thermocouples at a small temperature difference, this loss from the irreversibility of the heat exchange can be minimal.

Where heat is supplied (removed) through the surface of the junctions in monolithic thermocouples and the rate of heat exchange is not so significant, and the heat exchange surface is immeasurably smaller, the loss due to heat exchange irreversibility is large because of the high temperature heads between the heat exchanging media. Mounting fins on the junctions makes it possible to somewhat reduce such a loss. However, this is achieved at a substantial increase in construction cost and complexity.

The presence of internal heat exchange in permeable thermocouples introduces fundamental and important factors into their operation. In particular, a new possibility for influencing the power characteristics

of thermoelectric devices, the useful power (the temperature drop at the junctions) and the generator efficiency or the cold productivity and the cooling coefficient of refrigerating devices and conditioners is opened up.

As is well known [28], the temperature profile in the material of a monolithic thermocouple is described by the following equation:

$$T = T_1 + \frac{T_2 - T_1}{\delta} y + \frac{Q_v \delta}{2\lambda} y - \frac{Q_v}{2\lambda} y^2, \quad (10)$$

where  $Q_v$  is the internal heat generation in the material of the branches (Joule heating),  $\delta$  is the height of the thermocouple,  $\lambda$  is the thermal conductivity of the material of the branches (average for the p - n pair);  $T_2$  and  $T_1$  are respectively the temperatures of the hot and cold junctions.

It is apparent from the expression given above that the temperature profile has a non-linear character. The non-linearity of the temperature profile along the height of the thermocouple is determined by the magnitude of the internal heat generation. The Joule heat which is generated within the branches when the electric current flows through them, increases the excess heat flow to the cold junction and the temperature gradient, depending on the distance from the hot junction to the cold. In this case, less heat enters the thermocouple from the hot side than leaves it from the cold side. The difference in heat is equal to the Joule heat generated in the material of the branches when electric current flows through it.

It can be seen from equation (10) that the shape of the temperature profile in a monolithic thermocouple depends on the temperature drop at the surfaces, the height of the thermocouple, the heat conductivity of the material it is made from, and the magnitude of Joule heat generation.

However, in the case of a permeable thermocouple a significantly greater number of factors exert an influence on the shape of the temperature profile in the branches of the material. The direction of flow has the most influence: i.e., against the heat flow (from the cold to the hot junction) or in the direction coinciding with the heat flow (from the hot to the cold junctions). Additionally, the structure of the permeable material (finely porous or perforated) and the heat transfer coefficients within the branches also significantly change the shape of the profile.

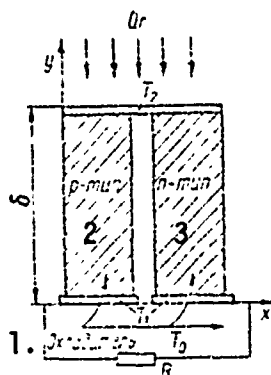


Figure 16.

Diagram of a permeable thermocouple.

1. Coolant,
2. p - type,
3. n - type.

When obtaining expressions for describing temperature profiles in permeable thermocouples, we will consider the thermocouple circuit shown in Fig. 16.

### 1. Method of Calculating the Temperature Fields

We will initially consider the case when a substance (gas, liquid) blows through the thermocouple directed from the cold to the hot junctions, i.e. in a direction contrary to the heat flow in the material of the branches. We will adopt the following basic symbols:  $T_2$  and  $t_2$  are respectively the temperature of the material and the blow-through medium at the hot side when  $y = \delta$ ;  $T_1$  and  $t_1$  are respectively the temperature of

the material and the blow-through medium at the cold side when  $y = 0$ .

The specific mass velocity of the blow-through medium,  $\rho v_w$  applies to the entire surface of the finely porous thermocouple and to the cross sectional area of the capillaries in the case of perforated thermocouples.

In investigating temperature fields in permeable thermocouples, in addition to the heat conducting processes it is necessary to consider the processes of convective heat exchange for the mass of the material of the branches and the blow-through medium fed through the surface of the pores or capillaries. This means that the temperature profiles in the material of the branches and in the blow-through medium will be closely interrelated within the boundaries of the thermocouple height.

We will consider the unidimensional problem of obtaining temperature profiles in the material of the branches and in the blow-through medium (see Fig. 16).

When the coolant is blown through the permeable wall it is heated up, extracting heat from the material of the wall. The coolant is heated due to the gain in the amount of heat passed by thermal conductivity

$$\lambda (F - F_{\text{nop}}) \frac{dT}{dy} - \left[ -\lambda (F - F_{\text{nop}}) \left( \frac{dT}{dy} + \frac{d^2T}{dy^2} dy \right) \right], \text{ из}$$

through an element of the wall,  $dy$ , and also due to the internal heat generated in this volume element (when electric current flows - the Joule heat), i.e.

$$\rho v_w c_p (F - F_{\text{nop}}) \frac{dT}{dy} dy + q_v (F - F_{\text{nop}}) dy, \quad (11)$$

where  $F_{\text{nop}}$  is the cross sectional area of the capillaries.

**THIS  
PAGE  
IS  
MISSING  
IN  
ORIGINAL  
DOCUMENT**



The constants A, B and C have a somewhat different form depending on the nature of the thermocouple material: porous or perforated.

From the equations introduced above, it is easy to find expressions for the determination of the temperatures of the material and the blow-through medium within the boundaries of the thermocouple height, having the determined the constants of integration from the conditions of temperature constancy for the material and the blow-through medium at its surface (where  $y = \delta$  and  $y = 0$ ). In this case we obtain the following expressions:

$$T = T_1 + ACy + (T_1 - t_1 - C) \frac{2B + A}{2B - A} \times \\ \times \left\{ \exp \left[ \left( B - \frac{A}{2} \right) y \right] - 1 \right\} + \\ + \left( \left( \frac{B}{A} + \frac{1}{2} \right)^2 \left\{ \exp \left[ \left( B - \frac{A}{2} \right) y \right] - 1 \right\} + \right. \\ \left. + \left( \frac{B}{A} - \frac{1}{2} \right)^2 \left\{ 1 - \exp \left[ - \left( B + \frac{A}{2} \right) y \right] \right\} \right) \frac{2AC_3}{2B - A}, \quad (16)$$

$$t = T_1 - C + ACy + (T_1 - t_1 - C) \frac{2A}{2B - A} \left\{ \exp \left[ \left( B - \frac{A}{2} \right) y \right] - \left( \frac{B}{A} + \frac{1}{2} \right) \right\} + \left( \left( \frac{B}{A} + \frac{1}{2} \right) \exp \left[ \left( B - \frac{A}{2} \right) y \right] + \right. \\ \left. + \left( \frac{B}{A} - \frac{1}{2} \right) \exp \left[ - \left( B + \frac{A}{2} \right) y \right] - \right. \\ \left. - 2 \frac{B}{A} \right) \frac{2AC_3}{2B - A}, \quad (17)$$

где  
where

$$C_3 = \frac{(T_2 - T_1 - AC\delta) \left( \frac{B}{A} - \frac{1}{2} \right) + \\ + (T_1 - t_1 - C) \left( \frac{B}{A} + \frac{1}{2} \right) \left\{ 1 - \exp \left( B - \frac{A}{2} \right) \delta \right\}}{\left( \frac{B}{A} + \frac{1}{2} \right)^2 \exp \left[ \left( B - \frac{A}{2} \right) \delta \right] - \\ - \left( \frac{B}{A} - \frac{1}{2} \right)^2 \exp \left[ - \left( B + \frac{A}{2} \right) \delta \right] - 2 \frac{B}{A}}. \quad (18)$$

For finely porous thermocouples where it is practically impossible to determine the heat exchange surface, the heat transfer coefficient,  $(\alpha_v)$ , characterizing the heat exchange per unit volume of material in the thermocouple branches is usually employed. For the case of perforated thermocouples, where the internal heat exchange surface can be determined relatively simply, the coefficient of heat transfer characterizing the transfer of heat through a unit surface of the capillaries is employed. When calculating the temperature fields based on the relationships given above, it is possible to employ these coefficients for heat transfer which take into account the various forms of the constants A, B and C.

The differential equations which describe the temperature profiles in permeable thermocouples, which are blown through in a direction coinciding with the direction of heat flow (from the hot to the cold junctions) and which are obtained by analogy with the expressions given above for the opposite blow-through direction [10], have the form

$$T = t - \frac{0.5 \alpha_v t_{\text{exp}}}{\alpha \pi d z_1} \cdot \frac{dz}{dy}, \quad (19)$$

$$\frac{d^2 T}{dy^2} - A \frac{dT}{dy^2} - \frac{\alpha_v d z_1}{\lambda (F - F_{\text{exp}})} \cdot \frac{dT}{dy} - \frac{\alpha_v A}{\lambda} = 0. \quad (19)$$

The general solution of this system can be presented in the following form:

$$T = C_1 - \left( \frac{B}{A} - \frac{1}{2} \right) C_2 \exp \left[ \left( B + \frac{A}{2} \right) y \right] +$$

$$+ \left( \frac{B}{A} - \frac{1}{2} \right) C_3 \exp \left[ - \left( B - \frac{A}{2} \right) y \right] - ACy + C, \quad (20)$$

$$t = C_1 - C_2 \exp \left[ \left( B + \frac{A}{2} \right) y \right] -$$

$$- C_3 \exp \left[ - \left( B - \frac{A}{2} \right) y \right] - ACy.$$

The constants of integration  $C_1$ ,  $C_2$  and  $C_3$  are determined from the boundary conditions for the temperature constancy of the blow-through medium and the material of the thermocouple branches at the surfaces of the junctions (where  $y = \delta$  and  $y = 0$ ). In this case, the expressions which describe the temperature profile for the indicated direction of flow, take the form:

$$T = T_1 - ACy + \frac{2B - A}{2B + A} (T_2 - t_2 - C) \frac{\exp\left[\left(B + \frac{A}{2}\right)y\right] - 1}{\exp\left(B + \frac{A}{2}\right)\delta} +$$

$$+ \left(\left(\frac{B}{A} - \frac{1}{2}\right)^2 \exp\left[-\left(B - \frac{A}{2}\right)\delta\right] \times\right.$$

$$\times \left\{1 - \exp\left[\left(B + \frac{A}{2}\right)y\right]\right\} - \left(\frac{B}{A} + \frac{1}{2}\right)^2 \exp\left[\left(B + \frac{A}{2}\right)\delta\right] \times$$

$$\times \left\{1 - \exp\left[-\left(B - \frac{A}{2}\right)y\right]\right\} \left. \frac{2AC_1}{(2B + A) \exp\left(B + \frac{A}{2}\right)\delta} \right. \quad (21)$$

$$t = T_1 - C - ACy - (T_2 - t_2 - C) \frac{\left(\frac{B}{A} - \frac{1}{2}\right) + \exp\left(B + \frac{A}{2}\right)y}{\left(\frac{B}{A} + \frac{1}{2}\right) \exp\left(B + \frac{A}{2}\right)\delta} +$$

$$+ \left(\left(\frac{B}{A} - \frac{1}{2}\right) \exp\left[-\left(B - \frac{A}{2}\right)\delta\right] \left\{\left(\frac{B}{A} - \frac{1}{2}\right) +\right.\right.$$

$$\left. + \exp\left(B + \frac{A}{2}\right)y\right\} + \left(\frac{B}{A} + \frac{1}{2}\right) \exp\left(B + \frac{A}{2}\right)\delta \times$$

$$\times \left\{\exp\left[-\left(B - \frac{A}{2}\right)y\right] - \left(\frac{B}{A} + \frac{1}{2}\right)\right\} \left. \frac{2AC_2}{(2B + A) \exp\left(B + \frac{A}{2}\right)\delta} \right. \quad (22)$$

where  
the

$$C_3 = \frac{\left(\frac{B}{A} + \frac{1}{2}\right)(t_2 - T_1 + C + AC\delta) \exp\left[\left(B + \frac{A}{2}\right)\delta\right] +$$

$$+ (T_2 - t_2 - C) \left[\frac{B}{A} - \frac{1}{2} + \exp\left(B + \frac{A}{2}\right)\delta\right]}{\left(\frac{B}{A} - \frac{1}{2}\right)^2 \exp\left[-\left(B - \frac{A}{2}\right)\delta\right] -$$

$$- \left(\frac{B}{A} + \frac{1}{2}\right)^2 \exp\left[\left(B + \frac{A}{2}\right)\delta\right] + 2 \frac{B}{A} \exp A\delta} \quad (23)$$

The equations which were obtained for describing the temperature profiles in the material of the thermocouple branches and in the heat carrier (coolant) blowing through them, both for the case of blow-through from the cold to the hot junctions (equations 16 and 17), and for the case of the opposite blow-through direction (equations 21 and 22) have a rather cumbersome form. They can be somewhat simplified in the design of devices which operate within a fixed range of blow-through medium flow rates, for the case of set geometric dimensions of the thermocouples and in certain other cases when terms of the second order of smallness appear and can be neglected without detracting from the computational accuracy. However, it is necessary to note that for the existing multiplicity of high capacity computers, the numerical solution of these equations presents no difficulties at all, without any simplification (algebraic).

As has already been noted, in the expressions given above for determining the temperatures in the material of the branches and in the medium being blown through them for flow in both directions, the values of the coefficients A, B and C have a different form depending on whether the thermocouple is finely porous or perforated.

These coefficients have the following form:

for finely porous thermocouples:

$$A = \frac{\alpha_0}{\rho c_p \delta}, \quad B = \sqrt{\left(\frac{A}{2}\right)^2 + \frac{\alpha_1}{\lambda}}, \quad C = \frac{\lambda \cdot F^2}{\delta^2 (1 - 1) \alpha_0};$$

for perforated thermocouples:

$$A = \frac{\alpha_0}{\rho c_p \delta}, \quad B = \sqrt{\left(\frac{A}{2}\right)^2 + \frac{\alpha_1 H}{\lambda}}, \quad C = \frac{\lambda \cdot F^2}{\delta^2 (1 - 1) \alpha_0 H}.$$

## 2. Analysis of the Temperature Fields

We will now consider the character of the change in temperature profiles in the blown-through thermocouples for various directions of flow depending on the operational conditions for specific examples. Let a thermocouple with a height of 1 cm have 25 capillaries per  $\text{cm}^2$  of surface, each with a diameter of 0.1 cm. The temperature profiles of the thermocouple described above are shown in Fig. 17 a and b for the material of the branches (solid line) and the medium blown through the capillaries (dotted line).

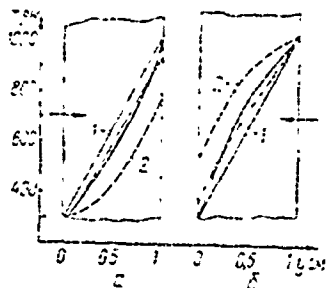


Figure 17. Temperature profiles in permeable thermocouples.

Fig. 17 a corresponds to the case where the flow direction is from the cold to the hot junctions, i.e. when the blow-through medium is heated in the capillaries. The temperature profiles shown in the figure were computed from formulas (16) and (17). The temperature profiles for the case where the blow-through medium flows in the opposite direction, i.e. when the medium is cooled inside the thermocouple, is shown in Fig. 17 b. These profiles were computed from formulas (21) and (22). The curves, 1, in Fig. 17 correspond to the small specific flow rate of the blow-through medium of  $10^{-5} \text{ kg/cm}^2 \cdot \text{sec}$ , while the curves, 2, are for a flow rate of  $10^{-4} \text{ kg/cm}^2 \cdot \text{sec}$ . The temperatures at the hot and cold sides were taken as 1,000 and 300° K respectively,

while the temperatures at the surface, through which the medium is blown, and of the blow-through medium, were taken as equal to each other for the sake of simplicity.

The considerable influence of the flow rate of the blow-through medium on the curvature of the profile can be seen in Fig. 17. If the temperature profiles in the material of the thermocouple branches are nearly linear (analogous to monolithic thermocouples) at a small mass rate of flow, then when the rate of flow is increased, they bend sharply. As has already been noted, the bending of the profile is caused by the temperature gradients at the hot and cold surfaces, thus also the heat entering the thermocouple at the hot side and leaving it at the cold side. The difference in these heats is explained by the heating or cooling of the blow-through medium within the capillaries.

As is evident from Fig. 17 a and b, for temperature equality between the blow-through medium at the inlet to the thermocouple and the responding surface of the thermocouple in proportion to the movement of the blow-through medium through the capillaries, this equality is not preserved and the difference in temperatures between the medium and the material increases. The irreversibility of the heat exchange arises due to the small heat transfer coefficient in the capillaries. Calculations based on the expressions given above, as well as experimental data [28] show that in finely porous systems, this irreversibility is much less and under specified conditions, approaches zero. However, in capillary thermocouples the heat exchange irreversibility is substantially less than in monolithic couples, even for extensive fin cooling of the junctions.

The diameter of the capillaries and the number of them per unit surface also exhibits a substantial influence on the curvature of the temperature profiles. For an insufficiently large number of capillaries, the internal heat exchange will not exhibit any influence on the temperature profile in the material of the thermocouple between perforations. Such a situation was observed when blowing air through perforated plates from the cold side to the hot [10].

The temperature profiles measured in the material of a perforated plate with 22 perforations per  $\text{cm}^2$  each with a diameter of 0.5 mm for various mass rates of flow of the blow-through medium,  $\rho v_w$ , are shown in Fig. 18. The dotted lines show the results of calculations based on the theoretical relationship (13). It can be seen that there is sufficiently good agreement between the theoretical and the experimental data.

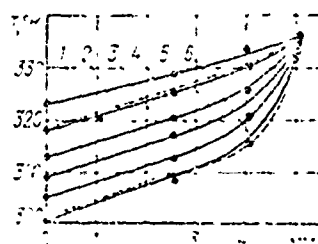


Рис. 18. Теоретические и экспериментальные температурные профили в перфорированной стенке  
 1 —  $\rho v_w = 1,72 \cdot 10^{-3} \text{ кг/с} \cdot \text{м}^2$   
 2 —  $\rho v_w = 3,16 \cdot 10^{-3} \text{ кг/с} \cdot \text{м}^2$   
 3 —  $\rho v_w = 0,151 \cdot 10^{-3} \text{ кг/с} \cdot \text{м}^2$   
 4 —  $\rho v_w = 0,375 \cdot 10^{-3} \text{ кг/с} \cdot \text{м}^2$   
 5 —  $\rho v_w = 0,574 \cdot 10^{-3} \text{ кг/с} \cdot \text{м}^2$   
 6 —  $\rho v_w = 0,655 \cdot 10^{-3} \text{ кг/с} \cdot \text{м}^2$

Figure 18. Theoretical and experimental temperature profiles in a perforated wall.

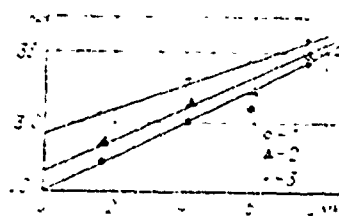


Рис. 19. Температурные профили в перфорированной стенке с малым числом отверстий  
 1 —  $\rho v_w = 1,25 \cdot 10^{-3} \text{ кг/с} \cdot \text{м}^2$   
 2 —  $\rho v_w = 0,725 \cdot 10^{-3} \text{ кг/с} \cdot \text{м}^2$   
 3 —  $\rho v_w = 0,625 \cdot 10^{-3} \text{ кг/с} \cdot \text{м}^2$

Figure 19. Temperature profiles in a perforated wall with a small number of perforations.

The results of blow-through of a perforated plate with 10 perforations per  $\text{cm}^2$  having a diameter of 0.8 mm are shown in Fig. 19. As was to be expected, for a small number of capillaries the bending of the temperature profile in the wall material was not observed even for large mass rates of flow of the air. The temperature through the thickness of the wall in this case changes in accordance with a linear law characteristic of monolithic walls.

In this way, the features of the temperature fields in permeable thermocouples make it possible to influence the thermal flows at the surface of the thermocouple to a greater or less degree, thus also influencing its power characteristics. A qualitative and quantitative analysis of such influence will be given below when considering specific circuits of thermoelectric devices having permeable thermocouples.

The features of temperature fields considered above for permeable thermocouples can also exert a significant influence on the method of averaging the parameters of the materials of the thermocouple branches operating in the given temperature range [9].

In monolithic thermocouples, where the temperature profile approaches the linear, the average temperature is located near the center of the thermocouple branch. In the case where thermocouples are blown through, a significant portion of the height of the thermocouple can operate at a slightly changing temperature and the average temperature will be located not in the center but closer to the hot or cold side, depending on the direction of blow-through.

Taking into account the fact that the properties of many thermoelectric materials change rather sharply with an increase in temperature, the



parameters for permeable thermocouples are to be averaged both for the temperature and for the height of the branches.

## Chapter IV

### The Design of Thermoelectric Generators with Permeable Thermocouples

The literature has dealt in adequate detail with generators having monolithic thermocouples, their design methods, operational analysis and the structural features of devices for various purposes; in the present work it proves to be expedient to cite the known data. At the present time, information on the design methods, structural features, etc. of generators with permeable thermocouples is contained only in periodicals. For this reason, we shall take up in detail the design methodology and analysis of the operation of generators with permeable thermocouples as well as consider their heat circuits. As has been noted in the preceding chapters, it is possible to consider two directions of flow for permeable thermocouples using a liquid or gaseous medium - from the cold junctions to the hot and vice versa. The direction of the medium flow, either in the direction of heat flow or vice versa, substantially influences the temperature profile in the thermocouple material (see Chapter III), thus also the thermal currents at the surfaces of the junction, which in turn has a very great effect on the operational modes of the generator and on its power characteristics. Under these conditions, the design methods of such generators will be entirely different.

## 1. The Design of a Generator Flushed by a Coolant Flowing From the Cold to the Hot Junctions

For the case of the indicated direction of medium flow, the temperature drop at the junction of the thermocouples with any possible heat source is created primarily due to the removal of heat by the cooling medium within the permeable thermocouples, and partially (in cases) at the surface of the cold junctions.

Practically any gases and liquids can be used as a cooling medium. A fuel or an oxidizer which react with one another upon exiting the surface of the hot junctions, thereby heating them, can be employed to create the temperature drop at the junctions of permeable thermocouples when operating generators using combustion products from organic fuels for heating the hot junctions.

We will now consider a generator with internally cooled thermocouples and hot junctions heated by combustion products from organic fuels, which is schematically shown in Fig. 20.

Liquid or gaseous fuel is fed into the device with an insufficiency or surplus of oxidant. In the operational mode where there is oxidant insufficiency, a mixture of unburned fuel and combustion products exists through the batteries. The unburned fuel continues to burn in the oxidant which is blown through the permeable thermocouples from the hot to the cold junctions.

With such a circuit, the cooling of the cold thermocouple junctions can be realized in two ways, depending on the temperature drops at the junctions necessary for obtaining the requisite useful power.

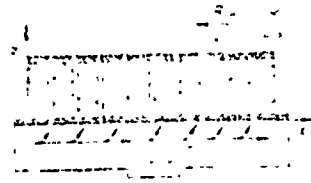


Figure 20. Circuit of a generator with internal cooling and heating of the hot junctions with combustion products.

In the first place, the coolant can be fed in against the heating flow and effect combined cooling of the cold junctions. In this case, a portion of the coolant flow being sucked through the permeable thermocouples, removes heat inside the capillaries. Another portion of the cooling flow, removing heat at the surface of the cold junctions, is subsequently utilized as primary air for oxidizing the fuel, returning the same heat which was removed from the cold junctions, to the combustion region.

Secondly, the temperature drop at the junctions of the thermocouples can be created only by blowing the cooling medium from the cold to the hot junctions. In this case, in order to realize the operation possibilities of the battery with a large temperature drop at the junctions, the coolant can be fed into various sections along the length (sectionally).

In both of the described heat circuits, the heat losses from the cold junction side of the generator is for practical purposes nonexistent. All of the heat is returned from the cooling medium (in the given case, the oxidant) to the combustion region.

It is assumed in the design of such a generator, that the following are known: its geometric dimensions, the temperature drop across the junctions  $\Delta T$ , the type of fuel (heat generating capability and composition), primary air flow rate  $G_B = \beta L_O$ , kg/kg ( $\beta$  is the coefficient of air surplus or insuff-

iciency), the initial oxidant flow rate ahead of the batteries  $G_0$  kg/sec, the initial oxidant temperature ahead of the batteries  $t_0^H$ , °K, and the specific coolant flow rate through the permeable thermocouples  $\rho v_w$ , kg/cm<sup>2</sup> · sec.

For a known type of fuel and coefficient of air insufficiency (surplus), the temperature of the heating mixture ahead of the batteries (at  $x = 1$ ) can be methodologically determined [22].

Utilizing this method, it is possible to obtain the dependence of the initial temperature of the combustion products of any organic fuel with a known basic composition on the coefficient,  $\beta$ , of oxidant insufficiency or surplus at the inlet to the device. Consequently, for the known initial data indicated above for the generator design, it is easy to determine the initial temperature of the heating flow ahead of the first thermocouples (where  $x = 1$ ).

The basic equations of thermal equilibria for the generator with permeable thermocouples based on Fig. 22 will have the following form.

Due to convective heat removal, heat from the heating gas is transferred to the hot thermocouple junctions, which can be described by the following equation which takes into account both the mixing process of the heating flow and the injected coolant:

$$B(G_0 + 1)c_p dt_3 + \rho v_w k_1 b (1 - x) c_i dt_3 - \rho v_w k_1 b c_p dx (t_3 - t_2) + q b dx = \alpha_1 b dx (t_3 - T_2), \quad (24)$$

where  $t_3$  is the running temperature of the heating flow;  $b$  is the generator perimeter (along the surface of the hot junctions);  $k_1$  is the ratio of the cross-sectional area of the capillaries to the overall area of the thermocouple.

The heat transfer coefficient,  $\alpha_1$ , from the heating gas flow to the hot thermocouple junctions where the medium is blown in through pores or capillaries, can be computed, for example, from formula (7). The additional specific quantity of heat  $q$  (with respect to the area of the hot junctions of the thermocouples) is liberated as a result of the additional burning of the fuel in

the oxidizer, injected through the permeable thermocouples when the generator is operating in a mode where  $\beta < 1$ , i.e. when a heating gas containing combustion products and unburned fuel reaches the first thermocouple:

$$q = \frac{BQ_p^H(1-\beta)}{b!} \quad (25)$$

Depending on the coefficient of primary air insufficiency and the rate of flow of secondary air blown through the thermocouples, the additional heat generation can take place at various distances from the beginning of the battery (from the cross-section where fuel is injected). This distance can be determined from the expression:

$$l-x = \frac{1-\beta}{\rho v_{\infty} F_1 b} L_0 B. \quad (26)$$

The heat which is transferred to the hot junctions of the thermocouples by convection from the heating flow, is expended in heat removed from their surface as a result of thermal conductivity of the material of the branches, and in Peltier heat absorbed at the surface of the hot junctions:

$$\alpha_1 b dx (t_3 - T_2) = k b dx \left( \frac{dT}{dy} \right)_{y=0} + \frac{k \lambda}{\delta (m+1)} \Delta T T_2 b d\lambda, \quad (27)$$

$$K = \frac{F - F_{\text{no2}}}{F}.$$

The difference in the heats entering at the surface of the hot junctions and leaving the thermocouples at the surface of the cold junctions is expended in useable power developed by the generator, and for heating the coolant from a temperature  $t_1$  at the boundary of the cold junctions up to the temperature at the boundary of the hot junctions,  $t_2$ :

$$\begin{aligned}
& \frac{2\lambda k}{\delta(m+1)} \Delta T T_2 b dx + \lambda k b dx \left( \frac{dT}{dy} \right)_{y=\delta} - \frac{2\lambda k}{\delta(m+1)} \Delta T T_1 b dx - \\
& - \lambda k b dx \left( \frac{dT}{dy} \right)_{y=0} = \\
& = \frac{2\lambda mk}{\delta(m+1)^2} \Delta T^2 b dx + \rho v_x k_1 c_p b dx (t_2 - t_1). \quad (28)
\end{aligned}$$

On the cold junction side of the battery, the Peltier heat which is generated at the surface, and the heat arriving there as a result of the thermal conductivity of the material of the thermocouple branches, with the exception of a slight amount of heat, is expended in heating the cooling medium which washes over the junction surface. The latter slight amount of heat is returned inside the thermocouples and further in the combustion zone with the injected oxidant, i.e.:

$$\begin{aligned}
G_1 c_p dt_0 - \rho v_x k_1 c_p b dx dt_0 - \rho v_x k_1 c_p b dx (t_1 - t_0) = \\
= \alpha_1 b dx (T_1 - t_0) + \lambda k b dx \left( \frac{dT}{dy} \right)_{y=0} + \\
+ \frac{2\lambda k}{\delta(m+1)} \Delta T T_1 b dx - \rho v_x k_1 c_p b dx (t_1 - t_0). \quad (29)
\end{aligned}$$

Having rewritten the equilibrium equations considered here in a form more convenient for solution, we obtain a system of equations which makes it possible to determine the temperature distribution of the junctions, coolant and heat carrier along the length of the battery, as well as all of its other characteristics:

$$\begin{aligned}
& \frac{B(G_1 + 1)c_p}{\alpha_1 b} \cdot \frac{dt_2}{dx} + \frac{\rho v_x k_1 c_p}{\alpha_1} (l - x) \frac{dt_3}{dx} = \\
& = \frac{\rho v_x c_p k_1}{\alpha_1} (t_1 - t_2) + \frac{\rho v_x c_p k_1}{\alpha_1} (t_3 - T_2). \quad (30)
\end{aligned}$$

$$\frac{\alpha_1}{k\lambda} (t_3 - T_2) = \frac{2\lambda T}{\delta(m+1)} T_2 + \left( \frac{dT}{dy} \right)_{y=\delta}, \quad (31)$$

$$\frac{2\lambda T^2}{\delta(m+1)^2} + \left( \frac{dT}{dy} \right)_{y=\delta} - \left( \frac{dT}{dy} \right)_{y=0} = \frac{\rho v_x c_p \Pi}{k} (t_2 - t_1), \quad (32)$$

$$\frac{G_1 c_p}{\alpha_0 b} \cdot \frac{dt_0}{dx} - \frac{\rho v_x c_p k_1}{\alpha_0} x \frac{dt_0}{dx} - \frac{\rho v_x c_p k_1}{\alpha_0} (t_1 - t_0) = T_1 - t_0, \quad (33)$$

$$\begin{aligned}
& \frac{\alpha_0}{k\lambda} (T_1 - t_0) + \left( \frac{dT}{dy} \right)_{y=0} + \frac{2\lambda T}{\delta(m+1)} T_1 - \frac{\rho v_x c_p \Pi}{k} (t_1 - t_0) = \\
& = 79 - \quad (34)
\end{aligned}$$

where  $z$  and  $\lambda$  are respectively the figure of merit for the material of the thermocouple branches and the coefficient of heat conductivity of the material, which are taken as the averages for the p - n pair. Additionally, the quantity,  $z$ , takes into account the imperfect contact of the thermocouples. The coefficient of heat transfer  $\alpha_0$  from the cold junctions to the cooling flow characterizes the irreversible heat loss from a portion of the coolant which washes the surface of the junctions. The magnitude of this coefficient can be determined from the criterion equation (8) obtained for the case where the medium is sucked through a finely porous surface.

In the solution of the system of equations (30) - (34), one equation is still needed - for the temperature of the coolant at the output of the capillaries (where  $y = \delta$ ), which is obtained from the expression describing the temperature distribution in the oxidant flowing in the permeable thermocouples (14):

$$\begin{aligned}
 t_2 &= T_1(1 + k_3) - t_1 k_3 - C(1 + k_3) + AC\delta + k_2(\Delta T - AC\delta), \\
 \text{and} \quad k_2 &= \frac{\left(\frac{B}{A} + \frac{1}{2}\right) \exp\left(\left(B - \frac{A}{2}\right)\delta\right) + \left(\frac{B}{A} - \frac{1}{2}\right) \exp\left[-\left(B - \frac{A}{2}\right)\delta\right] - 2\frac{B}{A}}{\left(\frac{B}{A} + \frac{1}{2}\right)^2 \exp\left(\left(B - \frac{A}{2}\right)\delta\right) - \left(\frac{B}{A} - \frac{1}{2}\right)^2 \exp\left[-\left(B - \frac{A}{2}\right)\delta\right] - 2\frac{B}{A}}, \\
 k_3 &= \frac{\left[1 - k_2\left(\frac{B}{A} + \frac{1}{2}\right)\right] \exp\left(\left(B - \frac{A}{2}\right)\delta\right) - \left(\frac{B}{A} + \frac{1}{2}\right)(t_2 - t_1)}{\frac{B}{A} - \frac{1}{2}}.
 \end{aligned} \tag{35}$$

Thus by solving the system of equations (30) - (35), we obtain expressions for determining the temperature distributions along the length of the batteries:

of the cold junctions:

$$T_1 = \frac{t_0 \left( \frac{\alpha_0}{\lambda R} + \frac{\rho^2 \epsilon_p \Pi}{\lambda} \right) + \left( \frac{dT}{dy} \right)_{y=0} + \frac{\rho^2 \epsilon_p \Pi}{\lambda} \cdot C}{\frac{\alpha_0}{\lambda R} + \frac{\rho^2 \epsilon_p \Pi}{\lambda} - \frac{z \Delta T}{\delta (m+1)}}, \quad (36)$$

of the coolant washing over the surface of the cold junctions:

$$t_0 = \left[ t_0'' + \frac{\left( \frac{dT}{dy} \right)_{y=0} \left( 1 + \frac{\alpha_1}{\rho^2 \epsilon_p k_1} \right) - C \left[ 1 - \frac{z \Delta T}{\delta (m+1)} \right]}{\frac{z \Delta T}{\delta (m+1)} \left( 1 + \frac{\alpha_1}{\rho^2 \epsilon_p k_1} \right)} \right] \times \\ \times \frac{C \left( \frac{\rho^2 \epsilon_p \Pi}{\lambda} + \frac{\alpha_1}{\lambda} - \frac{z \Delta T}{\delta (m+1)} \right)}{\frac{z \Delta T}{\delta (m+1)} \left( 1 + \frac{\alpha_1}{\rho^2 \epsilon_p k_1} \right)} - \\ - \left( 1 - \frac{\rho^2 \epsilon_p \Pi}{\lambda} x \right) - \\ - \frac{\left( \frac{dT}{dy} \right)_{y=0} \left( 1 + \frac{\alpha_1}{\rho^2 \epsilon_p k_1} \right) - C \left[ 1 - \frac{z \Delta T}{\delta (m+1)} \right]}{\frac{z \Delta T}{\delta (m+1)} \left( 1 + \frac{\alpha_1}{\rho^2 \epsilon_p k_1} \right)}, \quad (37)$$

of the heating gas:

$$t_1 = T_2 \left[ 1 + \frac{z \Delta T}{\delta (m+1)} \cdot \frac{\rho^2 \epsilon_p \Pi}{\alpha_1} \right] + \frac{k_1}{\alpha_1} \left( \frac{dT}{dy} \right)_{y=\delta}, \quad (38)$$

of the coolant at the inlet to the capillaries (where  $y = 0$ ):

$$t_1 = T_1 - C \quad (39)$$

of the coolant at the outlet of the capillaries:

$$t_2 = T_1 + k_7 \quad (40)$$

It should be remembered when carrying out calculations based on the given equations, that the running values of the temperatures  $t_0$ ,  $T_1$  and  $t_2$  are reflected in the relationships (37) - (40). For example, in the determination of the temperature of the heating gas in any section, it is necessary to substitute the temperature values  $t_2$ ,  $t_0$  and  $T_2$ , which correspond



to this section, in equation (38).

The order of performing the calculations for a generator with permeable thermocouples is as follows. First, the change in the temperature of the coolant flow along the length is determined from equation (37). After this the temperatures of the cold junctions of the thermocouples in the corresponding sections are computed from equation (36). Then the temperature changes in the coolant at the surface of the hot and cold junctions as well as the temperatures of the heating flow are found from equations (38) - (40).

The following conventional symbols are adopted for the relationships given above:

$$k_1 = \frac{\left(\frac{B}{A} + \frac{1}{2}\right) \exp\left(B - \frac{A}{2}\right) \delta + \left(\frac{B}{A} - \frac{1}{2}\right) \exp\left[-\left(B + \frac{A}{2}\right) \delta\right]}{\left(\frac{B}{A} + \frac{1}{2}\right)^2 \exp\left(B - \frac{A}{2}\right) \delta - \left(\frac{B}{A} - \frac{1}{2}\right)^2 \exp\left[-\left(B + \frac{A}{2}\right) \delta\right] - 2 \frac{B}{A}}$$

$$k_2 = \left(B + \frac{A}{2}\right) \left\{ \exp\left(B - \frac{A}{2}\right) \delta - \left(\frac{B}{A} + \frac{1}{2}\right) \left[ \exp\left(B - \frac{A}{2}\right) \delta - 1 \right] k_1 \right\},$$

$$k_3 = \frac{2 \frac{B}{A} \left(\frac{B}{A} + \frac{1}{2}\right)}{\left(\frac{B}{A} + \frac{1}{2}\right)^2 \exp\left(B - \frac{A}{2}\right) \delta - \left(\frac{B}{A} - \frac{1}{2}\right)^2 \exp\left[-\left(B + \frac{A}{2}\right) \delta\right] - 2 \frac{B}{A}},$$

$$k_4 = 1 - C + k_2 (\Delta T - AC \delta).$$

The temperature gradients at the surfaces of the hot and cold junctions of the thermocouples taking into account the adopted symbols will have the form:

$$\left(\frac{dT}{dx}\right)_{x=0} = 1C - \frac{H}{k_1} (\Delta T - AC \delta) k_1, \quad (41)$$

$$\left(\frac{dT}{dx}\right)_{x=L} = AC + 2 \left(\frac{B}{A} - \frac{1}{2}\right) (\Delta T - AC \delta) k_3, \quad (42)$$

It follows from these expressions that the temperature gradients at the hot and cold sides of the battery do not depend on the distance along the battery and are constant over all its length. The rate of flow of the medium being blown through them exerts the primary influence on the magnitude of the temperature gradients.

An expression for the determination of the temperature of the heating flow along the length of the battery can likewise be determined from equation (30). If equation (38) holds true for the case of generator operation with an initial coefficient of oxidant surplus (as well as for the determination of the requisite initial and final heating flow temperatures), then it is possible to obtain the temperature profile of the heating gas from equation (30), taking into account the additional heat generation when the unburned fuel is burned up in the operational mode where  $\beta < 1$ . In this case, we obtain the following expression:

$$t_1 = \left( t_2 - \frac{1}{\beta} \frac{1}{\gamma} \frac{1}{H} \frac{1}{S_1} \right) \left( 1 - \frac{1}{\beta} \right) + \frac{1}{\beta} \left( \frac{dT}{dx} \right)_{x=0} - \frac{1}{\beta} \left[ 1 - \frac{1}{\beta} \frac{1}{\gamma} \frac{1}{H} \frac{1}{S_1} \right] \left( 1 - \frac{1}{\beta} \right) + t_2 - \frac{1}{\beta} \frac{1}{\gamma} \frac{1}{H} \left[ \frac{1}{S_1} \frac{1}{\beta} \left( \frac{dT}{dx} \right)_{x=0} - \frac{1}{\beta} \right]. \quad (43)$$

In this fashion, by means of the equations introduced above, the distributions of all temperatures (of junctions, coolant and heat carrier) along the length of the battery can be determined. The fuel consumption which provides for the obtained temperature distributions, can be easily determined from a simultaneous solution of equations (38) and (43). Additionally, the fuel consumption can be determined from the equation of overall heat equilibrium of the generator considered here:

$$BQ_p'' = N + [B(1 + \beta L) + \rho c_p k F] c_p (t_3 - t_0'') + \alpha_0 F (T_1 - t_0') \quad (44)$$

The system of equations (37) - (44) makes it possible to carry out a complete thermal design of the generator, whose hot junctions are heated by the combustions products of an organic fuel, where the temperature drop at the junctions is created by blowing a coolant through the permeable thermocouples from the cold to the hot junctions.

The efficiency of this generator in the most general case is computed as the ratio of the obtained useful electrical power to the quantity of heat generated during the combustion of the fuel, i.e.:

$$\eta = \frac{N}{BQ_p^H} \quad (45)$$

All possible heat losses including also the heat loss with the exhaust gases are taken into account in this determination of the efficiency of the device. If one takes into account the fact that the heat of the exhaust gases following the generator can be utilized in some other heat-consuming device or in a second stage generator with lower temperature thermocouples, based for example on the thermal circuits of Fig. 5 e and f, then the efficiency of the heat-to-electrical energy conversion process itself in the device considered here can be evaluated having taken into account the thermoelectric conversion efficiency as the ratio of useful electric power to the heat passing through the surface of the hot junctions:

$$\eta_{th} = \frac{N}{BQ_p^H} \quad (46)$$

where  $\pi_2$  is the heat absorbed at the hot junctions as a result of the Peltier effect.

Some results of a theoretical analysis of the operation of the generator considered here, which were obtained using the given method for its design, are given below. To analyze the influence of various factors on the power characteristics of the generator, design variations were run through on the "Promin'" computer.

In the design variations, the following quantities were given and remained constant: the average characteristics for the p - n pair of the material of the thermocouple branches  $z = 0.5 \cdot 10^{-3} \text{ 1/}^\circ\text{K}$  and  $\lambda = 0.01 \text{ watts/cm} \cdot ^\circ\text{K}$ ; the diameter of the capillaries,  $d = 0.1 \text{ cm}$  and the number of them per unit surface of the battery  $z_1 = 25 \text{ holes/cm}^2$ , which determined the values of the quantities:

$$k_1 = \frac{F_{\pi op}}{F} = 0.196 \text{ and } k = \frac{F - F_{\pi op}}{F} = 0.804;$$

the physical characteristics of the cooling air  $\lambda_0 = 2.7 \cdot 10^{-4} \text{ watts/cm} \cdot ^\circ\text{K}$ ,  $c_{po} = 10^3 \text{ watt} \cdot \text{sec/kg} \cdot \text{deg}$ ,  $Pr_0 = 0.71$ ,  $\mu_0 = 1.8 \cdot 10^{-7} \text{ kg/cm} \cdot \text{sec}$ ; the initial temperature of the cooling air  $t_0^H = 300^\circ\text{K}$ ; the perimeter of the battery  $b = 10 \text{ cm}$ , as well as the geometric dimensions of the channel for passing the coolant. It was assumed that the generator is operated in the maximum power mode, i.e. for  $m = 1$ .

The fuel was assumed to be natural gas with a heat generating capacity of  $Q_p^H = 0.485 \cdot 10^8 \text{ watt} \cdot \text{sec/kg} \cdot \text{deg}$ , and the magnitude theoretically necessary for complete combustion of the air quantity  $L_0 = 16.76 \text{ kg/kg}$ . The dependence of the initial temperature of the combustion products,  $t_3^H$ , on the coefficient of oxidant surplus or insufficiency, as shown above, can

be easily obtained under these conditions.

In accordance with the method set forth here for generator design, the givens are the geometric dimensions of the battery and the temperature drop at the junctions of the thermocouples, (i.e. the useful electrical power), for a known initial flow rate and temperature of the coolant. In the calculation process, the distribution of the coolant temperature  $t_0$ , the hot and cold junction temperatures  $T_2$  and  $T_1$ , as well as the temperature distribution  $t_3$  of the combustion products for a known heat transfer coefficient  $\alpha_1$  from the hot side which is necessary for assuring these conditions is determined over the length of the battery.

The finding of the fuel consumption from a simultaneous solution of equations (38) and (43) or by using the dependence of the initial temperature of the fuel combustion on the coefficient of oxidant surplus, presupposes that the temperature distribution  $t_3$  of the hot gas over the length of the battery, which is calculated from formula (43), will be satisfied for the calculated conditions.

Under the conditions described, the necessary initial temperature  $t_3^H$  of the fuel combustion products can be assured for the case of two different operational modes of the device: for fuel combustion at the generator inlet with an insufficiency of primary oxidant and combustion with an excess of oxidant. The initial coefficient of oxidant surplus (insufficiency) changes along the length in connection with the injection of a portion of the oxidant through the permeable thermocouples along the length of the battery in the combustion region.

If the generator operates with an oxidant excess fed in at the inlet,

then as the combustion products move towards the exhaust, they are diluted by the injected coolant, reducing its own temperature not only because of the heat removal to the hot junctions of the thermocouples, but also due to the physical mixing with a colder cooling medium.

In the case where the requisite initial temperature of the combustion products is assured by the fuel combustion with a deficiency of primary oxidant, the oxidant feed through the capillaries promotes the generation of an additional quantity of heat along the length, due to the further burning of the unburned fuel ahead of the first thermocouples.

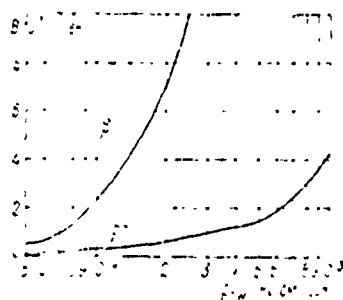


Figure 21. Dependence of fuel consumption  $B$  on the blow-through velocity of the oxidant  $\rho v_w$ .

The dependence of fuel consumption  $B$  on the mass rate of flow  $\rho v_w$  of the oxidant blown through the permeable thermocouples in a generator having a length of 30 cm, at whose junctions a temperature drop  $\Delta T = 500^\circ \text{K}$  is maintained and for a height of the thermocouple branches of  $\delta = 1 \text{ cm}$ , is shown in Fig. 21. However, for these conditions the change in the coefficient of oxidant surplus (insufficiency)  $\beta$ , along the length of the battery,  $l$ , is shown in Fig. 22. As can be seen from these figures, the operational mode of the battery during the combustion of fuel with a deficiency of primary air requires less of a fuel expenditure to obtain the same useful electrical power than the operational mode for an initial oxidant surplus.

The circumstances noted above are easily explained by the fact that the

operational mode requires a much greater flow rate of combustion products with the requisite initial temperature to maintain the necessary temperature of the mode when mixed with more cold air along the length of the battery. This air which is injected through the permeable thermocouples is necessary to maintain the designed temperature drop at the junctions.

In the operational mode of a generator with fuel combustion for an insufficiency of primary air ( $\beta < 1$ ), the reduction in the temperature of the heat carrier due to intermixing of the colder cooling medium (oxidant) injected through the capillaries, is compensated to a certain extent by the additional heat generation during the further burning of the fuel unburned in the primary air. In this case, the fuel consumption will be less in the mode of operation where  $\beta < 1$ , other conditions being equal. In the given case, the front section of the battery serves as a burner device. With a

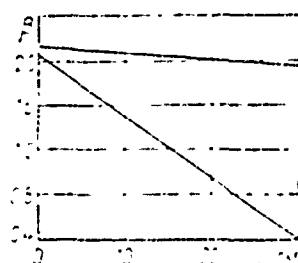


Figure 22. Change in the coefficient of oxidant surplus  $\beta$  along the length  $l$  of the thermo-battery.

reduction in the quantity of injected oxidant, this portion increases and for a flow rate  $\rho v_w = 5 \cdot 10^{-4} \text{ kg/cm}^2 \cdot \text{sec}$  amounts to 2/3 of the generator length.

The efficiency of this generator at a power of 75 watts (constant temperature drop at the junctions  $\Delta T = 500^\circ \text{ K}$ ) changes as a function of the specific rate of flow of the coolant blown in through the permeable

thermocouples according to the curves shown in Fig. 23. It can be seen from the figure that the efficiency at which the given useful electrical power is obtained from the generator increases according to the extent of reduction in the flow rate of the coolant blown through the thermocouples.

Fig. 24 shows the change in the temperatures of the coolant  $t_0$ , washing over the surface of the cold junctions,  $T_2$  of the hot junctions of the thermocouples and the initial temperature of the combustion products  $t_3$  in the section  $x = 1$ , i.e. at the inlet of the combustion products into the generator,  $t_3$  being necessary to assure the temperature  $t_0$  and  $T_2$ . It is apparent from the drawing that for the cooling mode considered here (the ratio of the medium blown through the capillaries to the total quantity of coolant reaching the cold junction is equal to 0.58) in the region of small flow rates of the injected medium, the coolant is heated up to significant temperatures, which entails an increase in the operational temperature level of the thermocouples, and consequently an increase in the initial temperature of the combustion products. However, the difference in temperatures between the hot junctions and the heating flow decreases in this case. This phenomenon can be easily explained by considering Fig. 25, in which the dependence of the ratio of the temperature gradients at the surfaces of the hot and cold junctions of the thermocouples on the rate,  $\rho v_w$ , at which the cooling medium flows through them is shown.

For low-flow velocities, the ratio  $(\frac{dT}{dy})_{y=\delta}/(\frac{dT}{dy})_{y=0}$  is not large and grows sharply with an increase in the coolant rate of flow through the capillaries. This condition in turn means that from the side of the cold junctions much more heat arrives for heating the cooling flow at small



injection velocities than in the case of large  $\rho v_{\omega}$ . Within the limits of increase for  $\rho v_{\omega}$ , the quantity of heat arriving at the surface of the cold junctions as a result of the thermal conductivity of the material of the thermocouple branches, and expended for heating the coolant, which washes over the latter, can approach zero. In this case, the cooling flow will be

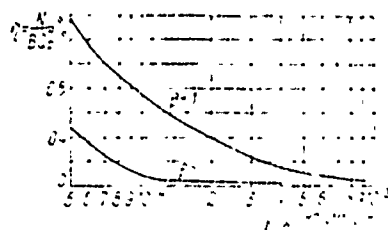


Figure 23. The dependence of the thermal battery efficiency  $\eta$  on the flow rate of the oxidant,  $\rho v_{\omega}$  blown through the capillaries.

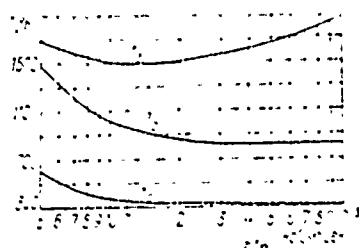


Figure 24. The change in the temperature of the heat carrier, coolant, and junctions as a function of the oxidant rate of flow  $\rho v_{\omega}$  in the cross-section  $x = 1$ .

heated up primarily by Peltier heat liberated at the surface of the cold junctions, which is likewise not very great due to their low temperature. This heat causes very rapid cooling which is clearly visible from Fig. 24, where for large injection velocities of the coolant, its temperature before the last thermocouples (counting from the inlet of the cooling flow) is almost not distinguishable from the initial temperature.

When the injection velocity of the coolant is increased, the heat outflow due to the thermal conductivity of the material of the branches from the hot junctions of the thermocouples increases sharply. This heat is expended primarily in heating the large quantity of coolant blown through the permeable

thermocouples to a rather high temperature. In this case, the initial temperature of the combustion products also begins to increase with an increase in the injection velocity of the cooling medium.

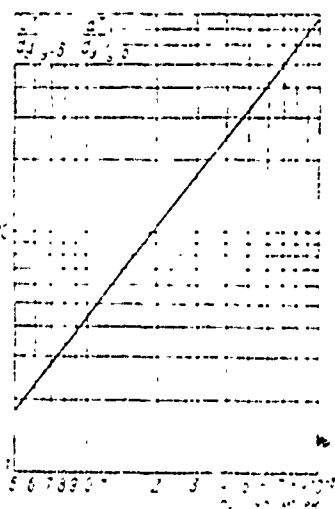


Figure 25. Dependence of the ratio of the temperature gradients at the junctions  $(\frac{dT}{dy})_{y=\delta} / (\frac{dT}{dy})_{y=0}$  on the oxidant rate of flow,  $\rho v_{\omega}$ .

The change in the coefficient of oxidant surplus (insufficiency)  $\beta$  along the length,  $l$ , of the generator for specific oxidant flow rates through the capillaries, and the temperature drop at the junctions  $\Delta T = 800^\circ \text{ K}$  is shown in Fig. 26.

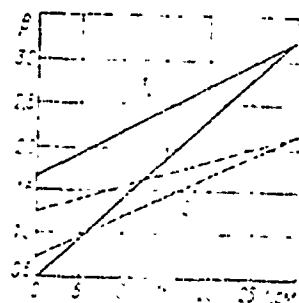


Figure 26. The influence of the flow rate of the injected oxidant on the coefficient of oxidant surplus,  $\beta$ .

This graph likewise confirms the expediency of generator operation in

a mode with an initial oxidant insufficiency. The dependencies  $\beta$  shown in this drawing assure the same temperature mode of generator operation, but at substantially different fuel consumptions.

The dependence of the efficiency of the generator on the injection velocity of the coolant shown in Fig. 23 was calculated from equation (45). As has already been noted, this equation takes into account the reduction in generator efficiency due to heat losses with the exhaust gases.

The loss of heat with the exhaust gases is a determining factor both in generators with permeable as well as in generators with monolithic thermocouples. If generators with permeable and monolithic thermocouples operate in the same temperature range and with the same temperature drop at the junction, then their efficiency computed from formula (45) will be the same under conditions of complete heat recovery from the cold junctions in both devices.

In contrast to generators with non-permeable thermocouples, an increase in the efficiency of generators with permeable thermocouples can be obtained by creating a greater temperature drop at the junctions (obtaining a greater useful power) due to higher rate of heat exchange when a coolant is blown through the capillaries. In this case, the coolant flow rate will also be substantially less than in devices with monolithic thermocouples, even where the cold junctions of the latter make extensive use of cooling fins.

A comparison of the operation of generators having permeable and non-permeable thermocouples without taking into account the loss in heat with the exhaust gases occasions certain difficulties due to the lack of clear-cut boundaries within which it would be possible to place both generators and assure similar conditions for their operation. In fact, the efficiency of generators with monolithic thermocouples is computed from the well-known

relationship [6]:

$$\eta = \frac{N}{P_2 + \lambda F \left( \frac{dT}{dy} \right)_{y=2\delta}} = \frac{N}{P_1 + N + \lambda F \left( \frac{dT}{dy} \right)_{y=0}}, \quad (47) \quad (47)$$

i.e., the useful electrical power is related to the quantity of heat entering the thermocouples from the hot junction side, or to the quantity of heat exiting at the surface of the cold junctions plus the useable power. In a permeable thermocouple, these heat quantities differ sharply from one another owing to the removal of heat to the coolant within the thermocouples. For this reason, the equation introduced above is not justified for the case of permeable thermocouples.

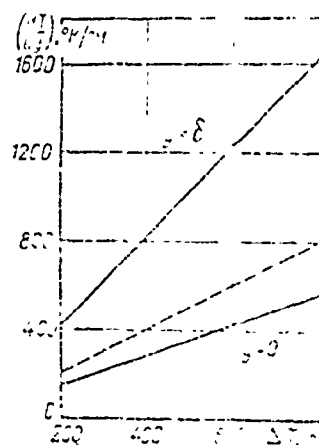


Figure 27. The values of the temperature gradients at the junctions of monolithic and permeable thermocouples.

Fig. 27. Dependence of the temperature gradients at the junctions of monolithic and permeable thermocouples on the temperature drop at the junctions.

The values of the temperature gradients at the surfaces of hot and cold junctions of monolithic and permeable thermocouples are shown in Fig. 27 as a function of the temperature drop at the junctions for a coolant flow rate through the permeable thermocouple of  $10^{-4} \text{ kg/cm}^2 \cdot \text{sec}$ . As can be seen from Fig. 27, the temperature gradients at the junctions of permeable thermocouples differ quite sharply. Here the ratio of the temperature gradients at the hot and cold junctions for the given permeable thermocouple

depends only on the flow rate of the coolant through the capillaries. An increase in the flow rate of the coolant through the capillaries causes a large increase in the difference of magnitudes of the temperature gradients at the surfaces of the cold and hot junctions of the permeable thermocouple. Consequently, if the efficiency of the permeable thermocouple is calculated similarly to the monolithic (the dotted line) according to formula (47), then in the calculation of the quantity of heat exiting at the cold side, it will be much higher than for the case of the calculation for the quantity of heat entering the thermocouple from the hot side. If it is assumed that the heat removed by the coolant in the thermocouple is returned to the heating flow and can be further utilized, then the efficiency of the permeable thermocouple, characterizing the conversion efficiency of thermal into electrical energy can be computed from formula (47). In this case, the useful power is related to the quantity of heat exiting the cold junction side plus the quantity of extracted power.

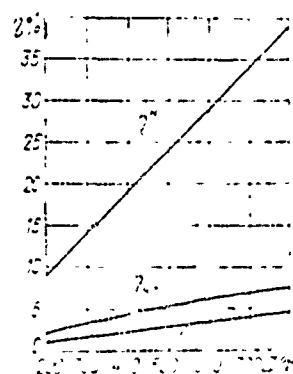


Figure 28. The dependence of energy conversion efficiency on the temperature drop at the junctions of the thermocouples.

In Fig. 28 the relationships of monolithic and permeable thermocouples to the temperature drop at the junctions are shown as calculated from formulas (47). The relationships shown in this figure are of purely theoretical

interest. In the comparison of the operational efficiency of generators with monolithic and permeable thermocouples, intended for any sort of concrete operating conditions, an individual approach is necessary which takes into account all the features of the device being designed.

## 2. Design of a Generator Where the Heat Carrier Blows Through From the Hot to the Cold Junctions

The circuit of a thermocouple operating as a generator of electrical power and having a heat carrier blown through from the hot to the cold junctions is shown in Figure 29 [13].

A hot heat carrier at an initial temperature of  $t_3$  blows through capillaries made in the branches of the generator thermocouples. In the given case, heat is delivered to the battery not only through the surfaces of the hot junctions of the thermocouples, but also within the capillaries. Such a battery can be employed, for example, to utilize the heat of combustion products exhausted from any kind of heat-utilizing plant. Naturally, under these conditions the flow rate of the hot heat carrier and its initial temperature ahead of the batteries are given.

Let us assume that the battery is fabricated from permeable thermocouples having the same geometric characteristics and its dimensions are known. This means that where the average parameters of the materials of the thermocouple branches are known, its internal electrical resistance,  $r$ , is known. If the electrical resistance of the load,  $R$ , and the requisite useful power consumed in it are known, then it is possible to find the temperature drop which should be maintained at the junctions of the given

battery from equation (6):

$$\Delta T = \sqrt{\frac{N\delta(m+1)^2}{2\lambda m b l k}}. \quad (48) \quad (48)$$

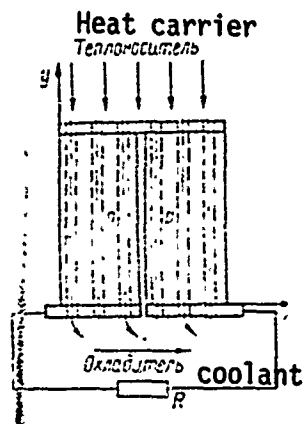


Figure 29. The circuit of a thermocouple where the heat carrier blows through from the hot to the cold junctions.

This drop is created by the cooling of the heat carrier from an initial temperature  $t_3$  ahead of the thermocouples to a temperature of the cooling flow  $t_0$ , i.e.

$$\rho v_{\perp} c_p k_1 b l (t_3 - t_0) = N + \Pi_1 + \rho v_{\perp} c_p k_1 b l (t_1 - t_0) + \lambda k b l \left( \frac{dT}{dy} \right)_{y=0}$$

or, simplifying this expression we obtain

$$\rho v_{\perp} c_p k_1 b l (t_3 - t_1) = N + \Pi_1 + \lambda k b l \left( \frac{dT}{dy} \right)_{y=0}, \quad (49) \quad (49)$$

where  $\Pi_1$  is the Peltier heat generated at the cold junctions of the permeable thermocouples.

The temperature of the hot heat carrier is reduced from the side of the hot junctions of the permeable thermocouples due to the absorption of the Peltier heat at the surface of the hot junctions and also due to the removal of heat as a consequence of the heat conductivity of the material of the

thermocouple branches, i.e.

$$\rho v_{\infty} c_p k_1 b l (t_3 - t_2) = \frac{z \Delta T^2}{\delta (m+1)} T_2 k b l + \lambda k b l \left( \frac{dT}{dy} \right)_{y=\delta}. \quad (50)$$

From expressions (49) and (50) it is not difficult to find the temperature of a heat carrier at the input to the capillaries (where  $y = \delta$ ), by calculating the temperature gradient at the surface of the hot junctions from equation (21):

$$\begin{aligned} \frac{\rho v_{\infty} c_p M}{\lambda} (t_3 - t_2) &= \frac{z \Delta T^2}{\delta (m+1)} + \frac{z \Delta T}{\delta (m+1)} T_1 + \\ &+ 2B \frac{\left( \frac{B}{A} - \frac{1}{2} \right) \exp A \delta}{M} \left\{ (t_2 - T_1) \left( \frac{B}{A} - \frac{1}{2} \right) + \right. \\ &+ \Delta T + C \left[ (1 + A \delta) \left( \frac{B}{A} + \frac{1}{2} \right) - 1 \right] \left. \right\} + \\ &+ \left( B - \frac{A}{2} \right) (\Delta T + T_1 - t_2 - C) - AC. \end{aligned}$$

from this equation we obtain:

(51)

$$t_2 = \frac{k_2}{k_3} T_1 + \frac{k_4}{k_3}, \quad (51)$$

where

$$\begin{aligned} k_2 &= 2B \frac{\left( \frac{B}{A} - \frac{1}{2} \right)^2 \exp A \delta}{M} - \frac{z \Delta T}{\delta (m+1)} - \left( B - \frac{A}{2} \right), \\ k_3 &= \frac{\rho v_{\infty} c_p M}{\lambda} + 2B \frac{\left( \frac{B}{A} - \frac{1}{2} \right)^2 \exp A \delta}{M} - \left( B - \frac{A}{2} \right), \\ k_4 &= \frac{\rho v_{\infty} c_p M T_1}{\lambda} - \frac{z \Delta T^2}{\delta (m+1)} - \\ &- 2B \frac{\left( \frac{B}{A} - \frac{1}{2} \right) \exp A \delta}{M} \left\{ \Delta T + C \left[ (1 + A \delta) \left( \frac{B}{A} + \frac{1}{2} \right) - 1 \right] \right\} - \\ &- \left( B - \frac{A}{2} \right) (\Delta T - C) + AC, \\ M &= \left( \frac{B}{A} + \frac{1}{2} \right)^2 \exp \left[ \left( B + \frac{A}{2} \right) \delta \right] - \\ &- \left( \frac{B}{A} - \frac{1}{2} \right)^2 \exp \left[ - \left( B - \frac{A}{2} \right) \delta \right] - 2 \frac{B}{A} \exp A \delta. \end{aligned}$$



The temperature of the heat carrier  $t_1$  at the outlet of the capillaries on the side of the cold junctions can be determined from equation (22) for the condition  $y = 0$ . Neglecting terms of the second order of smallness in this equation, we obtain an expression for the temperature of the heat carrier at the surface of the cold junctions:

$$t_1 = T_1 - C + \frac{\left(\frac{B}{A} - \frac{1}{2}\right) \exp\left(B + \frac{A}{2}\right) \delta}{AI} \times$$

$$\times \left\{ (t_2 - T_1) \left(\frac{B}{A} - \frac{1}{2}\right) + \right.$$

$$\left. + \Delta T + C \left[ (1 + A\delta) \left(\frac{B}{A} + \frac{1}{2}\right) - 1 \right] \right\}. \quad (52)$$

It is more expedient to maintain a high temperature of the hot junctions in generators (see Fig. 29), which permits the maximum utilization of the heat of the hot heat carrier by creating the maximum temperature drop at the junctions of the thermocouples. The maximum value of the temperature of the hot junctions can be obtained by equating it with the temperature of the heat carrier at the surface of the hot junctions (where  $y = \rho$ ), i.e. when  $T_2 = \Delta T + T_1 = t_2$ , or taking expression (51) into account

$$T_1 = \frac{k_1 - k_2 \Delta T}{k_1 - k_2}. \quad (53)$$

having substituted this in the expression for the values of the coefficients  $k_2$ ,  $k_3$  and  $k_4$ , we obtain an equation for determining the temperature of the cold junctions of the generator being considered:

$$\frac{\rho^2 \epsilon_p \Pi}{\delta} (t_2 - \Delta T) - 2B \frac{\left(\frac{B}{A} - \frac{1}{2}\right) \exp A\delta}{AI} \times$$

$$\times \left\{ 2\Delta T + C \left[ (1 + A\delta) \left(\frac{B}{A} + \frac{1}{2}\right) - 1 \right] \right\} -$$

$$- \frac{2\Delta T^2}{\delta(m+1)} + C \left( B + \frac{A}{2} \right)$$

$$T_1 = \frac{\frac{\rho^2 \epsilon_p \Pi}{\delta} (t_2 - \Delta T) - \frac{2\Delta T^2}{\delta(m+1)} + C \left( B + \frac{A}{2} \right)}{\frac{\rho^2 \epsilon_p \Pi}{\delta} - \frac{2\Delta T}{\delta(m+1)}}. \quad (54)$$

In such a manner, for a given initial heat carrier temperature  $t_3$  and temperature drop  $\Delta T$  at the junctions of the thermocouples, it is possible to determine the temperatures  $T_2$  of the hot and  $T_1$  of the cold junctions of the batteries and the temperature of the heat carrier at the input to the capillaries  $t_2$  and at their outlet  $t_1$  from equations (51), (52) and (54). After this it is necessary to carry out the calculations for the cooling system which makes it possible to maintain the given temperature drop at the junctions of the thermocouples within the design temperature range.

It follows from equation (49) that the Peltier heat generated at the junction surfaces of permeable thermocouples, the heat reaching the cold junctions due to thermal conductivity of the material of the branches, and the physical heat of the heat carrier leaving the surface of the cold junctions at a temperature  $t_1$  is removed from the side of the cold junctions of permeable thermocouples by the external coolant flow. These are the three components of thermal flow from the surface of cold junctions of permeable thermocouples, which should be dissipated by the coolant flow washing over their surface externally.

There is no information in the literature on the coefficient of heat transfer from a hot permeable surface to a cold external flow when a hot heat carrier is blown through the permeable surface. However, if it is assumed that the coefficient of heat transfer in the case under consideration is determined from the equations obtained for the case where a cold medium is injected into the hot heating flow, specifically in accordance with formula (7), then the quantity of heat removed in this case can be determined in the following fashion:

$$\alpha_1 (T_1 - t_0) = \lambda k \left( \frac{dT}{du} \right)_{u=0} = \frac{2\lambda \Delta T}{\delta (pi + 1)} T_1 k. \quad (55)$$

(55)

It is apparent from equations (49) and (55) that in the determination of the heat transfer coefficient from formula (7), it is additionally necessary to also take into account the increase in the temperature of the cooling medium due to the physical heat of the intermixed heat carrier which exits the surface of the cold junctions of the permeable thermocouples. If the initial rate of flow of the coolant and its temperature at the input to the thermocouples are known, then it is possible to write the following equation for thermal equilibrium:

$$(G_{\text{ex}} + \rho v_{\omega} k_1 b l) c_{p0} t_0^{\text{II}} - G_{\text{ex}} c_{p0} t_0^{\text{II}} = \rho v_{\omega} c_{pr} k_1 b l (t_1 - t_0) + \alpha_1 b l (T_1 - t_0), \quad (56)$$

or taking into account expressions (44) and (55).

$$\begin{aligned} (G_{\text{ex}} + \rho v_{\omega} k_1 b l) c_{p0} t_0^{\text{II}} - G_{\text{ex}} c_{p0} t_0^{\text{II}} = \\ = \rho v_{\omega} c_{pr} k_1 b l (t_3 - t_0) - \frac{z \lambda m}{\delta (m + 1)} \Delta T^2 k b l. \end{aligned}$$

Relating the initial coolant rate of flow to the area of the generator and dividing both parts of equation (56) by  $\rho v_{\omega} c_{pr} k_1 b l$ , we obtain an expression for the final temperature of the cooling medium

$$t_0^{\text{II}} = \frac{t_3 + \left[ \frac{\rho U_0}{\rho v_{\omega} k_1} \cdot \frac{c_{p0}}{c_{pr}} - 0.5 \right] t_0^{\text{I}} - \frac{\lambda}{\rho v_{\omega} c_{pr} H} \cdot \frac{z \Delta T^2}{\delta (m + 1)} \cdot \frac{m}{(m + 1)}}{\left( \frac{\rho U_0}{\rho v_{\omega} k_1} + 1 \right) \frac{c_{p0}}{c_{pr}} + 0.5}. \quad (57)$$

In this fashion, knowing the final temperature of the coolant it is possible to determine its average temperature over the length of the generator and find the coefficient of heat transfer for the design mode from equation (44):

$$\alpha_1 = \frac{\rho v_{\omega} c_{pr} k_1 (t_3 - t_1) - \frac{z \lambda T}{\delta (m + 1)} \cdot \frac{\lambda m}{(m + 1)} k}{T_1 - t_0}. \quad (58)$$

The magnitude of the heat transfer coefficient  $\alpha_1$  computed from this expression can be realistically assured by the choice of the necessary velocity of the basic cooling medium flow, which can be determined from equation (7) or from the other equations for the determination of the heat transfer coefficient when the medium is blown through the permeable wall. In such a generator, similar heat exchange conditions at the surface of the cold junctions can be realized by changing the cross-section of the channel for passing the coolant at its given initial flow rate.

Consequently, the system of equations which is obtained makes it possible to completely carry out the calculations for a generator with permeable thermocouples through which a heat carrier is blown from the hot to the cold junctions.

The efficiency of such a generator is defined as the ratio of the useful electric power to all of the expended heat:

$$\eta = \frac{N}{\rho v_{\infty} c_p k_1 b l (t_3 - t_0^h)} = \frac{z \Delta T^2}{\delta (m + 1)} \cdot \frac{\lambda}{\rho v_{\infty} c_p l l} \cdot \frac{n}{(m + 1) (t_3 - t_0^h)} \quad (59)$$

This expression likewise takes into account the heat loss with the exhaust gases.

To evaluate the efficiency of the conversion process of electrical into thermal energy, it is possible to utilize the expression without taking into account the influence of heat loss with the exhaust gases:

$$\eta' = \frac{N}{\rho v_{\infty} c_p k_1 b l (t_3 - t_1)} = \frac{z \Delta T^2}{\delta (m + 1)} \cdot \frac{\lambda}{\rho v_{\infty} c_p l l} \cdot \frac{m}{(m + 1) (t_3 - t_1)} \quad (60)$$

A comparison of the operational efficiency of generators having monolithic and permeable thermocouples, at the present time presents certain

difficulties due to a lack of adequate bases for methods of comparison.

If the attempt is made to compare these devices by assuming that batteries with the same geometric dimensions operate with the same temperature drop at their junctions, and that the flow rate of the heat carrier and its temperature ahead of the batteries are the same, then the efficiency of a non-permeable battery will have the following form, using the same conventional symbols:

$$\eta_{\text{un}} = \frac{z\Delta T^2}{\delta(m+1)} \cdot \frac{\lambda}{\rho v_w c_{pr} k_1} \cdot \frac{m}{(m+1)(t_3 - T_{2,\text{un}})} \quad (61) \quad (61)$$

This expression, just as (60), does not take into account the heat loss with the exhaust gases. Here  $P_{2\text{H}}$  is the minimum possible temperature of the exhausting combustion products, equal to the temperature of the hot junction for a non-permeable battery.

To compare the efficiency of the devices considered here, dividing expression (60) by (61), we obtain

$$\frac{\eta'}{\eta_{\text{un}}} = k \frac{t_3 - T_{2,\text{un}}}{t_3 - t_1} \quad (62) \quad (62)$$

The temperature of the heating gases following a non-permeable battery for the given condition of temperature equality of the hot junctions and the heat carrier at the outlet can be easily determined from the thermal equilibrium at the hot side:

$$\rho v_w k_1 c_{pr} b l (t_3 - T_{2,\text{un}}) = \frac{z\lambda\Delta T}{\delta(m+1)} T_{2,\text{un}} b l + \frac{\lambda}{\delta} b l \Delta T - 0.5 \frac{z\lambda\Delta T^2}{\delta(m+1)^2} b l \quad (63) \quad (63)$$

Отсюда

$$\text{whence} \quad T_{2,\text{un}} = \frac{t_3 - \frac{\lambda}{\rho v_w k_1 c_{pr}} \cdot \frac{\Delta T}{\delta} \left[ 1 - 0.5 \frac{z\Delta T}{(m+1)^2} \right]}{1 + \frac{\lambda}{\rho v_w k_1 c_{pr}} \cdot \frac{z\Delta T}{\delta(m+1)}} \quad (64) \quad (64)$$

It can be seen from equations (59) and (60) that the efficiency of a permeable generator taking into account the heat loss with the exhaust gases can be expressed in the following manner:

$$\eta = \frac{t_3 - t_1}{t_3 - t_0''} \eta' \quad (65) \quad (65)$$

For a generator with monolithic thermocouples, the efficiency can be expressed on analogy with a generator having permeable thermocouples, as:

$$\eta_{\text{mon}} = \frac{t_3 - T_{2\text{mon}}}{t_3 - t_0''} \eta_{\text{per}} \quad (66) \quad (66)$$

(here the conventional symbols are the same as for permeable thermocouples).

The relationship between the efficiency of generators having monolithic thermocouples and those which are permeable, in accordance with equations (62), (65) and (66), has the form

$$\frac{\eta}{\eta_{\text{mon}}} = k \quad (k < 1). \quad (67) \quad (67)$$

Consequently, for the conditions of comparison considered here, a battery with permeable thermocouples will be less efficient than one with monolithic couples.

This circumstance is justifiable only for the data from rather restricted conditions, when the same temperature drops at the junctions of thermocouples are assured in both cases by the hot and cold flows which have the same initial and final parameters.

However, this is observed up to a set value of  $\Delta T$ . In fact, in batteries with both permeable and impermeable thermocouples, which operate in the same temperature range of the heat carrier ( $t_3 - t_0$ ), the temperature drop at the junctions can increase up to the set limit. The

increase in the temperature drop at the junctions of the thermocouple causes an increase in the Peltier heat which is absorbed at the hot junctions, and an increase in the heat removed from them due to thermal conductivity of the material of the thermocouple branches. In this case, if the Peltier heat which is absorbed at the hot junctions is nearly the same in both cases (depends on the amount of empty space in the material of the branches, i.e. on the porosity or the capillary coverage), then the quantities of heat which are removed because of the thermal conductivity of the materials of the branches in monolithic and permeable thermocouples, differ sharply.

In a battery with non-permeable thermocouples, the temperature profile differs insignificantly from a straight line (see Chapter III), i.e. the magnitude of the heat flow will increase proportionally to the magnitude of the temperature drop at the junctions of the thermocouples. In a battery with permeable thermocouples, the temperature profile along the height of the thermocouple is very sharply bent, and the temperature gradient at the surface of the hot junctions for a temperature drop at the junctions the same as for a non-permeable thermocouple will be substantially less. This difference in heat flows entering the thermocouple through the surface of the hot junctions increases with an increase in the flow rate of the heat carrier blown through the permeable thermocouple. As an analysis of the expressions for determining the temperatures in a permeable wall shows, given in Chapter III an increase in the temperature drop at the junctions causes the temperature gradient at the surface of the junctions of a permeable thermocouple to grow more slowly in comparison with a monolithic one. In agreement with Fourier's law, this determines smaller heat flows

from the hot junctions in the permeable thermocouples.

An analysis of equations (50) and (63) makes it possible to clarify the redistribution of the influence of the absolute values of the magnitude of Peltier heating and the magnitude  $\lambda(-\frac{dT}{dy})_{y=\delta}$  on the reduction of the heat carrier temperature. Consequently, in non-permeable thermocouples, the heat which is removed due to the thermal conductivity of the material of the thermocouple branches in terms of the absolute magnitude greater than in a battery with permeable thermocouples, and the influence of an increase in the temperature drop at the junctions on the increase in the heat flow leaving the surface of the hot junctions in non-permeable thermocouples, is likewise greater than in permeable ones. This means that the maximum temperature which it is possible to achieve at the hot junctions of non-permeable thermocouples with an increase in  $\Delta T$ , other conditions being equal, will fall off significantly faster in comparison with permeable thermocouples.

For this reason, a battery with permeable thermocouples is capable of operating with a significantly greater temperature drop at the junctions than are monolithic thermocouples.

Thus, equation (67) is justified only up to a set magnitude of  $\Delta T$ , which is achieved in monolithic thermocouples (the value  $\Delta T$  is the maximum possible within the given range  $t_3 - t_0^H$ ). For a further increase in the temperature drop at the junctions of blown-through thermocouples, the efficiency of such a device will be higher than the maximum possible efficiency of a battery with monolithic thermocouples.

Consequently, the method given here makes it possible to carry out calculations for all of the thermal characteristics of a battery through



which a heat carrier blows from the hot to the cold junctions.

We will analyze the operation of a battery which is operating in the mode considered here on the basis of an example of a specific device, calculated in different design variants for changes in several parameters. For the design variants, it was assumed that the physical properties of the heat carrier and cooling flow are the same and equal respectively to:  $\mu = 2.4 \times 10^{-7}$  kg/cm · sec;  $c_p = 10^3$  watts x sec/kg · deg;  $\lambda = 3.8 \cdot 10^{-4}$  watt/cm · deg. The average characteristics of the material of the thermocouple branches are  $z = 0.5 \cdot 10^{-3}$  deg<sup>-1</sup> and  $\lambda = 0.01$  watt/cm · deg. The diameter of the capillaries were taken to be 0.1 cm and the the coefficients  $k_1 = \frac{F_{\pi op}}{F} = 0.196$  and  $k = \frac{F - F_{\pi op}}{F} = 0.804$ , which corresponds to 25 capillaries per cm<sup>2</sup> of battery surface. The ratio of the load resistance to the internal resistance of the battery was taken as  $m = 1$ , the temperature of the hot heat carrier ahead of the battery  $t_3 = 1500^\circ$  K, and the initial coolant temperature  $t_0^H = 300^\circ$  K.

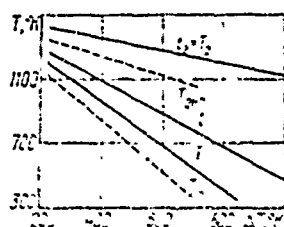


Figure 30. The temperatures of thermocouple junctions and the blow-through heat carrier as a function of the temperature drop maintained at the junctions.

The temperature of the junctions and the temperature of the heat carrier entering the capillaries and upon leaving them are shown in Fig. 30 as a function of the temperature drop at the junctions of permeable thermocouples, computed for a heat carrier flow rate through the capillaries of  $\rho v_w = 10^{-4}$  kg/cm<sup>2</sup> · sec.

However, for the sake of comparison the temperature relationships at the junctions of a non-permeable thermocouple (dotted line) shown here, which will be at the same initial temperature as in the case of a permeable thermocouple for the same rate of flow of the heating gas. It can be seen from the drawing, that it is possible to obtain much greater temperature drops at the junctions in a permeable thermocouple than in a monolithic thermocouple, other conditions being equal. For the given case, the maximum possible useful electrical power derives from a generator with permeable thermocouples will be 1.2 times greater in comparison with a generator having monolithic thermocouples. In this case, the weight of such a battery owing to the presence of the capillaries will be almost 20% less than a battery having monolithic thermocouples.

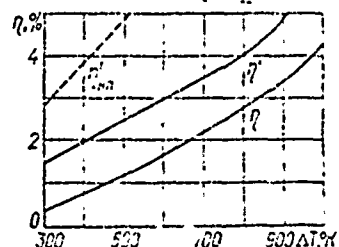


Figure 31. The influence of the temperature drop at the junctions on generator efficiency.

The dependence of the efficiency of the battery considered here on the temperature drop at the thermocouple junctions is shown in Fig. 31. As can be seen from the figure and formula (62), the efficiency of a battery with non-permeable thermocouples without taking into account the heat loss with the exhaust gases at any temperature drops across the junctions, is higher than the efficiency of a battery with permeable thermocouples for similar operational conditions. This is easily explained by the fact that for the same  $\Delta T$  at the junctions of the thermocouples (almost the same electrical powers), the temperature gradient at the cold side of the permeable battery, and thus the heat losses from the surface of the cold junctions,

are significantly greater than for a battery having monolithic thermocouples.

The interrelationship of the efficiency of batteries with permeable and monolithic thermocouples, computed taking into account the heat loss with the exhaust gases, follows from (67) and is determined only by the porosity for the selected method of comparison. However, if one considers thermobatteries not of the same geometric dimensions as in the given case, but of the same weight, i.e. the permeable thermobattery is taken to be larger by the amount of the empty space volume, then the efficiency of both batteries, taking into account the heat losses with the exhaust gases, will be identical for any heat carrier flow rates and temperature drops at the junctions under conditions of complete heat recovery in these circuits.

However, a battery with permeable thermocouples is capable of generating a greater useful electrical power than a battery of the same geometric dimensions with monolithic thermocouples.

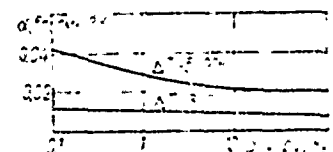


Figure 32. The dependence of the heat transfer coefficient  $\alpha$  at the cold junction side on  $\rho U_0 / \rho V_w k_1$ .

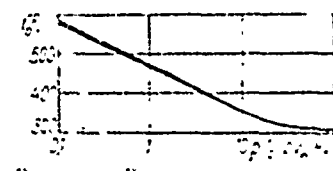


Figure 33. The influence of the ratio  $\rho U_0 / \rho V_w k_1$  on the average temperature of the coolant flow  $t_0^{CP}$ .

The coefficient of heat transfer  $\alpha$  on the cold junction side and the average temperature of the cooling flow  $t_0^{CP}$  over the length of the battery

are shown in Figs. 32 and 33 as a function of the ratio of the specific rates of flow of the coolant reaching the surface of the cold generator junctions, and the heat carrier leaving the permeable thermocouples at the surface of the cold junctions,  $\rho U_0 / \rho v_{\omega_1} k_1$ . It can be seen from these graphs that for an increase in the ratio  $\rho U_0 / \rho v_{\omega_1} k_1$ , at a fixed heat carrier flow rate the magnitude of the necessary heat transfer coefficient  $\alpha$  decreases slightly, but in this case, the average temperature of the coolant flow  $t_0^{CP}$  decreases markedly. This is of significance insofar as the generator can operate with a greater temperature drop at the thermocouple junctions, which means there is obtained a greater useful electrical power.

### 3. Two-stage Generator Design

The devices considered above are capable of operating as both independent generators and jointly in circuits with generators having monolithic thermocouples and with one another. As has already been noted, such combined circuits make it possible to obtain a more efficient conversion of heat and nuclear into electrical energy in many cases. By way of example, we will consider two combined circuits.

The operation of a two-stage generator based on the thermal circuit shown in Fig. 5 f makes it possible to avoid some of the significant drawbacks of each of the stages when operated independently. In such a circuit, each of the generators can operate in its own optimum mode. In this case, both generators operate only with one hot and one cold heat source. The efficiency of any combined cycle, including the one considered here [27], can be computed from the formula:

$$\eta_k = \eta_1 + \psi \eta_2 (1 - \eta_1) \quad (68)$$

where  $\eta_1$  and  $\eta_2$  are respectively the efficiency of the first and second generator.

In the given circuit, one of the generators can be considered as an electric generating device of the primary cycle, while the other is considered a high or low temperature addition to it. Insofar as the values  $\eta_1$  and  $\eta_2$  are small, the effect of combining the cycles of both generators is close to the effect obtained for summing these quantities, i.e. the efficiency of the jointly operating generators calculated from formula (68) will be almost twice as great as that for each of them operating independently. In this case, the magnitude of the coefficient  $\psi$  can be taken as equal to unity, since when there is complete heat recovery in the first stage, the same quantity of heat which is delivered to the first stage is supplied to the second stage of the generator.

Not only combustion products from organic fuels, but also nuclear reactors and radioisotope capsules can be used in such a combined heat cycle as a source of heat for heating the hot junctions of the first stage thermocouples. Under these conditions, the coolant blown through the permeable thermocouples of the first stage and heated in them, creating a temperature drop at the junctions, thereafter is heated to a higher temperature in the space between the heating surface and the hot junctions. The thermocouple junctions in this case are heated by radiation from the heating surface and by convection from the medium cooling the thermocouples in the space between the heating surface and the hot junctions. The hot gas obtained in such a manner is utilized as a heat carrier in the second stage of the two-stage generator.

During two-stage generator operation on the combustion products of an organic fuel, the thermal design of both stages can be carried out in accordance with the methods set forth in the present chapter.

To evaluate the efficiency of a generator employing such a heat circuit, we will use the results of the design variants for single stage generators having permeable thermocouples which were given above. Let the useful electric power of a two-stage generator be 500 watts, where materials with identical properties are used in both stages, whose characteristics were specified above. The optimal operational variant of the two stages in this case, will be the operational mode of the two-stage generator in which the first stage generates 200 watts of useful electrical power, while the second generates 300 watts. The efficiencies of these generators, which are defined as the ratio of the useful power developed to the fuel consumed for its heat generating capacity, were respectively 1.03% and 1.55%. The overall efficiency of the two-stage generator calculated in the same fashion was 2.58%. The primary loss is represented by the heat loss with the physical medium of the combustion products leaving the device. Consequently, the efficiency of the device considered here was the same as the sum of the efficiencies of both generators. The absolute value of the efficiency of a two-stage generator can be significantly greater when a higher quality material with a figure of merit  $z > 0.5 \cdot 10^{-3} \text{ deg}^{-1}$  is used to make the thermocouple branches.

The joint operation of generators based on the heat circuits shown in Fig. 5 b and c (circuit 5 e) can be considered as another circuit for a combination generator. For example, such a generator can be utilized for the cathodic protection of gas pipelines.

The device under consideration consists of two stages and can be built in the form of pipe walls or a rectangular channel. The first generator stage with monolithic thermocouples utilizes the heat of combustion products leaving the generator having permeable thermocouples.

The temperature drop at the junctions of the thermocouples of the first stage is created by means of blowing a gas over finned or non-finned cold junctions, which is supplied from the gas pipeline.

Following the cooling of the cold junctions of the monolithic thermocouples of the first stage, the natural gas is fed to the cold junctions of the permeable thermocouples of the second stage through channel 3, and creates at the junctions of the permeable thermocouples the requisite temperature drop (Fig. 34) blowing through them from the cold to the hot junctions. After this, upon exiting the surface of the hot junctions of the second stage, the gas burns in the air.

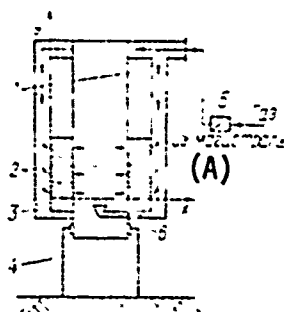


Figure 34. The circuit of a combination generator with permeable and monolithic thermocouples.

(A) Gas from the main line.

The air necessary for combustion is drawn in naturally owing to the difference in the specific weights of the combustion products and the surrounding medium. For this purpose, the device is set up above the ground surface on posts 4. Thus, the hot junctions of the second stage located in the combustion zone can be heated up to a high temperature. A sufficient rate of heat exchange, which takes place when the gas is blown through the pores

(capillaries) of the thermocouples, promotes a greater temperature drop at the junctions.

The combustion products give up a portion of their heat to the hot junctions of the second stage 2 of the generator, and thereafter enter the first stage 1 where they are cooled giving up heat to the hot junctions of the monolithic thermocouples. Convective cooling of the surface of the cold junctions of the first stage does not permit such a large temperature drop across them as in the case for the internal cooling of the second stage permeable thermocouples. However, the first stage increases the power efficiency of the generator, cooling the combustion products to a lower temperature, i.e. reduces the heat loss with the exhaust gases.

The requisite flow rate and pressure of the gas, which can be supplied directly from the gas line, are regulated by means of an automatic regulating device 5. The gas rate of flow can be varied depending on the magnitude of the electric current, or the temperature of the hot junctions of the second stage, or in accordance with any other parameter.

It is expedient to carry out the combustion process not just at the surface of the hot junctions of the second stage. Since the heat can be insufficient to heat the hot junctions of the first thermocouples, it is necessary to place burner 6 ahead of the second stage to obtain a sufficiently high temperature at the input.

In the device considered here, the heat losses from the cold junction side can be eliminated entirely. All of the heat removed from the surfaces of the cold junctions returns with the heated gas to the combustion zone.

The first and repeated starts of such a generator can be accomplished



using an electric ignition device, colocated with burner 5. The ignition device can be placed in operation automatically based on a temperature drop in the combustion products.

When the materials of the thermocouple branches of the first and second stages are specified, it is possible to select temperature drops at the junctions based on the conditions for most efficient operation of these materials. The optimum generator operation would be obtained when all thermocouples operate with an unchanging temperature drop at the junctions of each stage.

Coolant (natural gas) enters the second stage from the first, partially ( $\rho v \frac{k_1 \pi D l_H}{G_r}$ ) blows through the permeable thermocouples and burns at the surface of the hot junctions, and partially ( $G_r$ ) passes by the permeable thermocouples, feeding into the burner located at the generator input, i.e.

$$G_0 = G_r + \rho v \frac{k_1 \pi D l_H}{G_r}$$

where  $l$  is the length of the battery of the second stage;  $D$  is the internal diameter of the generator.

To burn this quantity of natural gas, air is fed in by a natural draft,  $G_B$ , kg/sec. The air surplus coefficient at the input to the generator will

be  $\beta = 1 + \frac{\rho v \frac{k_1 \pi D l_H}{G_r}}{G_r}$  since  $\beta_{L_0} = \frac{G_B}{G_r}$ . Consequently, for known

rates of gas flow through the burner and the permeable thermocouples, the air surplus coefficient is known at the input. For this reason, the temperature of the combustion products at the input can easily be found and the further design of the stage having permeable thermocouples can be based on the method given in paragraph I of this chapter.

The first stage with monolithic thermocouples is designed for the known temperature drop at the junctions  $\Delta T'$ , the rate of coolant flow (natural gas)  $G_0$  and its initial temperature  $t_0^H$ . Additionally, the temperature of the coolant at the outlet of the first stage  $t_0^K$  (where  $y = l_H$ ), the temperature of the combustion products when they enter the first stage  $t_3$  (when  $y = l_H$ ) and its gradient at this point become known from the calculations for the second stage.

The heat balance at the cold junction side of monolithic thermocouples can be written in the following form:

$$\alpha_0(T_1 - t_0) \pi D dy = G_0 c_p dt_0.$$

From this, the temperature distribution of the cold junctions over the length of the first stage is determined:

$$T_1 = \frac{G_0 c_p}{\alpha_0 \pi D} \cdot \frac{dt_0}{dy} + t_0. \quad (69) \quad (69)$$

The heat balance can otherwise be written as:

$$G_0 c_p dt_0 = \lambda' \pi D dy \left( \frac{dT'}{dx} \right)_{x=0} + \frac{z' \lambda'}{\delta' (m+1)} \Delta T' T_1 \pi D dy. \quad (70) \quad (70)$$

Determining the temperature gradient at the surfaces of the cold junctions from expression (10), we find from (70) that:

$$T_1 = \frac{G_0 \delta' (m+1)}{\pi D m z' \lambda'} \cdot \frac{dt_0}{dy} - \frac{1}{2} \cdot \frac{\lambda T'}{m+1} - \frac{m+1}{z'}. \quad (71) \quad (71)$$

Equating expressions (69) and (71) to each other, following integration we obtain the temperature distribution of the coolant over the height of the first stage with monolithic thermocouples:

$$t_0 = \left( \frac{1}{2} \cdot \frac{\Delta T'}{m+1} + \frac{m+1}{z'} + t_0'' \right) \exp \times \\ \times \left\{ \frac{t_{11} - y}{\left[ \frac{\alpha_0 \delta' (m+1)}{z' k' \Delta T'} - 1 \right] \frac{Q_0 c_p}{\alpha_0 \pi D}} \right\} - \left( \frac{1}{2} \cdot \frac{\Delta T'}{m+1} + \frac{m+1}{z'} \right). \quad (72) \quad (72)$$

Knowing the distribution of  $t_0'$ , it is possible to determine the temperature distribution at the cold junctions  $T_1'$  over the length of the generator from (69) or (71), thus also the distribution of the temperature at the hot junctions  $T_2'$ , since  $T_2' = T_1' + \Delta T'$ .

After this, the change in the temperature of the combustion products along the length of the stage with monolithic thermocouples is calculated. Insofar as the flow rates of the combustion products and the cooling medium in the non-permeable stage are fixed and the temperatures of the heating and cooling flows in the section  $y = l_H$  are known, the temperature drop which can appear at the junctions of the monolithic thermocouples will likewise be completely determined. This drop can be determined from the heat balance equation of the stage with monolithic thermocouples:

$$\alpha_1 (t_3 - T_2') = \alpha_0 (T_1' - t_0) \cdot \frac{z' k' m}{\delta' (m+1)^2} (\Delta T')^2. \quad (73) \quad (73)$$

Substituting the temperature values for the junctions from equation (69), we obtain:

$$(\Delta T')^2 + \frac{\alpha_1 \delta'}{k'} \cdot \frac{(m+1)^2}{z' m} \Delta T' + \\ + \frac{\alpha_1 \delta'}{k'} \left[ \frac{Q_0 c_p}{\alpha_0} \cdot \frac{(m+1)^2}{z' m \pi D} \left( \frac{\alpha_0}{\alpha_1} + 1 \right) \frac{dt_3}{dy} + \right. \\ \left. + \frac{(m+1)^2}{z' m} (t_0 - t_3) \right] = 0. \quad (74) \quad (74)$$

In this equation, the values of the temperatures  $t_0'$  and  $t_3'$  as well as the

temperature gradient  $\frac{dt'_0}{dy}$  are chosen for the section  $y = l_H$  following the calculation for the stage with permeable thermocouples:

$$t'_3 = t'_3|_{y=l_H}; \quad t'_0 = t'_0|_{y=l_H}; \quad \frac{dt'_0}{dy} = \left( \frac{dt'_0}{dy} \right)_{y=l_H}.$$

The temperature distribution of the hot gas can be found from the heat balance equation on the hot junction side of the monolithic thermocouples:

Отсюда

$$G_0(L_0 + 1)c_p dt'_3 = \alpha_1 \pi D dy (t'_3 - T_2).$$

whence

$$\int_{l_H}^{l_H} dy = \int_{t'_3}^{t'_3} \frac{dt'_3}{\frac{\alpha_1 \pi D}{G_0(L_0 + 1)c_p} (t'_3 - T_2)}. \quad (75) \quad (75)$$

When carrying out the calculations based on the given equations, the running value of the temperature of the hot junctions, which is determined from expression (69) taking into account the fact that  $T'_2 = T'_1 + \Delta T'$ , is to be used in expression (75).

Thus, using this method it is possible to carry out the complete thermal design of a combination generator, in which both permeable and monolithic thermocouples are employed.

The overall efficiency of the combined device can be determined from the relationship

$$\eta = \frac{N_1 + N_H}{G_0 Q_p}. \quad (76) \quad (76)$$

Such an expression for the efficiency also takes into account the heat losses with the exhaust gases.

## Chapter V

### Thermoelectric Cooling Devices with Permeable Thermocouples

## 1. Refrigerator Design Method

As has already been noted, permeable thermocouples used in the fabrication of thermoelectric devices differ from monolithic ones. Owing to the developed internal heat exchange surface in permeable thermocouples, the heat transfer between the liquid (gas) blown through them and the solid material of the branches takes place at low temperature differences, i.e. almost thermodynamically reversibly.

Such a heat exchange system gives the thermocouple operation its fundamental and essential characteristics, opening up the possibility for influencing the cooling coefficient of the refrigerator or conditioner.

We will analyze the operation of these thermocouples by considering the temperature curve in the material of the electrodes [12].

The nature of such a curve will change depending on the given operational conditions of the thermocouple. In Fig. 35 are shown two temperature curves,  $T = f(y)$ , derived for a refrigerating thermocouple on the assumption that the temperatures of the hot and cold junctions of permeable and monolithic thermocouples are respectively the same, and that consequently the thermoelectric effects are the same. The thermocouple is blown through by a coolant, which is cooled in moving from the hot to the cold junction.

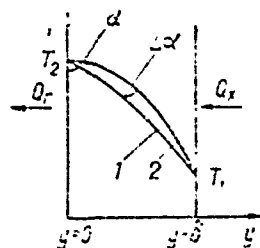


Figure 35. The character of temperature curves in blown-through and non-blown-through thermocouples.

Curve 1 which applies to the monolithic thermocouple, is bent upwards

in an arch due to the fact that the generation of jewel heat causes an increase in the quantity of heat along the y axis, transferred to the cold junction, thus also increasing the temperature gradient. The cooling coefficient  $\eta$  and the cold productivity  $Q_x$  are expressed in the following form:

$$\varepsilon = \frac{Q_c}{W}, \quad Q_x = Q_{\pi,r} - \frac{\lambda}{\lg \alpha} - W, \quad (77) \quad (77)$$

where  $Q_{\pi,r}$  is the Peltier heat generated per unit surface of the hot junction:

$$\operatorname{tg} \alpha = \frac{1}{\frac{(dt)}{(dy)_{y=0}}}, \text{ and } W \text{ is the expended power.}$$

Curve 2 is obtained in the transition to thermocouples with internal heat exchange. The position of curve 2 relative to curve 1 can be characterized by the increase in the angle  $\alpha$  by the magnitude  $\Delta\alpha$ . The additional bending of curve 2 is due to the same cause as the convexity of curve 1, i.e. the increase in the quantity of heat transferred to the cold junction along the y axis because of thermal conductivity. In turn, this is connected with the internal heat delivery from the cooling refrigerant. Thus for a permeable thermocouple,  $\varepsilon' = \frac{Q}{W}$ , where  $Q$  is the total cold productivity of the thermocouple consisting of the heat delivered due to the internal heat transfer from the cooling refrigerant  $\rho v_{\omega} c_p (t_r - t_x)$ , and from the heat supplied from without to the cold junction  $Q_x$ :

$$Q = \rho v_{\omega} c_p (t_r - t_x) + Q_x = Q_{\pi,r} - \frac{1}{\lg(\alpha - \Delta\alpha)} - W. \quad (78) \quad (78)$$

The quantity  $Q_x$  can be as small as desired or equal to zero. Expression (78) is distinguished from (77) only by the increase in the angle  $\alpha$ .

Consequently,  $\epsilon' > \epsilon$  always obtains, other conditions being equal.

For the equal conditions here, it is implied that besides the equality of the material properties, the flowing currents and temperatures of the hot and cold junctions of monolithic and permeable thermocouples are also equal. It is likewise considered that the difference in the temperatures of the filtered refrigerant and the material from which the permeable thermocouple is fabricated, is neglectably small. When these conditions are not observed, qualitatively different results will not result insofar as the magnitude  $\Delta\alpha$  always remains positive. The magnitude of the angle  $\Delta\alpha$  is subject to regulation by changing the quantity of the blown through refrigerant, and likewise depends on the temperature mode and the structural characteristics of the thermocouple.

It is apparent from formula (77), that for very large temperature differences at the junctions, for the case of very short thermocouples, when the angle  $\alpha$  becomes extremely small operational modes are possible in which  $Q_x = 0$ . In other words, for large temperature drops at the junctions (for very small branch heights) the cooling thermocouple does not operate. When finely porous or perforated thermocouples are used, such modes can be widely separated, since even for small magnitudes of the angle  $\alpha$ , it is possible to preserve a significant quantity for  $\alpha + \Delta\alpha$ , having provided for this the cooling medium flow rate which is necessary to obtain the requisite magnitude of  $\Delta\alpha$ .

The qualitative analysis of the operation of monolithic and permeable refrigerating thermocouples given above shows the advantages of the latter as far as the power characteristics are concerned. For this reason, it is expedient to quantitatively analyze in detail the operation of a permeable thermocouple.

The thermocouple of a refrigerating thermoelectric device is shown schematically in Fig. 36. The branches of the thermocouple are provided with capillaries for passing the cooled medium, which blows through from the hot to the cold junctions, giving up heat to the material of the branches of the thermocouples. Depending on the application conditions of a refrigerating battery having permeable thermocouples, the supply of the medium being cooled to the capillaries can be realized in two ways. In the first place, when the cooled medium circulates in a closed loop, its delivery to the capillaries of the thermocouple branches can be accomplished through channels made in the connecting plates of the hot junctions (Fig. 36 a)

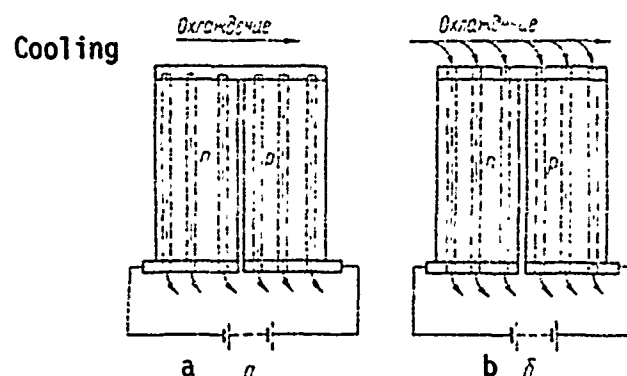


Figure 36. Circuits of permeable refrigerator thermocouples.

In this case, heat can be removed from the surface of the hot junctions by any heat carrier or by natural convection in the case of adequately developed fin cooling.

In the case where a refrigerating battery with permeable thermocouples operates in an open ended circuit, the removal of heat from the hot junctions can be accomplished by a flow of a medium, a portion of which is sucked through the capillaries of the thermocouples, being cooled in them (Fig. 36 b).

When electric current is delivered to the junctions, a temperature



difference is created by the Peltier effect:

$$\mathcal{W} = I^2 R + (T_2 - T_1) eI, \quad (79) \quad (79)$$

where  $I$  is the current passing through the thermocouple;  $e$  is the coefficient of thermal e.m.f.

In this case, the temperature profile along the height of the permeable electrode will be bent (see Fig. 35) and the temperature gradient at the hot side will be lower than on the cold side. Consequently, the transfer flow of heat due to thermal conductivity from the hot junctions will be less than the transfer flow of heat in the non-permeable thermocouples, other conditions being equal.

If it is assumed that  $Q'_x = 0$ , i.e. there is no heat delivered to the surface of the cold junction, then due to the Peltier effect only heat will be absorbed at the cold junctions, which is delivered to the cold junctions because of the thermal conductivity of the material of the thermocouple branches and the medium being cooled:

$$eIT_1 = \lambda (F - F_{\text{top}}) \left( \frac{dT}{dy} \right)_{y=0} + \lambda_{\text{v}} F_{\text{top}} \left( \frac{dT}{dy} \right)_{y=0}. \quad (80) \quad (80)$$

During the cooling of the gases, the heat which is delivered to the cold junctions due to the thermal conductivity of the gas is insignificantly small and in the future we will neglect the second term in (80).

As a result of the Peltier effect, in a non-permeable thermocouple not only heat is absorbed at the cold junctions which reaches them by thermal conductivity, but also heat which is extracted from the cooling substance. Consequently, in spite of the fact that the temperature gradient at the cold

side of a non-permeable thermocouple is smaller, the current magnitude necessary for maintaining the same temperature difference at the junctions will be greater for the same cold productivity, thus also the applicable power will be greater.

The heat delivered to the thermocouples from the cooled medium and the applicable power derived from the hot junction side (we neglect the magnitude  $Q'_x$ ):

$$Q = W + \rho v_{\infty} c_p F_{\text{nop}} (t_2 - t_1). \quad (81) \quad (81)$$

The areas of application of permeable thermocouples are limited by the necessity for operating with very small differences between the temperature of the hot junctions, which should be somewhat higher than the temperature of the surrounding medium and the temperature of the refrigerant, fed in through this junction for cooling. In fact, if the refrigerant has a higher temperature than the hot junction, then it can be cooled beforehand down to this temperature by thermal contact with the surrounding medium without wasting electrical power. If the temperature of the refrigerant returned for cooling is lower than the temperature of the hot junctions and equal to  $t_0$ , then at the input to the thermocouple, the refrigerant should be heated to a temperature close to the temperature of the hot junctions, and thereafter cooled down to the given temperature. In this case, naturally, it would be necessary to develop the superfluous cold productivity, and the ratio of the useful cold productivity to the total in this case is equal to the coefficient  $\frac{\rho v_{\infty} c_p (t_0 - t_1)}{\rho v_{\infty} c_p (t_2 - t_1) + Q'_x}$ , which becomes  $\frac{t_0 - t_1}{t_2 - t_1}$  when  $Q'_x = 0$ . The magnitude of the coefficient contrary to the total cold productivity and the cooling coefficient computed from it decreases for an increase in  $t_1$ .

The value of the current necessary to maintain the given temperature difference at the junctions when a set quantity of the substance being cooled is blown through, can be determined from (80):

$$I = \frac{zT_1 \alpha \pi d z_1}{2K\epsilon} - \sqrt{\left(\frac{zT_1 \alpha \pi d z_1}{2K\epsilon}\right)^2 - \frac{\left(B - \frac{A}{2}\right)\left(\frac{B}{A} + \frac{1}{2}\right)^2 \alpha \pi d z_1 (F - F_{\text{nop}}) \exp\left[\left(B - \frac{A}{2}\right)\delta\right]}{NK\rho} (t_2 - T_1), \quad (82)$$

где

where

$$\begin{aligned} A &= \frac{4\alpha}{\rho v_w c_p d}; \quad B = \sqrt{\left(\frac{A}{2}\right)^2 + \frac{\alpha \pi d z_1}{\lambda (F - F_{\text{nop}})}}, \\ K &= \frac{\left(B - \frac{A}{2}\right)\left(\frac{B}{A} + \frac{1}{2}\right) \exp\left(B + \frac{A}{2}\right)\delta}{N} \times \\ &\times \left[ (1 + A\delta)\left(\frac{B}{A} + \frac{1}{2}\right) - 1 \right] - A, \\ N &= \left(\frac{B}{A} + \frac{1}{2}\right)^2 \exp\left(B + \frac{A}{2}\right)\delta - \\ &- \left(\frac{B}{A} - \frac{1}{2}\right)^2 \exp\left(\frac{A}{2} - B\right)\delta - 2 \frac{B}{A} \exp A\delta. \end{aligned}$$

The temperature profile in the material of the thermocouple branches necessary for the calculation of the temperature gradient is taken from expression (21) when  $t_2 = T_2$ .

If the temperature of the medium being cooled ahead of the batteries and the temperature drop at the junctions are given, then having determined the current magnitude, it is possible to find the temperature of the cooled gas (22) when  $y = 0$ :

$$t_1 = T_1 - C + \frac{\left(\frac{B}{A} - \frac{1}{2}\right) \exp\left(B + \frac{A}{2}\right) \delta}{N} \times \\ \times \left\{ \left(\frac{B}{A} + \frac{1}{2}\right) [t_2 - T_1 + C(1 + A\delta)] - C \right\}, \quad (83) \quad (83)$$

где  
where

$$C = \frac{I^2 R}{\delta \alpha \pi d z_1}.$$

However, if the initial and final temperatures of the cooled medium are given for the design, then the necessary current and the temperature of the cold junction can be found from a simultaneous solution of equations (82) and (83).

For the current magnitude known from equation (79), it is possible to find the applicable electrical power and the quantity of heat which must be removed from the hot junctions from (81).

The efficiency of such a battery (the cooling coefficient) is defined as the ratio of the quantity of heat removed from the cooled medium to the consumed electrical power:

## 2. An Operational Analysis of a Cooling Device

We will consider a thermocouple with a surface of  $1 \text{ cm}^2$ , whose branches are made from solid solutions of  $\text{Bi}_2\text{Te}_3 - \text{Bi}_2\text{Se}_3$  (n - type) and  $\text{Bi}_2\text{Te}_3 - \text{Sb}_2\text{Te}_3$  (p - type). The average characteristics of the thermocouple materials for both branches are as follows:  $\lambda = 0.013 \text{ watt/cm} \cdot ^\circ\text{K}$ ;  $e = 350 \text{ } \mu\text{V}/^\circ\text{K}$ ; and  $\sigma = 1150 \text{ ohm}^{-1} \cdot \text{cm}^{-1}$ . The figure of merit for the material of the thermocouples, taking into account the imperfect connection, is  $z = 2.25 \cdot 10^{-3} \text{ } ^\circ\text{K}^{-1}$ . Air was assumed to be the medium being cooled,

whose temperature ahead of the thermocouple was taken as 323° K.

The cooling coefficient  $\epsilon$  is shown in Fig. 37 as a function of the air blow-through velocity  $\rho v_w$  for thermocouples of equal height, which have 25 capillaries with a diameter of 0.1 cm at a temperature of 290 °K at the cold junctions. As can be seen from the graph, the magnitude of the cooling coefficient  $\epsilon$  changes with a change in the flow rate along the curve, from a maximum, where this maximum shifts in the direction of smaller air flow rates for an increase in the height of the thermocouple. The distribution of the maximums of the efficiency of the thermocouples of different heights along one straight line makes it possible to easily select the height of a thermocouple for a given flow rate of the air being cooled.

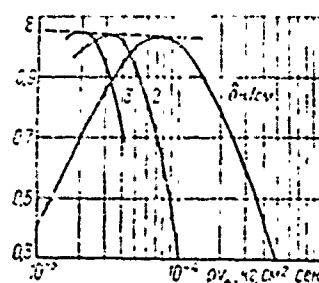


Рис. 37. Зависимость эффективности пористого холодильника  $\epsilon$  от удельного расхода охлаждаемого вещества  $\rho v_w$ .

Figure 37. The efficiency of a permeable refrigerator  $\epsilon$  as a function of the specific rate of flow of the medium being cooled  $\rho v_w$ .

The degree of air cooling in the thermocouple as a function of the flow rate is shown in Fig. 38. It turns out that for the same rate of flow of air through the capillaries, it is cooled to just the same extent in thermocouples of any height (within the limits of accuracy of the calculations). This means that the same quantity of heat will be extracted from the air being cooled in a thermocouple of any height, other conditions being equal. However, the efficiency of this heat removal will vary substantially for various  $\delta$  (see Fig. 37).

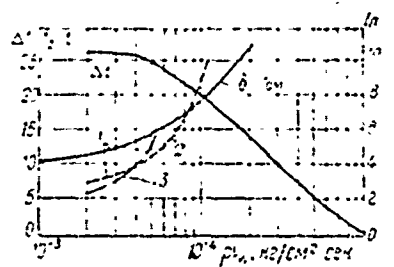


Рис. 38. Зависимость глубины охлаждения воздуха и тока  $I$  от расхода охлаждаемого вещества  $\rho v_{\omega}$ .

Figure 38. The depth of air cooling and the current  $I$  as a function of the flow rate of the medium being cooled,  $\rho v_{\omega}$ .

The nature of the change in the magnitude of the supply current  $I$  for a change in the flow rate of the air cooled in thermocouples of various heights is likewise shown in Fig. 38. The increase in current for a reduction in height is explained by the increase in the temperature gradient at the cold junctions of the thermocouple (Fig. 39), thus by an increase in the influx of heat, whose removal requires an increase in the Peltier effect.

In the known circuits of thermoelectric cooling devices having monolithic thermocouples, the requisite heat removal from the medium being cooled is realized by the Peltier effect at the cold junctions,  $\Pi = eIT_1$ . For large magnitudes of heat removal, the necessary current is quite significant, which in turn leads to greater internal heat generation as a result of Joule heating. The increase in Joule heating for an increase in the current level (when it is necessary to increase the heat removal from the medium being cooled) promotes a reduction in the cooling effect. Finally, the Joule heat can exceed the Peltier heat, and the cooling of the junction goes over into heating [6].

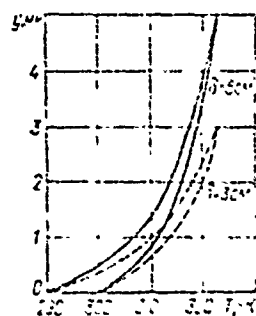


Figure 39. The influence of the height of the thermocouple  $y$  on the nature of the temperature profiles when  $\rho v_{\omega} = 10^{-4}$  kg/cm<sup>2</sup> · sec.

For the case of a circuit having permeable thermocouples, heat removal from the medium being cooled is realized not only at the surface of the junctions, but also within the thermocouple over its entire height. Heat is delivered to the cold junctions only because of the thermal conductivity of the materials of the branches. For this reason, the current which is required to maintain the given temperature difference at the junctions, as calculated from (82), will be less than for the usual devices considered at the same difference in temperatures at the junctions. Consequently, the Joule heat generation conversely affects the cold productivity of the cooling device (Fig. 40).

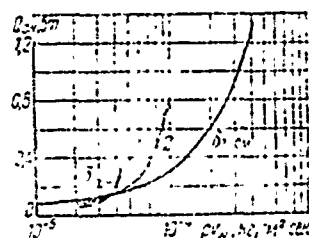


Figure 40. The dependence of the magnitude of the Joule heat  $Q_J$  on the flow rate of the medium being cooled,  $\rho v_w$ .

As is apparent from this graph, in the region of greater flow rates of the medium being cooled, an increase in the height of the thermocouple results in a rather significant increase in the Joule heat generation. However, in the region of low rates of flow, a completely opposite picture is obtained, the greater  $\delta$  is, the smaller is  $Q_J$ . In the region of small flow rates, the magnitude of the current grows less sharply for an increase in the flow rate of the substance being cooled, and in thermocouples with a greater height, a smaller quantity of Joule heat is generated. This parasitic heat generation also exerts a substantial influence on the efficiency of the cooling device (see Figs. 37 and 40). Thus, of the three

thermocouples of various heights which were considered, the most efficient will be the 3 cm high thermocouple in a range of flow rates up to  $2.5 \cdot 10^{-5}$ ; the 2 cm high thermocouple will be most efficient in a range of  $2.5 \cdot 10^{-5}$  --  $6 \cdot 10^{-5}$ ; and for greater flow rates, the thermocouple with a height of 1 cm.

Table 3

Таблица 3

1. $\Delta T$ , град	2. Параметр	3. Непродуваемый термоэлемент		4. Продуваемый термоэлемент	
		$\epsilon_{\max}$	$Q_{\max}$	$\epsilon_{\max}$	$Q_{\max}$
33	$\epsilon$	0,718	0,292	1,04	0,4
	$Q$ , см	0,33	0,8	0,31	0,6
	$I$ , а	9,2	24,2	6,2	15,8
	$W$ , см	0,46	2,74	0,298	1,5
53	$\epsilon$	0,216	0,148	0,3	—
	$Q$ , см	0,269	0,379	0,31	—
	$I$ , а	15,18	22,6	12,33	—
	$W$ , см	1,245	2,56	1,032	—

1.  $\Delta T$ , degrees
2. Parameter
3. Non-blown-through thermocouple
4. Blown through thermocouple.

A comparison of the thermocouples considered here with monolithic ones, carried out for the same cold productivities, shows that the cooling efficiency of the permeable thermocouple is 1.3 - 1.5 times higher than of the non-permeable one. It is necessary to note that these advantages were obtained for a thermocouple weighing substantially less, insofar as fins were lacking on the cold side and the weight of the thermocouple was reduced because of the capillaries.

The influence of a change in the temperature drop at the junctions on the characteristics of blown-through and non-blown-through thermocouples was considered for parallel designs. The results of the calculations for thermocouples with a height of 1 cm and an area of  $1 \text{ cm}^2$  are given in Table 3.



The temperature of the hot junctions in both cases was 323° K. The blown-through thermocouple was provided with 25 capillaries, each having a diameter of 0.1 cm.

As can be seen from the table, the blown-through thermocouple has advantages over the non-blown-through couple as far as the power characteristics are concerned.

These advantages lead us to hope that permeable thermocouples will be effectively employed for conditioning, deep cooling of gases and liquids in various devices, etc. However, the complex analysis of perforated batteries having permeable thermocouples and operating in specific circuits, requires additional research.

### Conclusion

The thermoelectric devices having permeable thermocouples dealt with in this book can be more advantageous than analogous devices having monolithic thermocouples. Much depends on the operational conditions and the function of these devices. For this reason, a comparison of the efficiency and determination of the practicability of using monolithic or permeable thermocouples, should be carried out separately for each specific circuit of a device employed under given specific conditions.

The bases for the theoretical calculations of various thermoelectric devices having permeable thermocouples are set forth in this book along with an analysis of their operation for the purpose of attracting the attention

of specialists to the practicability of their further, more detailed development.

For the practical application of such thermoelectric plants, it is still necessary to solve a number of problems. In particular, the problems of electrically connecting the permeable thermocouples, as well as of the technology of their manufacture from various thermoelectric semiconductor materials, both in a finely porous and perforated form, has been inadequately worked out at the present time.

The efforts directed towards these ends at the Institute for Problems of Materials Processing of the Academy of Sciences of the Ukrainian SSR are promising, but are rather narrowly directed towards the creation of thermoelectric modules for a high temperature thermoelectric generator.

The choice of the material for fabricating permeable thermobatteries is complicated by the fact that in practically all of the circuits considered, they operate in an oxidizing medium. Experiments conducted at the Institute for Engineering Heat Physics of the Academy of Sciences of the Ukrainian SSR have shown promise for the application of metallic thermocouples for the fabrication of permeable thermobatteries. The engineering and economic parameters of the thermoelectric generator with permeable thermobatteries which was developed and tested here are not inferior to the same indicators for devices utilized in the cathodic protection of gas pipelines and supplying low power radio equipment.

A more detailed, comprehensive thermodynamic analysis of thermoelectric devices having permeable thermocouples will inevitably lead to the creation of even more economical and refined thermal circuits. In particular, the

development of multistage thermoelectric refrigerators with permeable thermocouples for cooling the flow of a substance appears to be practicable. As the sample calculations show, the efficiency of such flow coolers will be much greater than the efficiency of devices with monolithic thermocouples constructed at the present time for similar service.

Thus, along with the refinement of devices having monolithic thermocouples and searching for new, higher quality thermoelectric materials, it is necessary to expand the efforts in the further investigation and creation of thermoelectric devices having permeable thermocouples.

---

## Bibliography

### ЛИТЕРАТУРА

1. Алатырцев Г. А. и др. Солнечный термогенератор мощностью 10 Вт. — В кн.: Теплоэнергетика. Изд-во АН СССР, М., 1961.
2. Алатырцев Г. А. и др. Экспериментальный солнечный термоэлектрогенератор. — В кн.: Преобразователи солнечной энергии на полупроводниках. «Наука», М., 1968.
3. Арифов У. А., Кулагин А. И. Некоторые вопросы геотермической энергетики в СССР. — Гелотехника, 1968, 3.
4. Даниель-Бек В. С., Рогинская Н. С. Термоэлектрод-генераторы. Связьиздат, М., 1961.
5. Норданашвили Е. К. Термоэлектрические источники питания. «Советское радио», М., 1968.
6. Ноффе А. Ф. Полупроводниковые термоэлементы. Изд-во АН СССР, М.—Л., 1960.
7. Канаев А. А., Копи И. З. Судовые и стационарные жидко-металлические энергетические установки. «Судостроение», Л., 1964.
8. Карпов В. Г., Чернявский В. В., Тайц Д. А. Использование термоэлектрических полупроводниковых кондиционеров на транспорте. Энергоснабжение и кондиционирование воздуха на транспорте (Материалы конференции). «Зинатне», Рига, 1965.
9. Котырло Г. К. О влиянии профиля температур в термоэлементах на усреднение характеристик полупроводниковых термоэлементов. — В кн.: Теплотехнические проблемы прямого преобразования энергии, 2. «Наукова думка», К., 1971.
10. Котырло Г. К. Температурные поля при охлаждении теплоносителя в пористых и перфорированных стенках. — В кн.: Теплофизика и теплотехника, 10. «Наукова думка», К., 1970.
11. Котырло Г. К., Лобунен Ю. Н. Некоторые результаты измерения температурных полей в продуваемых перфорированных пластинах. — В кн.: Вопросы технической теплофизики, 3. «Наукова думка», К., 1971.
12. Котырло Г. К., Щеголев Г. М. Анализ влияния профиля температур в проицаемой термоэлектрической охлаждающей батарее на ее энергетические характеристики. — ТФЖ, 1972, 22, 1.
13. Котырло Г. К., Щеголев Г. М. Термоэлектрические устройства, продуваемые веществом в направлении теплового потока. — В кн.: Теплофизика и теплотехника, 19. «Наукова думка», К., 1971.
14. Котырло Г. К., Щеголев Г. М. Экспериментальное исследование теплообмена при отсосе через проицающую сетку канала. — В кн.: Теплообмен в энергетических установках. «Наукова думка», К., 1967.
15. Малевский Ю. Н., Милевская Н. Г. Влияние линейного распределения теплового потока на эффективность термоэлектрод-генератора. — В кн.: Преобразователи солнечной энергии на полупроводниках. «Наука», М., 1968.

16. Манасян Ю. Г. Судовые термоэлектрические устройства и установки. «Судостроение», Л., 1968.
17. Миллионщиков М. Д. и др. Високотемпературний реактор — преобразователь «Ромашка». — Атомная энергия, 1964, 17, 5.
18. Михеев М. А. Основы теплопередачи. Госэнергоиздат, М.—Л., 1949.
19. Мугалев В. П. Исследование теплообмена и характеристик турбулентного слоя на пористой поверхности. — В кн.: Тепло- и массоперенос, 1. «Энергия», М., 1963.
20. Наер В. А., Семенов В. А. Влияние пульсаций тока на характеристики полупроводниковых термоэлементов охлаждающих и нагревающих устройств. — Изв. вузов, Энергетика, 1963, 6.
21. Николаев Ю. Д. и др. Термоэлектрический холодильник для автомобиля скорой медицинской помощи. — Автотракторное электрооборудование, 1969, 4.
22. Равич М. Б. Упрощенная методика теплотехнических расчетов. Изд-во АН СССР, М., 1958.
23. Современные термоэлектрические генераторы. (Обзор по материалам зарубежной печати). ППТЭ и ТЭ, 1967, 12 (65).
24. Фаворский О. Н., Каданер Я. С. Вопросы теплообмена в космосе. «Высшая школа», М., 1967.
25. Цветков А. Г. и др. Полупроводниковая термоэлектрическая камера ПТК-1. — Холодильная техника, 1971, 1.
26. Шаленый Э. Г. Полупроводниковые термоэтарен для кондиционирования воздуха. — В кн.: Холодильная техника и технология. «Техника», К., 1966, 2.
27. Щеголев Г. М. Термодинамический анализ высокотемпературных разомкнутых циклов. «Наукова думка», К., 1964.
28. Эккерт Э. Р., Дрейк Р. М. Теория тепло- и массообмена. Госэнергоиздат, М.—Л., 1961.
29. Энергетические установки для космических аппаратов «Мир», М., 1964.
30. Плевак Т. Улучшение характеристик термоэлектрического генератора путем применения испаряющего холодильника. ППТЭ и ТЭ, 1967, 3(36).
31. Pruscek R. Energieversorgungsanlagen mit nuklearen Energiequellen für Raumfliegergeräte. Chemie, Ingenieur, Technik, 1960, He 5.
32. Schuh N. F. Thermoelectric power systems Astronautics and Aerospace Engineering, 1963, 1, 4.
33. Welch J. R. Reactors: key to large scale underwater operations. Nucleonics, 1965, 24, 6.
34. Ureda B. F. SNAPS hot Launch Operations. IEEE Transactions of Nuclear Science, 1965, NS-13, 1.